

AWARD NUMBER: W81XWH-15-C-0089  
JW140111

TITLE: GMP Production and Clinical Trial of a Self-Assembling Protein Nanoparticle  
and Toll-Like Receptor Liposomal MPL Adjuvanted Malaria Vaccine

PRINCIPAL INVESTIGATOR: Dr. Evelina Angov

CONTRACTING ORGANIZATION: Henry M. Jackson Foundation  
Bethesda, MD 20817

REPORT DATE: July 2019

TYPE OF REPORT: Annual

PREPARED FOR: U.S. Army Medical Research and Materiel Command  
Fort Detrick, Maryland 21702-5012

DISTRIBUTION STATEMENT: Approved for Public Release;  
Distribution Unlimited

The views, opinions and/or findings contained in this report are those of the author(s) and should not be construed as an official Department of the Army position, policy or decision unless so designated by other documentation.

# REPORT DOCUMENTATION PAGE

*Form Approved*  
OMB No. 0704-0188

Public reporting burden for this collection of information is estimated to average 1 hour per response, including the time for reviewing instructions, searching existing data sources, gathering and maintaining the data needed, and completing and reviewing this collection of information. Send comments regarding this burden estimate or any other aspect of this collection of information, including suggestions for reducing this burden to Department of Defense, Washington Headquarters Services, Directorate for Information Operations and Reports (0704-0188), 1215 Jefferson Davis Highway, Suite 1204, Arlington, VA 22202-4302. Respondents should be aware that notwithstanding any other provision of law, no person shall be subject to any penalty for failing to comply with a collection of information if it does not display a currently valid OMB control number. **PLEASE DO NOT RETURN YOUR FORM TO THE ABOVE ADDRESS.**

<b>1. REPORT DATE</b> July 2019		<b>2. REPORT TYPE</b> ANNUAL		<b>3. DATES COVERED</b> 1JUL2018 - 30JUN2019	
<b>4. TITLE AND SUBTITLE</b>  GMP Production and Clinical Trial of a Self-Assembling Protein Nanoparticle and Toll-Like Receptor Liposomal MPL Adjuvanted Malaria Vaccine				<b>5a. CONTRACT NUMBER</b> W81XWH- 15-C-0089	
				<b>5b. GRANT NUMBER</b>	
				<b>5c. PROGRAM ELEMENT NUMBER</b>	
<b>6. AUTHOR(S)</b>  Dr. David Lanar  E-Mail: <a href="mailto:clarior@hjf.org">clarior@hjf.org</a>				<b>5d. PROJECT NUMBER</b>	
				<b>5e. TASK NUMBER</b>	
				<b>5f. WORK UNIT NUMBER</b>	
<b>7. PERFORMING ORGANIZATION NAME(S) AND ADDRESS(ES)</b>  Henry M. Jackson Foundation Bethesda, MD 20817				<b>8. PERFORMING ORGANIZATION REPORT NUMBER</b>	
<b>9. SPONSORING / MONITORING AGENCY NAME(S) AND ADDRESS(ES)</b>  U.S. Army Medical Research and Materiel Command Fort Detrick, Maryland 21702-5012				<b>10. SPONSOR/MONITOR'S ACRONYM(S)</b>	
				<b>11. SPONSOR/MONITOR'S REPORT NUMBER(S)</b>	
<b>12. DISTRIBUTION / AVAILABILITY STATEMENT</b>  Approved for Public Release; Distribution Unlimited					
<b>13. SUPPLEMENTARY NOTES</b>					
<b>14. ABSTRACT</b>  There are two main efforts in this project: First, the manufacture of a protein nanoparticle, (FMP014) as the protein base for a malaria vaccine. Second, the development and manufacture of an adjuvant system (Army Liposome Formulations) that was designed to increase the immune response to the protein nanoparticle FMP014. The first year of this three year project was focused on the GMP manufacture of these two key components and was reported last year. The results of second year of this project, reported here, are focused on the evaluation of the two components, both chemically and immunologically. To evaluate the components chemically we focused on identification of the bio-physical characteristics (identification by sequence analysis, size assembled nanoparticle, identification by monoclonal and stability over time) of each component; for evaluation of the immunological characteristics we focused on the immune responses (titer to NANP repeat and C-terminal epitopes, demonstration of induction of protective antibodies; and induction of cellular cytokines in mice and non-human primates) when the FMP014 and adjuvant were combined and injected into the animals. In addition we began an evaluation of the potential toxicity of the components either individually or combined. These efforts were accomplished by a standard multi-dose toxicology study in rabbits. This investigation is still in progress. The results of these evaluations are reported here.					
<b>15. SUBJECT TERMS</b>  None listed					
<b>16. SECURITY CLASSIFICATION OF:</b>			<b>17. LIMITATION OF ABSTRACT</b>	<b>18. NUMBER OF PAGES</b>	<b>19a. NAME OF RESPONSIBLE PERSON</b>
<b>a. REPORT</b>	<b>b. ABSTRACT</b>	<b>c. THIS PAGE</b>			USAMRMC
Unclassified	Unclassified	Unclassified	Unclassified	58	<b>19b. TELEPHONE NUMBER</b> (include area code)

## Table of Contents

	<u>Page</u>
<b>1. Introduction.....</b>	<b>2</b>
<b>2. Keywords.....</b>	<b>3</b>
<b>3. Accomplishments.....</b>	<b>4</b>
<b>4. Impact.....</b>	<b>7</b>
<b>5. Changes/Problems.....</b>	<b>9</b>
<b>6. Products.....</b>	<b>11</b>
<b>7. Participants &amp; Other Collaborating Organizations.....</b>	<b>14</b>
<b>8. Special Reporting Requirements.....</b>	<b>16</b>
<b>9. Appendices.....</b>	<b>17</b>

## 1. INTRODUCTION

The JW14011 project consisted of two main cGMP product development efforts with the goal of translation into first-in-human, Phase I clinical trial to assess the safety, reactogenicity, immunogenicity and efficacy of a novel malaria vaccine candidate. Initially, the Malaria Vaccine Branch (MVB) focused on the development and manufacture of the malaria target, a self-assembling protein nanoparticle (SAPN) based on displaying polypeptide epitopes from the *P. falciparum* Circumsporozoite protein (CSP) on the surface of SAPN. The final molecule was designated, FMP014, for Falciparum Malaria Protein #14. Concomitantly, the Military HIV Research Program (MHRP) focused their efforts on the development and manufacture of an adjuvant system, Army Liposome Formulations, (ALF) designed to increase the immune response to the protein nanoparticle FMP014 and militarily relevant targets of interest (i.e. HIV, Campylobacter, Dengue, etc.). The initial years of this multi-year project focused on the GMP manufacture of the two key components (antigen and adjuvant). Results from these cGMP manufactures and the evaluation of the two vaccine components, chemically and immunologically, were reported previously and will only be briefly summarized here.

Briefly, for the evaluation of the biophysical characteristics of the FMP014 SAPN molecule, various tests were performed to assess the identity, purity and homogeneity of the molecule. These tests included full plasmid nucleotide sequence of the clone, N-terminal sequencing of the protein monomer, mass spectrometry to assess the size of the monomer, dynamic light scattering to analyze the size of the final-assembled SAPN, and SDS-PAGE/Western blotting to verify the homogeneity and stability of the monomer protein over time. For the evaluation of the immunological characteristics induced by the FMP014/adjuvant vaccine candidate, we focused on measuring immune responses such as the antibody titer to NANP repeat and C-terminal epitopes, induction of protective antibodies; and induction of cellular cytokines in mice and non-human primates (NHP). To assess the safety of FMP014 and the various ALF adjuvants including ALFQ, ALFQA and ALFA, several Repeat-dose toxicity studies in New Zealand white rabbits were performed. Overall, there was no antigen or adjuvant related safety signal triggered causing concerns for advancing FMP014 and ALFQ or the other adjuvants evaluated into First in human, Phase I clinical trials.

For the evaluation of the ALF adjuvants, ALFQ and ALFA, for product release and ongoing stability testing, we have used Liquid Chromatography Tandem Mass Spectrometry

(LC/MS/MS) as the analytical method for lipids quantification. LC/MS/MS measurements were performed by Avanti Polar Lipids (Alabaster, AL).

*Extensive delays were experienced due to unexpected outcomes during standard stability testing of the ALF adjuvants.* Briefly, the regulatory timelines for implementing a Phase 1 clinical trial of the FMP014/ALFQ were delayed due to an Out of Specification (OOS) OOS-279 investigation initiated by Avanti Polar Lipids (contractor that performed the analytical methods to quantitate the lipids and adjuvant components) pursuant to failures in stability testing of ALFQ lot #1974 and ALF43 lots #1962 and #1967 for 2-8°C stability samples at the 12 month stability time point. While initial investigations found no obvious reasons for the testing failures, subsequent investigations identified several inconsistencies in the performance of the analytical methods by Avanti Polar Lipids. Most notably, there was an uncontrolled change to the instrumentation which could have had an effect on the qualification status of the methods and instrument. Secondly, it was determined that possible laboratory errors related to the routine preparation and use of the working calibration standards may have impacted their stability (and concentration). Pursuant to Avanti's internal QC investigation, Avanti's Quality Unit deemed the methods performance unreliable and the system suitability parameters an insufficient measure of assay performance. These failures were associated with the performance of the analytical methods and not to the final adjuvant products, ALF43 (ALFA) and ALFQ. Avanti Polar Lipids initiated methods development under a Corrective and Preventative Action proposal, (CAPA-039), September 2017, to better understand the capabilities of all five adjuvant component test methods and to improve their system suitability parameters to better monitor test method performance. Approximately one year later (Sept 2018), following extensive methods development, all cGMP lots of adjuvants were retested using the requalified methods and calibrated standards. All adjuvant lots passed identity and composition testing within the established specifications. Based on these positive results, MVB/MHRP initiated translational efforts of the FMP014 (PfCSP- SAPN) formulated in ALFQ to a Phase 1 trial with Controlled Malaria Infection Challenge (CHMI). The focus of the work shifted to the development of clinical protocol and completion of the CMC sections of the IND; substantially undertaken from Oct 2018 through the end of this annual reporting period (31 July 2019).

## **2. KEYWORDS:**

Plasmodium falciparum	SAPN
Malaria	Nanoparticle
Vaccine	Adjuvant

### **3. ACCOMPLISHMENTS:**

#### **What was accomplished under these goals in Year 4?**

Following the requalification of the analytical methods used to assess adjuvant components, lipids, 3D-PHAD and QS-21, ~September 2019, efforts were focused on the clinical study design, and the development of a clinical human-use protocol and the completion and compiling of the CMC sections of the IND.

#### **Key Reviews and Approvals**

WRAIR Scientific Review Committee (SRC) approval: 17 June 2019

Sponsors Protocol Review Board (PRB) approval: 21 June 2019

WRAIR Investigation Review Board (IRB) approval with stipulation: 10 July 2019

#### **3.1 Clinical Study Design**

The study is designed as a single center, open-label immunization with Controlled Human Malaria Infection (CHMI). The trial design is described and illustrated in Figure 1. Healthy, malaria-naïve adults (males and non-pregnant, non-lactating females), aged 18 to 55 years old (inclusive) will be recruited from the surrounding area to participate in this immunization with CHMI study. Up to 40 subjects will be enrolled (defined as receiving experimental product) into one of 5 experimental cohorts in two parts. In part A two experimental cohorts of 5 subjects each will receive a series of three vaccinations at 0, 1, and 2 months at a two doses (the “low dose” arm and the “high dose arm”). In part B three experimental cohorts of 10 subjects will receive a series of 3 vaccinations at 0, 1, 6 months (called the “delayed dose” arm), the “delayed fractional dose” arm is vaccinated at 0, 1, and 6 months with the 6 month dose being 1/5 the other doses, and the “standard” arm” at the 4th, 5th, and 6th month (after the first vaccination of the other two arms in part B). As both the adjuvant and the antigens will be first-in-human inter- and intra-cohort safety staggers will be used. In part A, low and high dose groups will be staggered by 14 days, with the “low dose” arm vaccinated prior to “high dose” arm. In addition, both arms will utilize an internal safety stagger, with one subject vaccinated on Day 1, followed by the remainder of each cohort 24-72 hours later (if no stopping criteria are met). After the third vaccination of cohorts from part A are complete, a SMC meeting will occur. Part B will start only after the Safety Monitoring Committee (SMC) evaluates safety data from Part A and part B will start if the study is determined to be safe to proceed and at either the high or low dose used in part A.

Up to 6 subjects will be enrolled (defined as receiving malaria challenge) later in the trial to serve as challenge controls. Additional subjects may be recruited as alternates to ensure that 6 control subjects undergo each challenge. Any alternates not challenged will be released from the study at day of challenge.

All subjects in part B will undergo CHMI 3-4 weeks after the final vaccine is administered. Challenge will consist of exposure to *Plasmodium falciparum* 3D7 sporozoites through the bites of infected mosquitoes. Between post-challenge day 5 and post-challenge day 20, subjects will be evaluated daily for the development of malaria infection utilizing validated qPCR. Subjects will be monitored post-challenge in a clinic setting; a hotel phase will not be utilized. Subjects who do not become parasitemic by Day 20 will be seen every other day in the clinic until diagnosis or Day 28. All subjects without parasitemia through Day 28 after challenge will be treated empirically.

All subjects diagnosed with malaria infection will be prescribed a standard treatment regimen consisting of chloroquine (CQ), atovaquone-proguanil (AP; Malarone®), or artemether/lumefantrine (AL; Coartem®), to begin on the day that parasitemia is detected. For purposes of confirming treatment effectiveness, daily qPCR will be continued after diagnosis until two consecutive negative qPCR results has been recorded. If a treated subject has not met the effectiveness threshold by Day 20, they will be followed daily in the CTC for blood draws and continued testing until they meet criteria.

All part B experimental subjects will be followed for an additional 56 days following completion of the original challenge phase for safety and immunogenicity, and then released from the trial.

Part A subjects will not undergo CHMI. Instead, they will be followed for an additional 112 days (4 months post-third immunization) for safety and immunogenicity, and then released from the trial.

### **3.2 Criteria for Evaluation**

#### **Safety:**

1. Occurrence of solicited adverse events (AE) during the study period (enrollment to final follow-up visit).
2. Occurrence of unsolicited AEs at any time during the study period (enrollment to final follow-up visit).

3. Occurrence of serious adverse events (SAE) at any time during the study period (enrollment to final follow-up visit).

**Efficacy:**

1. Vaccine efficacy defined as the proportion of subjects who do not have a positive qPCR following CHMI.
2. Identification of parasitemia by positive qPCR after the *P. falciparum* challenge.
3. Time to parasitemia defined as quantification of time to positive qPCR in subjects that develop a positive qPCR.

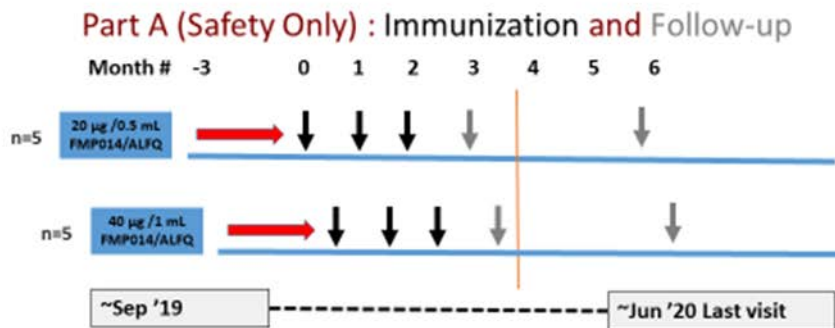
**Immunogenicity:**

1. Measure antibody, innate, and cellular responses to PfCSP present in serum/blood at specified time-points: prior to vaccination (or challenge for control subjects) and on study days specific for each group.

**3.3 Clinical Schema**

The study design is illustrated in Figure 1, below:

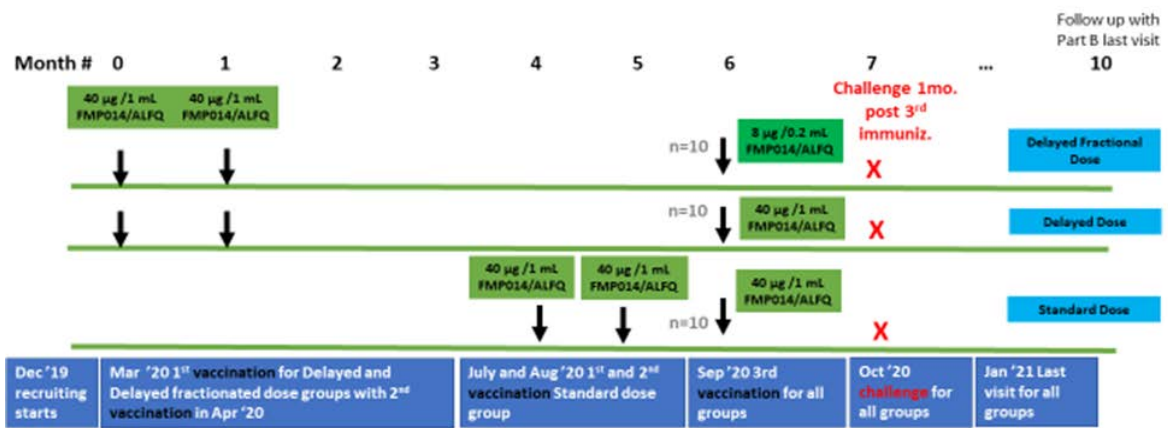
Part A (Safety)



Part B (Immunogenicity and Efficacy)



## Part B: Immunization and Challenge



Note: For Part B, SMC may choose to proceed with lower dose (20 µg of FMP014 and 0.5 mL ALFQ), depending on safety evaluation from part A of the study. In this case the fractional dose would be 4 µg of FMP014 and 0.1 mL ALFQ.

### What opportunities for training and professional development has the project provided?

Attend local and international conferences to present the study data.

### How were the results disseminated to communities of interest?

Regular monthly working group meetings, presentation at national and international conferences as either oral or poster presentations, final published manuscripts:

### What do you plan to do during the next reporting period to accomplish the goals?

1. Receive final WRAIR IRB approval for the FMP014/ALFQ clinical protocol
  1. Submit the FMP014/ALFQ IND to the U.S. FDA for review
  2. Obtain USOTG/Sponsor approval for implementing the clinical trial at the WRAIR Clinical Trials Center (CTC)
  5. Initiate recruiting and screening for subjects to participate in the clinical trial of the FMP014/ALFQ (Fall 2019)
  6. Perform all immunizations and sample collections
  7. Provide information on the safety and any adverse events through reporting to the Sponsor
  8. Complete immunizations and perform CHMI
4. **IMPACT**

**What was the impact on the development of the principal discipline(s) of the project?**

The development of the self-assembling nanoparticles approach used for FMP014 is an innovative approach for vaccine antigen design and display, one that has increasingly gained attention. The nanoparticle design for FMP014, produces a highly repetitive, symmetrical display of CSP-derived antigens. Results from animal models yielded encouraging results for safety, tolerability and protective efficacy. In addition, the FMP014 design is highly stable relative to long term storage, and thus is economical for production and distribution. The use of WRAIR's ALFQ adjuvant is also groundbreaking, its composition is similar to the highly potent and protective AS01 adjuvant developed by GSK. While the AS01 adjuvant has been essential to the success of the malaria vaccine candidate, RTS,S, it is not available to the US Army for developing clinically relevant vaccines. Application of ALF-like adjuvants in humans, has proven that the immunostimulatory molecules (QS-21 and 3D-PHAD) are safe and suitable for enhancing immune responses, and support the Phase I studies of FMP014/ALFQ. Results from safety testing of FMP014/ALFQ in mice, rabbits and rhesus macaques support the further testing of this vaccine candidate in human subjects. The objective of the current study is to develop a novel malaria vaccine based on the CSP antigen that is both safe and effective in healthy, naïve adults. Importantly, because of improvements in the antigen and adjuvant, the vaccine has the potential for eliciting potent and long-lasting protection against infection.

**What was the impact on other disciplines?**

The ALF adjuvants are being applied to evaluate other vaccine approaches being developed by WRAIR research community as well as with external collaborations.

In MVB Dr. Evelina Angov and Dr. Sheetij Dutta are evaluating the ALFQ adjuvant in preclinical studies using PfCelTOS, PfCel-PfCel SAPN and the soluble *P. falciparum* CSP (FMP013), PfCSP-repeat specific tobacco mosaic virus nanoparticles, respectively.

In collaboration with Dr. Evelina Angov, Dr. Martha Sedegah and Dr. Peter Burkhard have received CDMRP funding to evaluate the next generation of SAPN antigen display approach as a multi-epitope/multi-antigen delivery system for malaria. This project will initiate in OCT FY20 and is funded for three years.

### **What was the impact on technology transfer?**

1. Scalable, cGMP processes for manufacture of both the antigen (FMP014) and adjuvants (ALF43 and ALFQ) were developed.
2. Methods for the qualification of the adjuvant components were developed by Avanti Polar Lipids. APL plans to validate these methods in the future.
3. A US Patent for ALFQ as an adjuvant has been approved and will issue shortly.

### **What was the impact on society beyond science and technology?**

Nothing to report

## **5. CHANGES/PROBLEMS**

### **Changes in approach and reasons for change**

The company, Avanti Polar Lipids, who manufactures the liposomes and phospholipids that are used to manufacture the base component, ALF55, of the ALF adjuvants experienced significant delays in the quantitative analysis of the GMP vialled products. During the second-third quarter of FY17, adjuvant stability testing yielded an out of specifications finding for ALF adjuvants. Due to an Out of Specifications (OOS) investigation initiated by Avanti Polar Lipids, Inc. on March 27, 2017 and the pursuant investigations into the matter, it was determined that additional methods development is required to establish well qualified and validated methods for quantifying and identifying the ALFQ adjuvant components and degradants of the GMP batch lots for product release and stability testing. The impact of this action is the invalidation of the lot release for the GMP adjuvant ALFQ Lot #1974 and #2010.

### **Actual or anticipated problems or delays and actions or plans to resolve them**

GMP product re-testing and release occurred in Sept 2018 using the final re-qualified methods to quantify lipids, 3D-PHAD and QS-21. All adjuvants passed composition testing and were re-released in October 2018. Ongoing monthly, and quarterly stability testing indicates that the adjuvant is stable.

### **Changes that had a significant impact on expenditures**

1. The returning of clinical trial funds to CDMRP in FY17 July, due to invalidation of testing results for the stability time point (T12) of the ALFQ lots led to the cancellation of the clinical trial. Returning of the funds to CDMRP impacted the ability to perform the clinical trial activities in the out-year FY18-FY19.
2. Upon resolution of the methods requalification and release of the adjuvants for testing, the funds assigned to the clinical trial were returned to WRAIR (~March 2019) as FY19 funds (2 year funds expiring in 30 Sept 2020).
3. Pilot BioProduction Facility closure at WRAIR for remodeling had a significant impact on the ability to formulate any new ALFQ adjuvant lots.

### **Significant changes in use or care of human subjects, vertebrate animals, biohazards, and/or select agents**

Nothing to report

### **Significant changes in use or care of human subjects**

Nothing to report

### **Significant changes in use or care of vertebrate animals.**

Nothing to report

### **Significant changes in use of biohazards and/or select agents**

Nothing to report

## 6. PRODUCTS:

### Publications, conference papers, and presentations:

#### Journal publications

All subject matter discussed in the reports and presentations relates to either the malaria antigen FMP014, or the ALF adjuvants, ALFQ and ALFA (ALF43).

1. Cawlfeld A, Genito CJ, Beck Z, Bergmann-Leitner ES, Bitzer AA, Soto K, Zou X, Hadiwidjojo SH, Gerbasi RV, Mullins AB, Noe A, Waters NC, Alving CR, Matyas GR, Dutta S. Safety, toxicity and immunogenicity of a malaria vaccine based on the circumsporozoite protein (FMP013) with the adjuvant army liposome formulation containing QS21 (ALFQ). *Vaccine*. 2019 May 28. pii: S0264-410X(19)30696-6. doi:10.1016/j.vaccine.2019.05.059. [Epub ahead of print] PubMed PMID: 31151801.
2. Ramakrishnan A, Schumack NM, Gariepy CL, Eggleston H, Nunez G, Espinoza N, Nieto M, Castillo R, Rojas J, McCoy AJ, Beck Z, Matyas GR, Alving CR, Guerry P, Poly F, Laird RM. Enhanced Immunogenicity and Protective Efficacy of a *Campylobacter jejuni* Conjugate Vaccine Coadministered with Liposomes Containing Monophosphoryl Lipid A and QS-21. *mSphere*. 2019 May 1;4(3). pii: e00101-19. doi: 10.1128/mSphere.00101-19. Erratum in: *mSphere*. 2019 May 22;4(3): PubMed PMID: 31043512; PubMed Central PMCID: PMC6495334.
3. Krebs SJ, Kwon YD, Schramm CA, Law WH, Donofrio G, Zhou KH, Gift S, Dussupt V, Georgiev IS, Schätzle S, McDaniel JR, Lai YT, Sastry M, Zhang B, Jarosinski MC, Ransier A, Chenine AL, Asokan M, Bailer RT, Bose M, Cagigi A, Cale EM, Chuang GY, Darko S, Driscoll JI, Druz A, Gorman J, Laboune F, Louder MK, McKee K, Mendez L, Moody MA, O'Sullivan AM, Owen C, Peng D, Rawi R, Sanders-Buell E, Shen CH, Shiakolas AR, Stephens T, Tsybovsky Y, Tucker C, Verardi R, Wang K, Zhou J, Zhou T, Georgiou G, Alam SM, Haynes BF, Rolland M, Matyas GR, Polonis VR, McDermott AB, Douek DC, Shapiro L, Tovanabutra S, Michael NL, Mascola JR, Robb ML, Kwong PD, Doria-Rose NA. Longitudinal Analysis Reveals Early Development of Three MPER-Directed Neutralizing Antibody Lineages from an HIV-1-Infected Individual. *Immunity*. 2019 Mar 19;50(3):677-691.e13. doi: 10.1016/j.immuni.2019.02.008. Epub 2019 Mar 12. PubMed PMID: 30876875.
4. Karch CP, Matyas GR, Burkhard P, Beck Z. Glycosylation of the HIV-1 Env V1V2 loop to form a native-like structure may not be essential with a nanoparticle vaccine. *Future Virol*. 2019 Feb;14(2):51-54. doi: 10.2217/fvl-2018-0174. Epub 2019 Jan 10. PubMed PMID: 30815025; PubMed Central PMCID: PMC6378949.
5. Karch CP, Bai H, Torres OB, Tucker CA, Michael NL, Matyas GR, Rolland M, Burkhard P, Beck Z. Design and characterization of a self-assembling protein Nanoparticle displaying HIV-1 Env V1V2 loop in a native-like trimeric conformation as vaccine antigen. *Nanomedicine*. 2019 Feb;16:206-216. doi: 10.1016/j.nano.2018.12.001. Epub 2018 Dec 18. PubMed PMID: 30576800.

6. Singh P, Beck Z, Matyas GR, Alving CR. Saturated phospholipids are required for nano- to micron-size transformation of cholesterol-containing liposomes upon QS21 addition. *J Liposome Res.* 2018 Nov 23;1-4. doi: 10.1080/08982104.2018.1538239. [Epub ahead of print] PubMed PMID: 30350748.

7. Karch CP, Matyas GR, Burkhard P, Beck Z. Self-Assembling Protein Nanoparticles: implications for HIV-1 vaccine development. *Nanomedicine (Lond).* 2018 Sep;13(17):2121-2125. doi: 10.2217/nmm-2018-0222. Epub 2018 Oct 1. PubMed PMID: 30270731.

### **Books or other non-periodical, one-time publications.**

Nothing to report

### **Other publications, conference papers, and presentations.**

1. Matyas, G.R., Torres, O.B., Sulima, A., Beck, Z., Jacobson, A.E., Rice, K.C., A Stable Heroin Analog Vaccine Formulation that Induces Long Duration Antibody Titers that Block the Antinociceptive Effects of Heroin and Hydromorphone. International Narcotics Research Conference, San Diego, CA July 12-16, 2018 (poster).

2. Karch, C.P., Matyas, G.R., Burkhard, P., Beck, Z. Innovative HIV-1 vaccine design using glycosylated V1V2 Envelope proteins displayed on a Self-Assembling Protein Nanoparticle. Innovative Vaccines Against Resistant Infectious Diseases and Emergent Threats. New York Academy of Sciences, New York, NY May 20, 2019 (poster).

3. Angov, E., Dutta, S., Beck, Z., Matyas, G.R., Nguay, V. Strategic Overview: WRAIR's Next Generation Adjuvanted *P. falciparum* CSP Vaccine Candidates in Clinical Development, PfCSP-SAPN and full length, soluble PfCSP. Malaria Vaccines for the World, Oxford, UK, May 8-10, 2019 (talk).

4. Karch, C.P., Matyas, G.R., Burkhard, P., Beck, Z. De novo Designed Self-Assembling Protein Nanoparticle Platform for HIV-1 Vaccine Development. Annual Conference on Vaccinology Research, Baltimore, MD, April 3-5, 2019 (poster).

5. Rao, M., Onkar, S., Peachman, K.K., White, Y., Trinh, H.V., Jobe, O., Zhou, Y., Dawson, P., Eller, M.A., Matyas, G.R., Alving, C.R. Liposome-Encapsulated HIV-1 gp120 Induces Potent V1V2-Specific Antibodies in Humans. International Society for Vaccines, Atlanta, GA, October 28-30, 2018 (talk).

6. Godin, S., Lanar, D., Matyas, G.R., PfCSP Self-Assembling Protein Nanoparticle (SAPN) Malaria Vaccine in Combination with Army Liposomal Adjuvant Containing Monophosphoryl Lipid A and QS21 (ALFQ) and ALFQ and Alhydrogel (ALFQA): Local and Systemic Toxicity Study Following Four Intramuscular Injections to Male and Female New Zealand White Rabbits with a 28-Day Recovery Period. American College of Toxicology, West Palm Beach, FL Nov 4-7, 2018 (poster).

7. Gutman, E., Irvin, T., Torres, O.B., Matyas, G.R., Alving, C.R. Jacobson, A. E., Rice, K.C. Design and synthesis of a novel hapten for use in heroin vaccines: testing the facial recognition hypothesis, 2018 Behavior, Biology, and Chemistry Conference: Translation

Research in Addiction, San Antonino, TX, March 2-3, 2019 (poster).

8. Matyas, G.R., Dutta, S., Laird, R.M., Ramakrishnan, A., McCoy, A.J., Beck, Z. Army Liposome Formulations, ALFA and ALFQ, Are Potent Adjuvants. HIV Research for Prevention, Madrid, Spain, October 21-25, 2018 (poster).

9. Pegu, P., Tucker, C., Wiczorek, I., Molnar, S., Martinez, E., Florese, R., Polonis, V., Matyas, G.R. Immunogenicity of HIV-1 DNA and Protein Prime-Boost Vaccine Regimen in Combination with Novel Adjuvants. HIV Research for Prevention, Madrid, Spain, October 21-25, 2018 (poster).

10. Sulima, A., Jalah, R., Torres, O.B., Imler, G.I., Deschamps, J., Beck, Z., Alving, C.R., Jacobson, A.E., Matyas, G.R., Rice, K.C. Broad spectrum long acting heroin vaccine. Improved synthesis of 6-AmHap, a hapten for a broad-spectrum conjugate heroin vaccine for phase 1 clinical trials. Middle Atlantic Regional Meeting: Combating the Opioid Crisis with Chemistry Bethesda, American Chemical Society, University of Maryland, Baltimore, MD, May 30- June 1, 2019 (talk).

11. Matyas, G.R., Torres, O.B., Sulima, A., Whalen, C., Beck, Z., Jacobson, A.E., Rice, K.C. A Stable Heroin Hapten (6-AmHap) Vaccine Formulation Slated for a Phase 1 Clinical Trial Induces Long Duration Antibody Titers that Block the Antinociceptive Effects of Heroin and other Opioids. College of Problems of Drug Dependence, San Antonio, TX, June 15-19, 2019 (talk).

12. Matyas, G.R., Dutta, S., Laird, R.M., Ramakrishnan, A., McCoy, A.J., Beck, Z. Army Liposome Formulations, ALFA and ALFQ, Are Potent Adjuvants. International Society for Vaccines, Atlanta, GA, October 28-30, 2018 (poster).

### **Invited Scientific Lectures**

1. Development of a Heroin Vaccine That Induces Antibodies That Also Bind to Abused Prescription Opioids; Vaccines for the Treatment of Opioid Disorder; National Institute of Allergy and Infectious Diseases, National Institutes of Health, Rockville, MD; October 24, 2018.

2. Breaking ~~Bad~~ Good: Developing a Vaccine Against Opiate Addiction; Emory Vaccine Center, Emory University, Atlanta, GA November 14, 2018.

3. Can You Make a Vaccine to Heroin?; Department of Pharmacology, Michigan State University, East Lansing, MI; February 27, 2019.

### **Army Presentation**

1. Briefed Col Jerome Buller, Commander, U.S. Army Institute of Surgical Research on: Heroin Vaccine Research, March 15, 2019

### **Website(s) or other Internet site(s)**

Nothing to report

### **Technologies or techniques**

Nothing to report

### **Inventions, patent applications, and/or licenses**

US Patent for the ALFQ has been approved and will issue shortly.

### **Other Products**

Nothing to report

## **7. PARTICIPANTS & OTHER COLLABORATING ORGANIZATIONS**

### **What individuals have worked on the project?**

Name:	Dr. Evelina Angov
Project Role:	Principle Investigator
Researcher Identifier (e.g. ORCID ID):	0000-0003-2814-3057
Nearest person month worked:	12
Contribution to Project:	Dr. Angov is the Project PI.
Funding Support:	N/A

Name:	Dr. Gary Matyas
Project Role:	Consultant
Researcher Identifier (e.g. ORCID ID):	
Nearest person month worked:	12
Contribution to Project:	ALFQ expertise
Funding Support:	N/A

Name:	Dr. Peter Burkhard
Project Role:	Consultant
Researcher Identifier (e.g. ORCID ID):	
Nearest person month worked:	12
Contribution to Project:	invented these protein nanoparticles as a



	platform for vaccine design
Funding Support:	N/A

**Has there been a change in the active, other support of the PD/PI(s) or senior/key personnel since the last reporting period?**

Dr. Stephen Kaba, departed from the laboratory as of 31 July 2018.

**What other organizations were involved as partners?**

Organization name:	Avanti Polar Lipids
Location of the organization	Alabaster, AL, USA
Partner's contribution to the project:	
In kind support	Partner manufactures the ALF (with 43% or 55% cholesterol) portion of the adjuvants used with FMP014

Organization name:	Desert King International
Location of the organization	San Diego, CA, USA
Partner's contribution to the project:	
In kind support	Partner manufactures the QS21 that is part of the adjuvant used with FMP014

Organization name:	Alpha-O peptides
Location of the organization	Allschwil, Switzerland
Partner's contribution to the project:	
Collaboration	Dr. Burkhard designed the SAPN FMP014

Organization name:	WRAIR Pilot Bioproduction Facility (PBF)
Location of the organization	Silver Spring, MD, USA
Partner's contribution to the project:	
Collaboration	PBF staff performs the scale-up and performs release testing of the drug product and substance

Facilities	The project staff uses the partners facilities for stability sample storage
------------	---

Organization name:	WRAIR Veterinary Medicine Support
Location of the organization	Silver Spring, MD, USA
Partner's contribution to the project:	
In kind support	Partner makes equipment such as cages etc. available to the project staff when needed
Facilities	Project staff uses the partner's facilities to perform all animal work
Collaboration	Partner's staff works with the project staff to ensure and maintain the safety of the animals used in the studies
Personnel exchanges	Project staff uses the partners facilities to immunize and bleed the mice for the studies

Organization name:	WRAIR Entomology Branch
Location of the organization	Silver Spring, MD, USA
Partner's contribution to the project:	
In kind support	Partner helped train staff in mosquito dissection
Facilities	Project staff uses entomology facilities to retrieve mosquitoes for dissection
Collaboration	Partners staff provides the mosquitoes for mouse challenge studies and works with project staff in the event help is required with dissections
Personnel exchanges	Project staff uses the entomology facilities while training and collecting mosquitoes

## 8. SPECIAL REPORTING REQUIREMENTS

### COLLABORATIVE AWARDS:

Nothing to report

### QUAD CHARTS:

Quad Chart July 2019 – Attachment 1

## **9. APPENDICES:**

Attachment 1 – Quad Chart July 2019 – Annual Report updated.

Attachment 2 – Manuscript – Cawlfild A., et al. Safety and toxicity study using cGMP ALFQ and malaria candidate, FMP013.

Attachment 3 – Manuscript – Ramakrishnan A., et al. Immunogenicity of campylobacter formulated in ALFQ adjuvant vaccine candidate.

# GMP Production and Clinical Trial of a Self-Assembling Protein Nanoparticle and Toll-like Receptor Liposomal MPL Adjuvanted Malaria Vaccine.



PI: Evelina Angov

Org: WRAIR / HJF Foundation

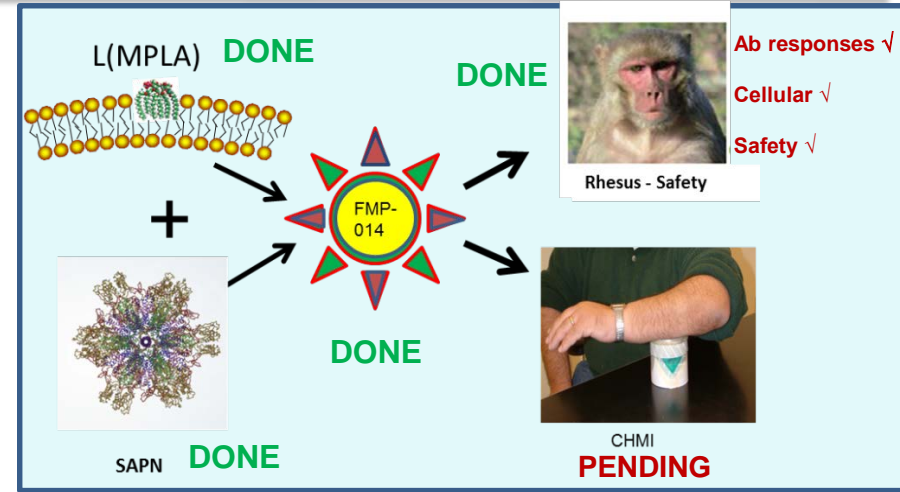
Award Amount: 7.5 Million

## Study/Product Aim(s)

- GMP Manufacture and Vialing of nanoparticle FMP014 ✓
- GMP Manufacture & Vialing of adjuvants ALF and ALFQ ✓
- Safety and Immunogenicity study in NHP ✓
- Repeat dose toxicity study in rabbits ✓
- Develop qualified methods (LC-MS/MS) used for measuring adjuvant composition (lipids, cholesterol, 3D-PHAD, QS21). ✓
- Perform FMP014/ALFQ clinical development activities for Phase 1/2a clinical trial with Controlled Human Malaria Infection (CHMI). (tentative start late FY19/early FY20). ✓
- Received approval with stipulations from WRAIR IRB, 15 July 2019.

## Approach

Test novel SAPN malaria vaccine FMP014 formulated in ALFQ in human subjects; subjects will receive three doses at 0,1, 6 months followed by a Controlled Human Malaria Infection by bites of infected mosquitoes.



**GMP lots of ALFQ adjuvant pass testing using qualified methods, adjuvant products are released from quarantine, 28 Sept 2018.**

## Timeline and Cost

Activities	CY 15	16	17	18	19	20
Produce FMP014	Actual (to date)	Proposed				
Produce ALFA, ALFQ, ALFQA		Actual (to date)	Proposed			
QC/QA FMP014 and ALFs; NHP Studies			Actual (to date)	Proposed		
Conduct Clinical Trial w/ CHMI (substantially delayed, ~2 yrs)					Actual (to date)	Proposed
<b>Estimated Budget (\$K)</b>	<b>\$3,000</b>	<b>\$1,500</b>	<b>\$3,000</b>		<b>\$1,751</b>	

Updated: (22 July 2019)

Proposed (Green bar)  
Actual (to date) (Blue bar)

## CY16-18 Goals – Product validation

- ✓ Produce cGMP Products
- ✓ Show safety, immunogenicity of FMP014/adjuvants in rabbits and NHP

## CY19 Goal (new)

- ✓ Submit Type C information package to the FDA
- ✓ Obtain IRB approval with stipulations
- ❑ Pending - Sponsor and FDA approval for clinical trial. – ~4<sup>th</sup> QTR FY19

## FY19/CY20 Goal (new)

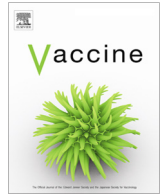
- ❑ Initiate Clinical Trail with FMP014/ALFQ with CHMI, ~late FY19/early FY20

## Comments/Challenges/Issues/Concerns

- ✓ Adjuvants, re-released Sept 2018 after requalification of methods
- ❑ Clinical Trial: delayed ~ 2 yrs due to invalidation of product release for cGMP ALF and ALFQ adjuvants.

## Budget Expenditure to Date

- ❑ Total Projected Expenditure: \$7,500,000.00
- ❑ HJF Total Budget \$2,537,483.00: Expended: \$2,220,001, Remaining: \$317,482
- ❑ Actual Expenditure to date : ~\$5,431,518.00
- ❑ ~\$1,751 M for clinical trial returned to CDMRP July 2017
- ❑ ~\$1.751 M transferred to WRAIR in MAR2019. FY19 2 year funds, expiring Sept 30, 2020.



# Safety, toxicity and immunogenicity of a malaria vaccine based on the circumsporozoite protein (FMP013) with the adjuvant army liposome formulation containing QS21 (ALFQ)

Alicia Cawlfeld<sup>a,1</sup>, Christopher J. Genito<sup>b,1</sup>, Zoltan Beck<sup>c,d</sup>, Elke S. Bergmann-Leitner<sup>e</sup>, Alexis A. Bitzer<sup>b</sup>, Kimberly Soto<sup>b</sup>, Xiaoyan Zou<sup>f</sup>, Sri H. Hadiwidjojo<sup>f</sup>, Robert V. Gerbasi<sup>f</sup>, Anna B. Mullins<sup>a</sup>, Amy Noe<sup>g</sup>, Norman C. Waters<sup>h</sup>, Carl R. Alving<sup>c</sup>, Gary R. Matyas<sup>c</sup>, Sheetij Dutta<sup>b,\*</sup>

<sup>a</sup> Department of Veterinary Medicine, Walter Reed Army Institute of Research, 503 Robert Grant Avenue, Silver Spring, MD 20910, USA

<sup>b</sup> Structural Vaccinology Laboratory, Walter Reed Army Institute of Research, 503 Robert Grant Avenue, Silver Spring, MD 20910, USA

<sup>c</sup> Military HIV Research Program, Walter Reed Army Institute of Research, 503 Robert Grant Avenue, Silver Spring, MD 20910, USA

<sup>d</sup> Henry M. Jackson Foundation for the Advancement of Military Medicine, 6720A Rockledge Drive, Bethesda, MD 20817, USA

<sup>e</sup> Flow-cytometric Center, Malaria Vaccine Branch, Walter Reed Army Institute of Research, 503 Robert Grant Avenue, Silver Spring, MD 20910, USA

<sup>f</sup> Malaria Department, Naval Medical Research Center, 503 Robert Grant Avenue, Silver Spring, MD 20910, USA

<sup>g</sup> Leidos Life Sciences, 5202 Presidents Court, Suite 110, Fredrick, MD 21703, USA

<sup>h</sup> Malaria Vaccine Branch, Walter Reed Army Institute of Research, 503 Robert Grant Avenue, Silver Spring, MD 20910, USA

## ARTICLE INFO

### Article history:

Received 3 September 2018

Received in revised form 16 May 2019

Accepted 20 May 2019

Available online 28 May 2019

### Keywords:

Malaria

Vaccine

Circumsporozoite protein

FMP013

ALFQ

Rhesus

## ABSTRACT

Antibodies to Circumsporozoite protein (CSP) confer protection against controlled human malaria infection (CHMI) caused by the parasite *Plasmodium falciparum*. Although CSP is highly immunogenic, it does not induce long lasting protection and efforts to improve CSP-specific immunological memory and duration of protection are underway. We have previously reported that the clinical grade CSP vaccine FMP013 was immunogenic and protective against malaria challenge in mice when combined with the Army Liposomal Formulation adjuvant containing immune modulators 3D-PHAD<sup>TM</sup> and QS21 (ALFQ). To move forward with clinical evaluation, we now report the safety, toxicity and immunogenicity of clinical grade FMP013 and ALFQ in Rhesus macaques. Three groups of Rhesus (n = 6) received half or full human dose of FMP013 + ALFQ on a 0-1-2 month schedule, which showed mild local site reactions with no hematologic derangements in red blood cell homeostasis, liver function or kidney function. Immunization induced a transient systemic inflammatory response, including elevated white blood cell counts, mild fever, and a few incidences of elevated creatine kinase, receding to normal range by day 7 post vaccination. Optimal immunogenicity in Rhesus was observed using a 1 mL ALFQ + 20 µg FMP013 dose. Doubling the FMP013 antigen dose to 40 µg had no effect while halving the ALFQ adjuvant dose to 0.5 mL lowered immunogenicity. Similar to data generated in mice, FMP013 + ALFQ induced serum antibodies that reacted to all regions of the CSP molecule and a Th1-biased cytokine response in Rhesus. Rhesus antibody response to FMP013 + ALFQ was found to be non-inferior to historical benchmarks including that of RTS,S + AS01 in humans. A four-dose GLP toxicity study in rabbits confirmed no local site reactions and transient systemic inflammation associated with ALFQ adjuvant administration. These safety and immunogenicity data support the clinical progression and testing of FMP013 + ALFQ in a CHMI trial in the near future.

© 2019 The Author(s). Published by Elsevier Ltd. This is an open access article under the CC BY license (<http://creativecommons.org/licenses/by/4.0/>).

## 1. Introduction

Malaria caused by the parasite *Plasmodium falciparum* kills hundreds of thousands of children annually, and emergence of

multi-drug-resistant strains indicates an urgent need for an efficacious vaccine for those living in endemic areas [1]. A vaccine is also needed by those who travel to malaria-endemic areas, such as tourists and troops. The most promising malaria vaccines to-date have targeted the circumsporozoite protein (CSP), present abundantly on the surface of the mosquito-transmissible sporozoite stage of the parasite. Antibodies against various regions of the CSP molecule have been associated with protection against malaria

\* Corresponding author.

E-mail address: [sheetij.dutta.civ@mail.mil](mailto:sheetij.dutta.civ@mail.mil) (S. Dutta).

<sup>1</sup> Both authors contributed equally.

challenge in mice and humans [2–5]. The first generation of CSP vaccines contained soluble protein or peptides combined with Aluminum-based adjuvants. Human trials with these first-generation CSP vaccines showed low levels of inconsistent protection against controlled human malaria infection (CHMI) [6] and naturally transmitted malaria [7]. A significant and reproducible improvement in efficacy was observed when a hepatitis B particle based CSP vaccine, RTS,S, was combined with a rationally designed molecular adjuvant, AS02 (GlaxoSmithKline Vaccines, Belgium) [8]. Oil-based AS02 has subsequently been replaced by a liposomal formulation (AS01) [9,10], though both adjuvant formulations contain two key immune-stimulators: monophosphoryl lipid A (MPLA), which is a potent TLR4 agonist derived from bacterial membrane, and QS21, a saponin extracted from the bark of *Quillaja saponaria*. QS-21 can activate the NOD-like receptor P3 (NLRP3) inflammasome complex present within the antigen presenting cell cytosol [11], resulting in a potent Th1-biased immune response. These two immune-modulators synergize to induce NK cells and CD8+T cells to produce a burst of IFN $\gamma$  in the draining lymph nodes [12]. Based on extensive Phase-3 trials in Africa, a pediatric formulation of RTS,S has been approved for Phase 4 trials in three African countries under the trade name Mosquirix<sup>®</sup> [13]. While the AS01 adjuvant was key to the success of RTS,S, AS01 was never combined with a soluble CSP in humans to determine if soluble immunogens could be as protective as RTS,S if adjuvanted with AS01. Soluble protein vaccines are relatively simple to scale-up and often more cost-effective to manufacture and stabilize for storage than particulate vaccines. Indeed, a soluble protein vaccine adjuvanted with AS01, “Shingrix”, was recently licensed by GlaxoSmithKline (GSK), showing >90% efficacy against herpes zoster virus in adults [14,15].

The CSP molecules on the parasite contain tetra-peptide repeating units (NANP) flanked by a conserved amino terminal region (N-term) and a polymorphic, cysteine-rich carboxy-terminal region (C-term). The RTS,S vaccine antigen does not contain the N-term sequence. While RTS,S confers sterile protection against the homologous 3D7 strain parasite in controlled infection, *i.e.* CHMI, the efficacy of RTS,S against diverse parasite populations in the field remains below 50% [4,13]. Protection against CHMI appears to be enhanced if the interval between boosts is increased and booster dose is decreased [16], but it remains to be seen if this delayed and fractional dose schedule will improve RTS,S mediated protection in the field. Another possible strategy to improve a vaccine is immune-broadening aimed at enhancing the immunogenicity of functional, but less dominant, protective epitopes. Several B- and T-cell epitopes that have been mapped to the N-term and C-term of CSP that are now being targeted for immune-broadening [5,17–19]. As a step in that direction, the Walter Reed Army Institute of Research (WRAIR) Malaria Vaccine Branch has produced a nearly full-length recombinant CSP vaccine: Falciparum Malaria Vaccine-013 (FMP013) [20]. FMP013 was expressed and purified from *E. coli* and contains the central repeat (19 NANP+3 NVDP), C-term and N-term regions of CSP. A cGMP lot of FMP013 was produced and has now met the purity and stability criteria for human vaccines [20]. FMP013 was tested in mice with a variety of available investigational and commercial adjuvants including a particle delivery platform [21]. Army liposomal formulation ALFQ, which contains QS21 along with a synthetic MPLA analog (3D-PHAD<sup>®</sup>, Avanti Polar Lipids) emerged as the most potent adjuvant for FMP013 [22,23]. In mice, three doses of 2.5  $\mu$ g FMP013 in 50  $\mu$ l ALFQ containing 20  $\mu$ g 3D PHAD<sup>™</sup> and 10  $\mu$ g QS21 induced high IgG antibody titers, high IgG2c antibodies that conferred sterile *in vivo* protection against transgenic *P. berghei* parasites expressing a functional copy of *P. falciparum* CSP. FMP013 + ALFQ also augmented the numbers of splenic germinal center-derived activated

B-cells, antibody secreting cells, CD4+T-cells and antigen-specific IFN- $\gamma$  producing cells [23].

While mouse models frequently are the first animal platform for early down-selection and detailed immunology of investigational vaccines, data from these models have not translated to development of human malaria vaccines. The Rhesus monkey (*Macaca mulatta*) model has repeatedly proven as a much better predictor of human responses. Most notably, the AS01 adjuvant was first found to be superior to AS02 in Rhesus and this was later confirmed in humans [9,10,24]. The Rhesus model also mirrored human immune responses against an adenovirus-RTS,S prime-boost vaccine [25,26] and an irradiated sporozoite vaccine [27]. Furthermore, the safety and toxicological data on the ASOX series of adjuvants was initially collected in Rhesus [24,28–31]. The Rhesus model has therefore remained on the critical path of down-selecting CSP vaccines in preclinical models at WRAIR.

Here we tested the safety and immunogenicity of FMP013 formulated with ALFQ in Rhesus monkeys. The 1 mL adjuvant dose containing 200  $\mu$ g 3D PHAD<sup>™</sup> and 100  $\mu$ g QS21 was at 10X the dose shown to be safe in mice [23]. GSK’s AS01 dose adjuvant (Shingrix<sup>™</sup> vaccine) contains 50  $\mu$ g QS21, hence ALFQ was also tested at half dose. FMP013 doses of 40  $\mu$ g and 20  $\mu$ g tested here was based on previous experience in Rhesus [32]. We report that FMP013 formulated in ALFQ was safe in the Rhesus model and a GLP toxicology study in rabbit model substantiated these findings. The immunogenicity of FMP013 met the go-criteria based on historical published data on RTS,S vaccine in humans. An investigational new drug (IND) application for a clinical trial of the FMP013 + ALFQ vaccine is being filed with the U.S. Food and Drug Administration based on these findings.

## 2. Methods

### 2.1. Ethics statement

Research was conducted under an IACUC-approved animal use protocol in an AAALACi accredited facility in compliance with the Animal Welfare Act and other federal statutes and regulations relating to animals and experiments involving animals and adheres to principles stated in the Guide for the Care and Use of Laboratory Animals, NRC Publication, 2011 edition.

### 2.2. Rhesus

Colony-bred adult rhesus macaques of Indian origin (*Macaca mulatta*), were housed at the WRAIR animal facility and used under the IACUC-approved protocol number 16-MVD-25L. Macaques were naïve and had never been used in an experimental study. All animals were quarantined for a period of 4 weeks and free from any overt clinical signs of illness and deemed to be in good health, testing negative for Macacine herpesvirus 1, measles, Simian Retrovirus, Simian Immunodeficiency Virus, Simian T-cell Leukemia Virus and tuberculin skin test. Animals were pair-housed in a controlled environment as previously described [32], in accordance with WRAIR Veterinary Service Programs standard operating procedures.

### 2.3. Rhesus vaccination

Three groups of 6 Rhesus macaques were given FMP013 and ALFQ corresponding to proposed human doses, according to Table 1. Sample size of n = 6 was determined to give a statistical power of 0.84 to discern >2-fold difference in serum antibody titer using an online power calculator (<http://www.stat.uiowa.edu/>

**Table 1**  
Rhesus vaccine antigen and adjuvant dose by group.

Groups	Dose 1	Dose 2	Dose 3
LO Ag	20 µg CSP	20 µg CSP	20 µg CSP
LO Adj	0.5 mL ALFQ	0.5 mL ALFQ	0.5 mL ALFQ
LO Ag	20 µg CSP	20 µg CSP	20 µg CSP
HI Adj	1 mL ALFQ	1 mL ALFQ	1 mL ALFQ
HI Ag	40 µg CSP	40 µg CSP	40 µg CSP
HI Adj	1 mL ALFQ	1 mL ALFQ	1 mL ALFQ

~rlength/Power). Vials of lyophilized cGMP grade FMP013 were suspended in 0.4 mL sterile water and brought up to 2X desired concentration with PBS, then combined with an equal volume of cGMP grade ALFQ (Table 1). The formulation was rolled on a rotary platform for 1 h ± 20 m before administration. Macaques were anesthetized with Ketamine HCl at 5–10 mg/kg in combination with acepromazine at 0.05–0.1 mg/kg. A small patch was shaved and vaccines were administered intramuscularly (IM) in the outer thigh muscle. Injection sites were alternated between right and left thigh for each administration day. Rhesus macaques were bled 2 weeks prior to the first dose and at 2 weeks after each vaccination for serology.

#### 2.4. Rhesus safety and tolerability assessment

Animals were examined on days 0, 1, 3, and 7 after each immunization. Fever cutoff was set at any temperature exceeding two times the standard deviation above the 6-month average rectal temperature for each individual animal. We inspected the injection site at each time point for skin warmth, erythema, swelling, muscle induration, ulceration, abscess, or any other abnormalities around the vaccine site. The grading scales for local skin reactions were: 0, absent; 1, mild; 2, moderate; 3, severe [24]. Two ml of blood was collected from the femoral vein for complete blood count (CBC) and serum chemistry at each time point (assessed parameters are listed in the supplement).

#### 2.5. ELISA

Direct and avidity ELISA were performed by the International Malaria Serology Reference Center (WRAIR, Silver Spring, MD) against the full-length CSP, (NANP)<sub>6</sub> peptide or a C-term CSP peptide (PF16; [33]) exactly as described by Regules et al. [16]. As a result the secondary antibody used for the Rhesus ELISA was heterologous, HRP-conjugated anti-human IgG (Southern Biotech, Birmingham, AL). For a region-specific ELISA, the protocols were similar to above except the plates were coated with GST fusion proteins representing the N-term, repeat or C-term of CSP. Rabbit ELISA required the use of anti-rabbit IgG H + L secondary antibody (Southern Biotech, Birmingham, AL). ELISA titer was defined as the serum dilution that resulted in optical density (OD) of 1.0 as predicted by a 4-parameter curve fitting equation (Biotek, Winooski, VT). Avidity ELISA was conducted with nearly full-length FMP013 (FL) as reported previously [16].

#### 2.6. IgG purification

Protein G (Thermo Fisher Scientific Waltham, MA) was used for IgG purification using 3 mL serum from 1 monkey in each group. Purified IgG was dialyzed against PBS, concentrated using Amicon<sup>®</sup> Centrifugal Filter Units (Millipore Sigma), and quantified by optical density measurement at 280 nm.

#### 2.7. Inhibition of liver stage development assay (ILSDA)

Purified rhesus IgG was tested by ILSDA [34]. Briefly, the NF54 strain of *Plasmodium falciparum* (Pf) sporozoites obtained from salivary gland dissections of infected *Anopheles* mosquitoes were mixed with a positive control monoclonal antibody NFS1 or polyclonal Rhesus IgG at a final concentration of 160 µg/ml and incubated at room temperature for 20 min. The sporozoite-antibody mixtures were then introduced into the wells containing cryopreserved human hepatocytes (BioIVT, Baltimore, MD) and incubated at 37 °C for 3 h to allow sporozoites to infect hepatocytes, washed to remove non-invaded sporozoites, and incubated at 37 °C for 96 h. Pf 18 s rRNA levels were quantified to determine the level of inhibition of liver stage development by quantitative real-time PCR (qRT-PCR) analysis.

#### 2.8. IL-2/IFN $\gamma$ Fluorospot assay

Antigen-specific interferon (IFN)- $\gamma$  and interleukin 2 (IL-2) cytokine-secreting T cells were measured by Fluorospot (Ucytech Biosciences, Utrecht, Netherlands) following the manufacturer's instructions. Monkey anti-CD3 mAb (Mabtech Inc., Cincinnati, OH) was used as an internal positive control. Each well was treated with 25 µl CD28 and CD49d (BD Biosciences, San Diego, CA) cell stimulants, 25 µl of antigen and 50 µl of cells ( $2.5 \times 10^5$ /well). Plates were incubated at 37 °C, 5% CO<sub>2</sub>, 100% humidity for 40–48 h. Fluorospot plates were analyzed using the Autoimmun Diagnostica (AID) GmbH Fluorospot reader (Strassberg, Germany) equipped with filters for FITC (excitation 490 nm/emission 510 nm) and Cy3 (excitation 550 nm/emission 570 nm).

#### 2.9. Mesoscale cytokine analysis

PBMC (pre-immune and 4wp3) were thawed and stimulated for 48 h with CSP peptide pools (1 µg/mL) or Fl CSP (5 µg/mL). The cytokine in the culture supernatants were measured using the Meso Scale Discovery 10-plex NHP pro-inflammatory panel kit to quantitate the amounts of IL-2, IFN- $\gamma$ , IL-12/IL-23p40 (Th1); IL-4, IL-5 (Th2); TNF- $\alpha$ , IL-1 $\beta$ , IL-6, IL-8 (pro-inflammatory), and IL-10 (immunomodulatory) according to the manufacturer's protocol. Plates were read using a MESO QuickPlex SQ120 (Meso Scale Diagnostics, Rockville, MD).

#### 2.10. Rabbit toxicology

The repeat dose rabbit toxicity study of FMP013 vaccine (Lot#1891) and ALFQ adjuvant (Lot#1974) was conducted at SNBL USA, Ltd. (Everett, WA) according to Good Laboratory Practice regulations (GLP). New Zealand White rabbits aged 13–16 weeks (Charles River Laboratories) were randomized to four groups in a weight-stratified manner to achieve similar dosing group body weight distributions (Table 2) and acclimated for 14 days. Lyophilized FMP013 was reconstituted with sterile water for injection and diluted to 40 µg/mL with either saline or ALFQ, mixed at medium speed on a bottle roller for 1 h at room temperature and used

**Table 2**  
Rabbit vaccine antigen and adjuvant dose by group.

Groups	Dose 1	Dose 2	Dose 3	Dose 4
1	Saline	Saline	Saline	Saline
2	1 mL ALFQ	1 mL ALFQ	1 mL ALFQ	1 mL ALFQ
3	40 µg CSP	40 µg CSP	40 µg CSP	40 µg CSP
4	40 µg CSP	40 µg CSP	40 µg CSP	40 µg CSP
	1 mL ALFQ	1 mL ALFQ	1 mL ALFQ	1 mL ALFQ

**Table 3**  
Rabbit bleed schedule.

Study Day	0	1	3	8	14	27	28	40	41	42	43	45	51	56	70
Vaccination	X				X		X			X					
Chemistry and count	X	X	X					X			X	X			X
C-reactive protein	X		X	X					X			X	X		X
Serology						X				X				X	X
Necropsy												X			X

within 3 h. Four groups of 10 male and 10 female rabbits were dosed IM on study days 0, 14, 28, and 42 (Table 2) alternating between right and left quadriceps for each administration day. Samples of each administered formulation were tested by SDS-PAGE for homogeneity, compatibility and stability assessments.

### 2.11. Rabbit toxicology readouts

For each animal, clinical observations were performed twice daily beginning on the second day of acclimation, with additional clinical observations performed on dosing days (1 h post dose administration). Dermal draize scoring of injection sites was performed prior to each dose administration and at 3 and 24 h post dose administration. Body temperature was assessed twice during acclimation and on dosing days at the following time points: pre-dose, 4 h post dose, and 24 h post dose. Body weight was assessed twice during acclimation, on study days 0 (pre-dose) and 3, and then weekly thereafter. Food consumption was estimated daily. Ophthalmological evaluations were performed during acclimation and during the week prior to necropsy. Blood collections for hematology were performed according to the schedule in Table 3. A terminal necropsy was performed with half of the animals in each group (5 males and 5 females) on study day 45 and a recovery necropsy was performed with the remaining animals on study day 70. Macroscopic examination was performed at necropsy. Organs were weighed and relative weights calculated as percentages of final body weight and brain weight. For histology, tissues were collected, fixed, processed and stained, and examined microscopically.

### 2.12. Protein analysis

Reconstituted vials of FMP013 + ALFQ were frozen following rabbit vaccination and analyzed for homogeneity and integrity. A 10  $\mu$ l aliquot was applied on to a 4–12% acrylamide gel and analyzed by electrophoresis and silver staining.

### 2.13. Statistical analysis

Rhesus immunological data was analyzed as the mean group value for each parameter. ELISA titers were log transformed and analyzed by ANOVA with Tukey's correction (GraphPad Prism software, La Jolla, CA). Rabbit toxicology was analyzed using Provantis software (InStem, Philadelphia, PA). Briefly, homogeneity of variance was assessed using Bartlett's test on both raw and log-transformed data, followed by a Kruskal-Wallis's H test and Dunn's modification to Steel's test if the results were significant. If the Bartlett's test was not statistically significant, a one way analysis of variance (ANOVA) was applied, followed by a Dunnett's test to determine significant differences between the saline control and each test group. Statistical significance is indicated on figures: \* ( $p < 0.05$ ), \*\* ( $p < 0.01$ ), \*\*\* ( $p < 0.001$ ) or \*\*\*\* ( $p < 0.0001$ ).

## 3. Results

### 3.1. Safety and reactogenicity in Rhesus

As indicated in Table 1, Rhesus macaques ( $n = 6$ ) were assigned to the following 3 groups based on low (LO) or high (HI) antigen and adjuvant dose (Ag and Adj, respectively): LO Ag + LO Adj, LO Ag + HI Adj and HI Ag + HI Adj. The vaccinated animals were closely monitored for adverse events during the study. No major vaccine-related effects on body weight or food consumption were observed during the entire course of the study. Local reactions at the vaccine site were scored on a 0–3 scale and a mean score was calculated for each group (Fig. 1A). Compared to the 0.5 mL ALFQ dose group (LO Ag + LO Adj; blue bars), the local reactions such as skin warmth, erythema, muscle swelling and muscle induration were more commonly associated with 1 mL adjuvant groups (red and green bars in Fig. 1A). No apparent wounds, ulcers or abscesses were noted and local reactions were considered mild and self-resolving by day 7 post vaccination. Two macaques in the HI Ag + HI Adj group developed an ecchymosis skin reaction around the vaccine site on day 3 post dose 2, which cleared by day 7. Anesthetized animals before vaccinations showed a baseline body temperature between 101.6 and 104.5°F. Out of 54 vaccinations, we recorded 26 episodes of fever (Fig. 1B); five episodes were  $>104^\circ\text{F}$ , though none exceeded 104.5°F, and all fevers spontaneously resolved by day 7 post vaccination. The LO Ag + HI Adj group had the most frequent fever events overall, most notably post 1st and 2nd vaccinations (red bars, Fig. 1B).

Blood was collected on days 1, 3 and 7 after each vaccination and toxicological changes were recorded. Supplementary data shows plots of group means for data on blood chemistry (Fig S1, S2 and S3) and blood cell count parameters (Fig S4, S5, S6), as well as the upper/lower limit and average baseline values for each parameter. Numerical values (mean  $\pm$  SD) are shown in Table S1–S3. Specifically, we saw no significant elevations in key biochemical and enzymatic markers of liver or kidney toxicity following FMP013 + ALFQ vaccinations. Increased creatine kinase (CK) on day 1 and 3 after vaccination was observed and the impact was highest in the HI Ag + HI Adj group (Fig. 2A and Fig. S1–3). Elevation of CK in any group did not reach statistical significance over baseline due to a wide range and several high CK values that were observed before the 1st vaccination; nevertheless, most macaques showed CK values returning to normal by day 7 post vaccination (Fig. 2A and Fig. S1–3). Hematological cell count revealed a normal RBC count, hemoglobin and hematocrit level in all groups throughout the study (Fig. 2B and Fig. S4–6). In contrast, a significant increase in WBCs, neutrophils and monocytes was attributed to the vaccine, most frequently seen on day 1 post 1st and 2nd vaccine (Fig. 2C–E, Fig. S4–6). Likewise, a trend of transient increase in platelet counts was observed on day 7 post each vaccination in all groups (Fig. 2F and Fig S6). A sporadic and transient increase in eosinophils was observed both before and during the vaccination period, most likely due to a prior whipworm (gastrointestinal parasite) infection that was treated a week before the study began (Fig S4–6). All blood cell count elevations that were statistically



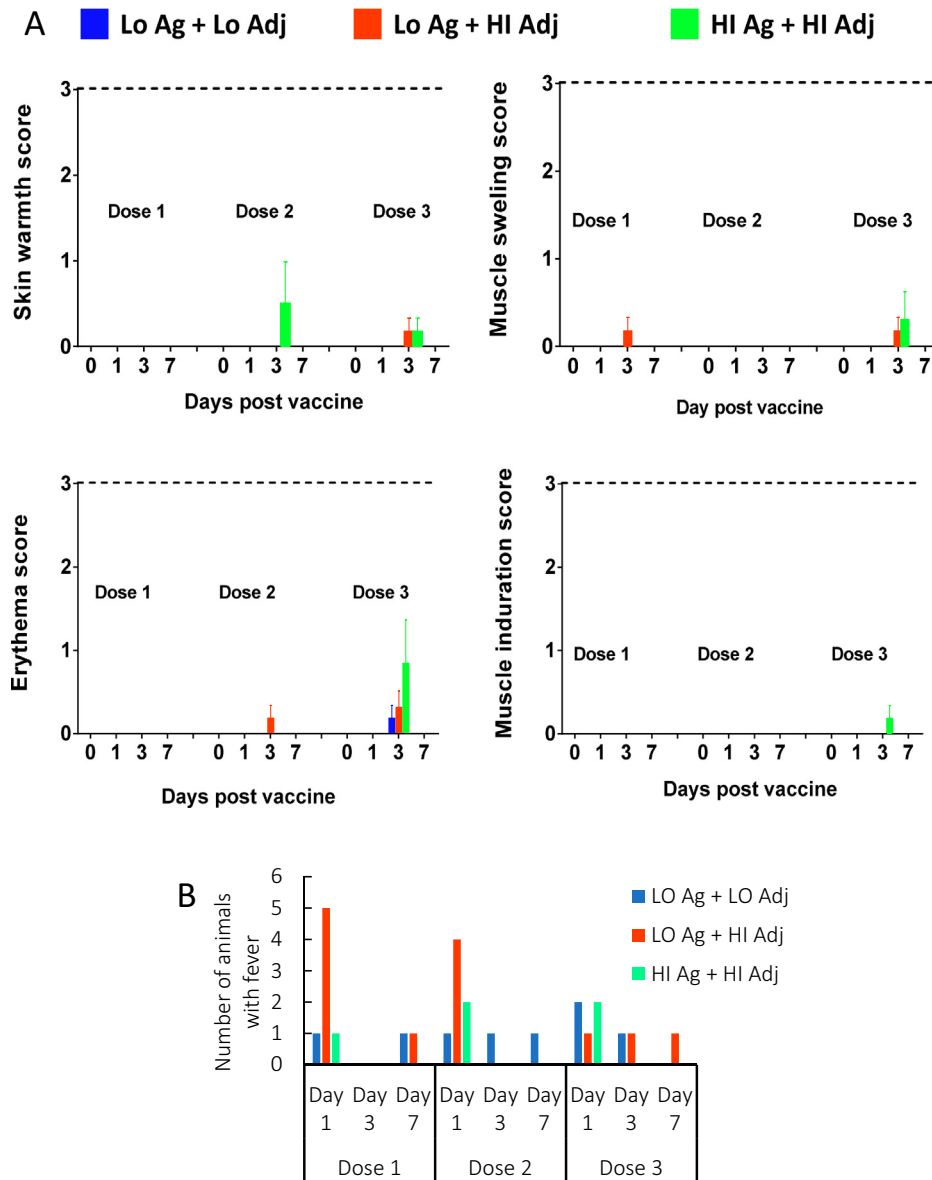


**Fig. 1.** Local reactions and fevers in Rhesus macaques vaccinated with FMP013 + ALFQ. (A) Group local adverse events score (Mean + SEM for  $n = 6$ ); dotted line represents max possible score. Bars were omitted if no reaction was observed. No group mean score was significantly above 0, as determined by a one-tailed one sample  $t$ -test. (B) Number of macaques that developed a fever on day 1, 3, and 7 after each of 3 doses.

significant and vaccine related (WBC, neutrophils, monocytes and platelets) returned to normal before the next vaccination time-point. Having observed only mild and transient reactions and no serious safety signals, we concluded that both the high and low dose FMP013 + ALFQ vaccines were safe and well-tolerated in the Rhesus model.

### 3.2. Immunogenicity and fine specificity

Serum was collected two weeks after each dose and antibody acquisition against FL (full-length CSP), C-term and NANP repeat antigens was determined by ELISA (Fig. 3A, B, C respectively). All monkeys seroconverted after the 1st vaccination and subsequent vaccinations boosted titers. FL and C-term antibody profiles were similar, but the repeat NANP ELISA revealed suboptimal boosting after 2nd and 3rd vaccination with 0.5 mL ALFQ (Fig. 3C, blue line). Overall, the 20  $\mu$ g FMP013 + 1 mL ALFQ dose (LO Ag + HI Adj) showed the best antibody acquisition profile over 3 vaccina-

tions (Fig. 3A, B, C, red lines). Group antibody titers were statistically analyzed at 2 weeks post 3rd vaccination (Fig. 3D, E, F). The 0.5 mL ALFQ group showed a trend towards lower mean FL, NANP and C-term responses compared to the 1 mL ALFQ groups, although this effect was not statistically significant (Fig. 3D, E, F; blue bars). Differences in antibody responses were not significant between 20  $\mu$ g and 40  $\mu$ g FMP013 doses with 1 mL adjuvant (red vs. green bars), although the 20  $\mu$ g antigen dose appeared to perform slightly better. Since FMP013 antigen contains the N-term, repeat and C-term of CSP, we next mapped region-specific ELISA titers using GST fusion proteins representing the N-term, repeat or C-term regions of CSP. Antibodies to all three regions of CSP were induced by FMP013 + ALFQ, with the highest numerical titers observed against the C-term region and lowest titers against the N-term region (Fig. 3G). Antibody avidity measured by urea wash against the FL antigen showed no difference between groups (Fig. 3H). In addition to potent antibody response against the repeat region, FMP013 induced a

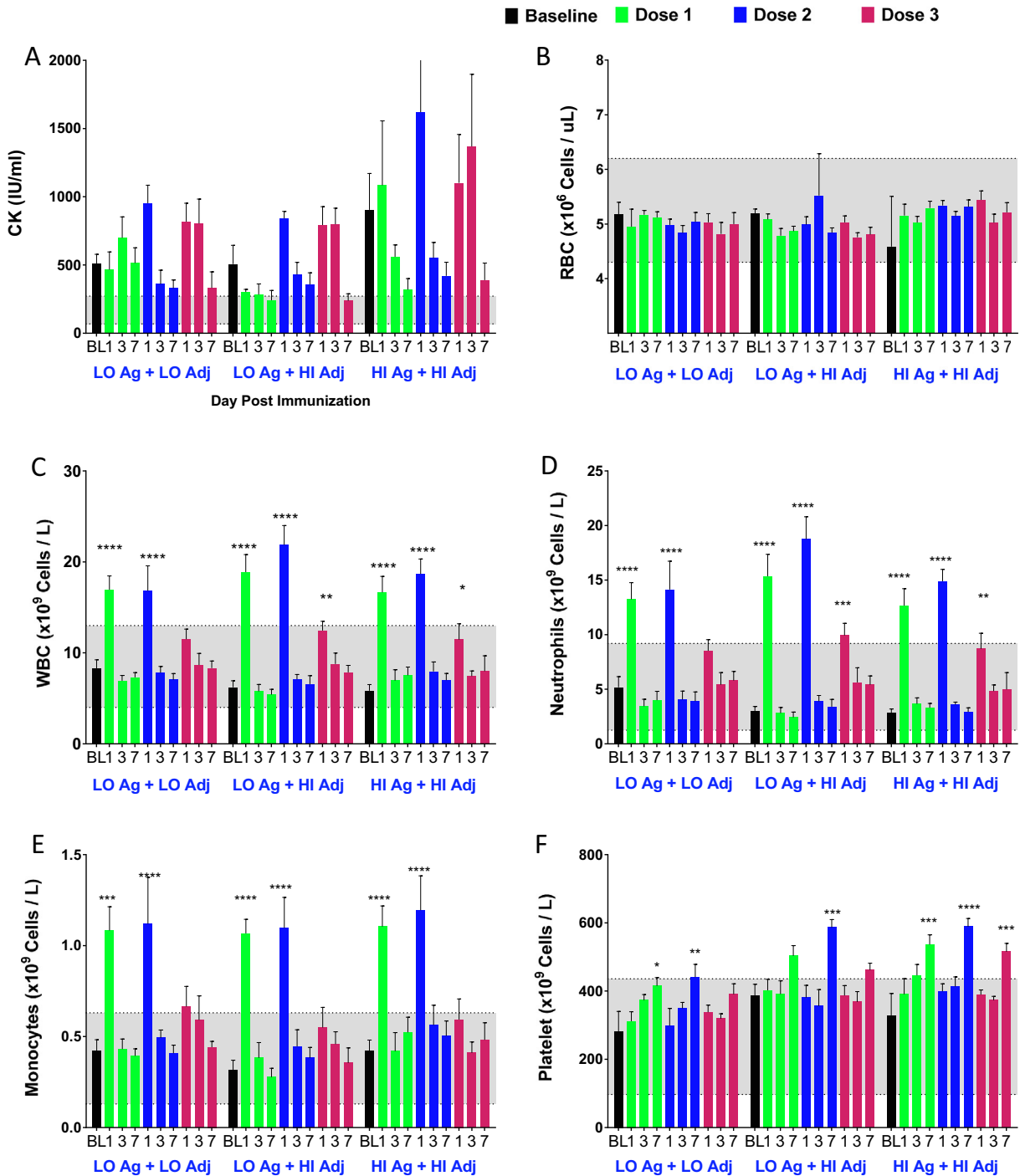


**Fig. 2.** Blood chemistry and complete blood count changes for Rhesus macaques vaccinated with FMP013 + ALFQ. Group Mean + SEM (n = 6) (A) creatine kinase levels, (B) red blood cell count, (C) WBC, (D) neutrophil, (E) monocyte and (F) platelet cell counts on days 1, 3, and 7 after each of 3 vaccinations (green, blue, and red bars in sequential order). Mean baseline (BL) for each group and reference range (shaded area) are shown. Significance above baseline was determined using ANOVA and Dunnett's correction for multiple comparisons.

broad range of anti-CSP responses, against C-term and N-term epitopes.

### 3.3. Comparison to historical immunogenicity data

We showed previously that Rhesus macaques (n = 5) vaccinated with 25 µg FMP013 in 0.5 mL Aluminum Hydroxide (containing 0.15 mg Al<sup>3+</sup>) or 25 µg FMP013 covalently linked to a Qβ phage particle in 0.5 mL Aluminum Hydroxide produced antibody responses

against the NANP repeat antigen [32]. We were able to compare the NANP titers from this past study to the present study, since both data were obtained by the International Malaria Serology Reference Center using a standardized ELISA protocol (Fig. 3F, grey bars). Mean NANP titer of the LO Ag + HI Adj and HI Ag + HI Adj groups were statistically superior (>3-fold) to FMP013 in Alum or FMP013 linked to Qβ particles. In another study, Regules *et al.* reported titers for RTS,S + AS01 vaccinated humans (standard dose at 0–1–2 month interval) as part of the MAL071 clinical study [16].

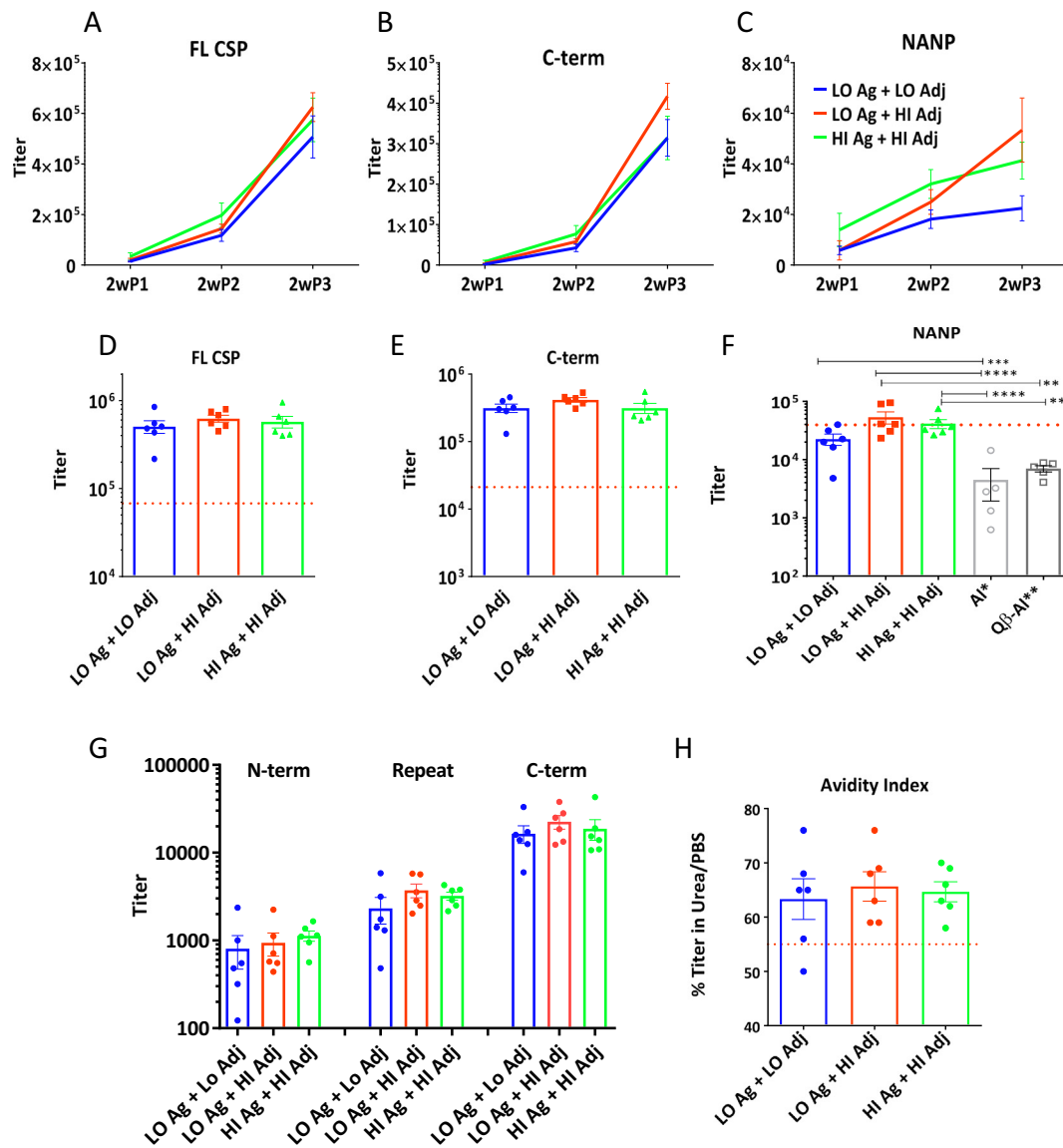


**Fig. 3.** Antibody profile induced by FMP013 + ALFQ vaccination of Rhesus macaques. Kinetics of antibody acquisition are shown ELISA titer (OD = 1) against (A) FL CSP, (B) C-term or (C) NANP plate antigen 2 weeks after each vaccine dose. (D–F) Comparison of ELISA titer at 2 weeks post 3rd vaccination. (G) ELISA titers against the N-term, Repeat and C-term regions of CSP measured using GST fusion coat antigens. (H) Antibody avidity index at 2 weeks post 3rd vaccination. AI\* and Q $\beta$ -AI\*\* NANP titers (F) refer to historical data obtained from macaques receiving FMP013 vaccine adjuvanted in Aluminium hydroxide or vaccinated with FMP013 conjugated to Q $\beta$  phage and formulated in Aluminium hydroxide. Red dotted lines represent historical mean ELISA titer or avidity against RTS,S + AS01 in humans reported by Regules *et al.* Statistical significance was determined by ANOVA and Tukey's correction for multiple comparisons. Bars represent group mean  $\pm$  SEM (n = 6).

Since identical human ELISA protocols were used in both studies, it was encouraging to note that the mean FL titers, C-term titers and antibody avidity of FMP013 + ALFQ in Rhesus were numerically greater than RTS,S + AS01 in humans, with comparable NANP titers (red dotted lines in Fig. 3D, E, F, H). A major caveat of this observation is that direct numerical comparisons of ELISA titers may be confounded by differences in the cross-reactivity of secondary anti-human antibodies to Rhesus immunoglobulin.

### 3.4. Functional activity

While FMP013 + ALFQ induces protective immunity in mice [23], there are no transgenic parasites available to challenge Rhesus monkeys vaccinated with *P. falciparum* CSP vaccines. Alternatively, IgG from 3 monkeys (one from each group) was purified and tested in an inhibition of sporozoite development assay (ILSDA) using *P. falciparum* sporozoites and primary human hepa-

cytes [34]. The assay was performed at  $\sim$ 1:75 dilution of whole serum, considering Rhesus monkeys have  $\sim$ 12 mg IgG per ml serum [35]. The assay was repeated 3 times to account for variability in the quality of primary human hepatocytes, the quality of sporozoite isolation and non-specific inhibition by pre-immune IgG. IgG from one animal in the LO Ag + HI Adj group animal showed  $\sim$ 2 log reduction in mean parasite 18 s rRNA burden that was significantly higher than pre-immune serum inhibition (Fig. 4A, shaded bar). An ELISA revealed that the relative NANP titer of this inhibitory IgG sample was about 2-fold higher than the non-inhibitory samples (Fig. 4B).

### 3.5. T-cell responses

PBMCs collected at 4 weeks post 3rd vaccination were stimulated by a pool of overlapping CSP peptides (Megapool) or the nearly full-length FMP013 protein (FL-CSP). The frequency of

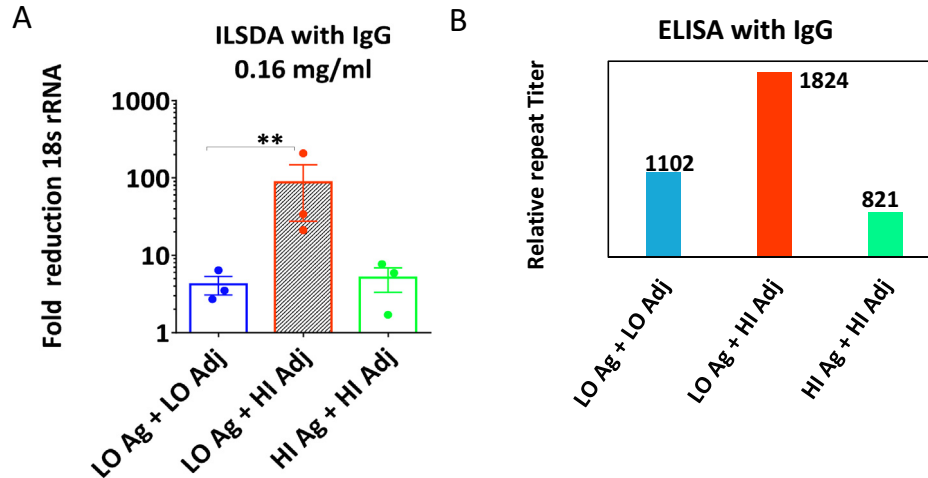


**Fig. 4.** (A) Functionality of purified Rhesus IgG assessed in an inhibition of liver stage development (ILSDA) assay, measured by fold reduction in *P. falciparum* sporozoite 18 s RNA using 0.16 mg/ml total IgG purified from one animal in each group (~1:75 dilution of whole serum). This assay was performed in triplicate in three independent experiments. Shaded bar represents significantly higher inhibition activity than pre-immune serum (B) Relative NANP titer obtained from ELISA of the purified IgG used in (A).

CSP-specific cytokine producing cells was then determined by Fluorospot. Significant IL-2 and IFN- $\gamma$  producing cells were detected, though IFN- $\gamma$  responses failed to achieve statistical significance over baseline pre-immune PBMCs (Fig. 5). No antigen or adjuvant dose effects were observed between groups. A Th1-biased T-cell response was further confirmed in vaccinated Rhesus by a 10-plex MesoScale assay (Fig. S7). Cytokine analysis shows a predominant TH1 profile (IL-2, TNF- $\alpha$ , IL-12/23p40) with some contribution by IL-5 (TH2, mediating antibody responses) and IL-6 (pro-inflammatory, supporting B cell responses). The IL-2 responses were highest in the HI/HI group regardless of the in vitro stimulation (FL-CSP vs. CSP peptides (Fig. S7)).

### 3.6. Rabbit toxicology

To supplement safety data from the Rhesus trial, FMP013 and ALFQ were tested in four groups of 10 male and 10 female New Zealand White rabbits according to Table 2. Whole blood and serum samples were collected for toxicology readouts following the bleed schedules shown in Table 3. Following four doses of 40  $\mu$ g FMP013 + 1 mL ALFQ administered at 2 week intervals, no injection site reactions, no change in body weight, no temperature elevation and no reduction in food consumption was noted. On day 1 after the 1st and 4th vaccine, a statistically significant increase in mean neutrophil counts was observed for ALFQ and FMP013 + ALFQ but not in saline and FMP013 groups (Fig. S8A), returning

to normal levels at subsequent assessment time point. Coagulation assessment showed ALFQ administration caused elevated fibrinogen on day 1 and day 3 post vaccination in ALFQ and FMP013 + ALFQ groups, also returning to normal at the subsequent assessment time point (Fig. S8B). A broad range of CRP concentrations were found in the rabbits, including moderately high values observed during the acclimation period prior to 1st vaccination. CRP concentrations trended higher on day 3 post 1st and 4th vaccine in ALFQ or FMP013 + ALFQ groups (Fig. S8C). One animal in the FMP013 alone group also demonstrated higher than normal CRP at 28 days post 4th vaccination; however similar elevations were observed during acclimation period.

Results of terminal procedures and pathology demonstrated no abnormal observations or differences between groups by gross pathology or organ weight. At terminal necropsy (study day 45), histological assessments of the injection sites demonstrated increased incidence and severity of subcutaneous or muscular inflammatory cell infiltration in ALFQ and FMP013 + ALFQ groups. At recovery necropsy (study day 70), most of these findings had resolved and thus considered reversible. A few animals in the saline and FMP013 alone groups also demonstrated some inflammatory cell infiltration at injection sites during the terminal necropsy, though no animals in either group demonstrated such findings during the recovery necropsy. Based on the evaluated parameters, results of the repeat dose rabbit toxicity study demonstrated that intramuscular administration of FMP013 alone

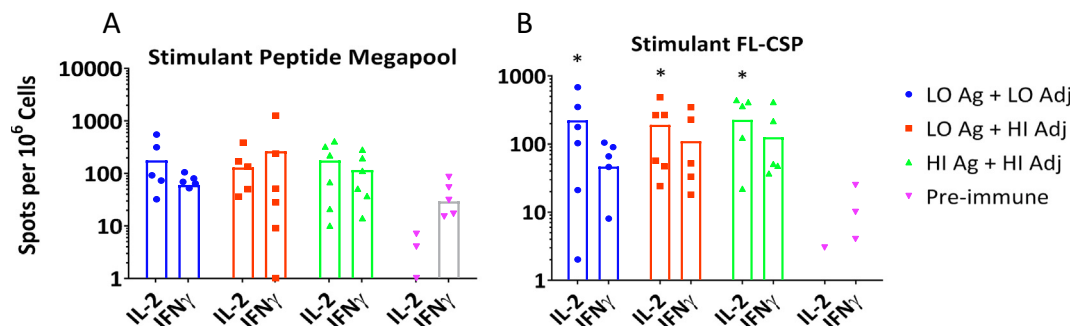


**Fig. 5.** T-cell response induced by FMP013 + ALFQ vaccination of Rhesus macaques. T-cell response determined by IL-2 and IFN- $\gamma$  Fluorospot at 4 weeks post 3rd vaccination. Rhesus PBMCs were stimulated with either (A) a peptide pool spanning the full length CSP sequence or (B) FL CSP vaccine antigen. Bars represent mean + SEM spots formed per million cells (n = 6). Cellular responses significantly above pre-immune baseline are shown using ANOVA and Dunnett's correction for multiple comparisons.

or in combination with ALFQ was well tolerated by study animals without any adverse effects.

### 3.7. Rabbit immunogenicity and stability of the formulation

Sera from male and female rabbits ( $n = 10$ ) were pooled separately and analyzed for seroconversion (Fig. S9). No antibodies were detected in saline and ALFQ groups; FMP013 alone was minimally immunogenic ( $\sim 1000$  endpoint titer) but FMP013 + ALFQ showed about one log higher titers and boosting post 2nd and 3rd vaccination. FMP013 antigen analyzed by SDS-PAGE after formulation in ALFQ migrated as a single band on silver stained gel, confirming that the antigen did not breakdown or aggregate after the 4 h storage at room temperature during vaccination of rabbits (Fig. S10). Overall, the observations of FMP013 + ALFQ obtained from study in rabbits correlate the safety and immunogenicity data from Rhesus macaques. Combined, these outcomes support FMP013 + ALFQ proceeding to clinical trial.

## 4. Discussion

Vaccination of Rhesus macaques with FMP013 + ALFQ did not induce ulceration or abscesses at the vaccine site, with only transient local reactions notable, particularly in the groups receiving 1 mL of ALFQ. This included an episode of ecchymosis observed at the vaccine site in two macaques at day 3 post 2nd vaccination. Ecchymosis is an acute inflammatory response that could be elicited by immune-modulators in ALFQ, though ecchymosis can often result from needle injury during vaccination. We believe that latter was the case because 1 mL ALFQ containing vaccines have been administered in multiple studies more than 100 times in Rhesus of Indian and Chinese origin (including this study) with no recurrence of vaccine site ecchymosis (unpublished data). Additionally, no ecchymosis reaction or any other local reaction was observed in rabbits after four 1 mL administrations of the vaccine. In our studies, administration of 1 mL ALFQ caused only mild and transient local reactions that are not uncommon for vaccines currently approved for use in adults and infants.

Transient elevation of white blood cell counts (WBC), particularly neutrophil counts, was observed in both Rhesus and rabbit models. A similar elevation of WBC has been reported for other adjuvants, including AS01 in Rhesus [36–38]. We also report a trend towards increased platelet counts in Rhesus. While increased platelet counts could suggest mild hemotoxicity or an inflammatory response to the vaccine, this observation was almost exclusively noted at the last scheduled phlebotomy after each vaccination (day 7), suggesting that this could be due to multiple phlebotomies within a short time period. Regardless of the cause, the platelet count abnormalities resolved before the next vaccination time-point and, most importantly, the hematocrit, RBC count, and hemoglobin remained stable in all studied macaques and rabbits. The current dataset further confirms that the unique cholesterol and lipid ratio of ALFQ reduces RBC lysis caused by free QS-21, as has previously been shown [39]. Eosinophil levels were higher than normal after vaccination in some of the macaques both before and during the vaccination period. Eosinophil elevation is a marker of hypersensitivity and its elevation could be associated with a previously treated parasitic worm infection in the colony. Overall, the cellular changes in blood observed after FMP013 + ALFQ administration in Rhesus and rabbits were transient and they normalized prior to the next vaccination time-point. Elevation of cellular markers of inflammation is caused by a robust innate immune response to vaccination which may lead to a strong adaptive response required for protective immunity against malaria [40].

No evidence of gross toxicity with respect to elevation in liver enzymes or kidney function panel was apparent following FMP013 + ALFQ administration in rabbits and Rhesus. The levels of fibrinogen and CRP were transiently elevated in rabbits after ALFQ administration, both of which are acute-phase proteins that elevate during systemic inflammation [41]. ALFQ administration caused CK elevation and transient fevers in Rhesus, both of which are markers of tissue damage and have been also reported to elevate following AS01 administration in Rhesus [24,30]. Overall, a transient systemic inflammation was confirmed by cellular and biochemical excursions in both Rhesus and rabbits, most likely linked to the potent immune-modulators 3D-PHAD<sup>®</sup> or QS21 in ALFQ.

The 20  $\mu\text{g}$  FMP013 + 1 mL ALFQ dose (containing 200  $\mu\text{g}$  3D-PHAD<sup>®</sup> + 100  $\mu\text{g}$  QS21) showed the best immunogenicity and functional antibody profile that was also superior to previously reported immunogenicity of FMP013 in Aluminum Hydroxide and as a Q $\beta$  particle conjugate [32]. We also show numerical non-inferiority of 20  $\mu\text{g}$  FMP013 + 1 mL ALFQ induced titers in Rhesus to the historical RTS,S + AS01B induced titers in humans [16]. The 0.5 mL AS01B volume contains 50  $\mu\text{g}$  MPLA and 50  $\mu\text{g}$  QS21 which has been safely administered to adults and children in RTS,S and Shingrix<sup>™</sup> vaccine trials [14] and MPLA dose up to 200  $\mu\text{g}$  has been safely tested in humans [42]. The safety data obtained from two animal models with a relatively high dose of immune-modulators in ALFQ reaffirms our hypothesis that using a specific lipid and cholesterol ratio in ALFQ can reduce QS21-mediated cell lysis [39] and other toxic adverse effects. With only minor and transient adverse effects observed in Rhesus and rabbits, we proposed that 20  $\mu\text{g}$  FMP013 + 1 mL ALFQ be the full-human dose of this vaccine.

Rhesus data confirm previous mouse data that high titers of antibodies could be induced by FMP013 + ALFQ vaccine [23]. We also showed previously that soluble FMP013 conjugated to virus-like particle Q $\beta$  specifically enhanced the NANP repeat responses [32, 21]. Here, soluble FMP013 + ALFQ induced high repeat and C-term responses along with measurable N-term responses. Epitopes outside of the repeat region of CSP may be important to induce protection. The C-term appears to have a protective role in RTS,S field trials in humans [4] and monoclonal antibodies against a protease cleavage site [5] and a junctional epitope [43] in the N-term have protected mice. Since the N-term is absent in RTS,S, the epitope broadening reported using nearly full-length soluble FMP013 may augment the degree and longevity of protection. Furthermore, cost-effectiveness of manufacturing and stability of soluble proteins could be critical for disease elimination efforts against malaria. Regulatory approvals are being sought for the conduct of a CHMI trial with FMP013 + ALFQ in the near future.

## Acknowledgements

We thank COL Viseth Ngauy, WRAIR, for comments on the manuscript. We thank Lisa Dlugosz and Tanisha Robinson for Rhesus sample processing and data collection. We thank Dawn Wolf and Marcia Caputo for their diligent work with Rhesus handling and sample collection. We thank Lorraine Soisson and Carter Diggs, USAID, for their advice on trial design.

## Disclaimer

Material has been reviewed by the Walter Reed Army Institute of Research and the US Agency for International Development. There is no objection to its presentation and/or publication. The opinions or assertions contained herein are the private views of the author, and are not to be construed as official, or as reflecting

true views of the Department of the Army, the Department of Defense, or the US Agency for International Development.

### Ethics approval

Research was conducted under an approved animal use protocol in an AAALACi accredited facility in compliance with the Animal Welfare Act and other federal statutes and regulations relating to animals and experiments involving animals and adheres to principles stated in the Guide for the Care and Use of Laboratory Animals, NRC Publication, 2011 edition.

### Funding

The funding for this work was provided by the USAID Malaria Vaccine Development Program and the Department of the Army. The work of ZB, CRA and GRM was supported through a Cooperative Agreement Award (no. W81XWH-07-2-067) between the Henry M. Jackson Foundation for the Advancement of Military Medicine and the U.S. Army Medical Research and Materiel Command (MRMC). The funding bodies had no role in the design of the study and collection, analysis, and interpretation of data and in writing the manuscript.

### Declaration of Competing Interest

SD and the US Army hold the patent on FMP013 antigen. SD, ZB and CA have filed for a patent on FMP013 + ALFQ formulation.

### Appendix A. Supplementary material

Supplementary data to this article can be found online at <https://doi.org/10.1016/j.vaccine.2019.05.059>.

### References

- [1] Ashley EA, Pyae Phyo A, Woodrow CJ. *Malaria*. *Lancet* 2018;391:1608–21.
- [2] Kaba SA, McCoy ME, Doll TA, Brando C, Guo Q, Dasgupta D, et al. Protective antibody and CD8+ T-cell responses to the *Plasmodium falciparum* circumsporozoite protein induced by a nanoparticle vaccine. *PLoS ONE* 2012;7:e48304.
- [3] White MT, Bejon P, Olotu A, Griffin JT, Riley EM, Kester KE, et al. The relationship between RTS, S vaccine-induced antibodies, CD4(+) T cell responses and protection against *Plasmodium falciparum* infection. *PLoS ONE* 2013;8:e61395.
- [4] Neafsey DE, Juraska M, Bedford T, Benkeser D, Valim C, Griggs A, et al. Genetic diversity and protective efficacy of the RTS, S/AS01 Malaria vaccine. *New England J Med* 2015;373:2025–37.
- [5] Espinosa DA, Gutierrez GM, Rojas-Lopez M, Noe AR, Shi L, Tse SW, et al. Proteolytic cleavage of the *Plasmodium falciparum* circumsporozoite protein is a target of protective antibodies. *J Infect Dis* 2015.
- [6] Fries LF, Gordon DM, Schneider I, Beier JC, Long GW, Gross M, et al. Safety, immunogenicity, and efficacy of a *Plasmodium falciparum* vaccine comprising a circumsporozoite protein repeat region peptide conjugated to *Pseudomonas aeruginosa* toxin A. *Infect Immun* 1992;60:1834–9.
- [7] Sherwood JA, Copeland RS, Taylor KA, Abok K, Oloo AJ, Were JB, et al. *Plasmodium falciparum* circumsporozoite vaccine immunogenicity and efficacy trial with natural challenge quantitation in an area of endemic human malaria of Kenya. *Vaccine* 1996;14:817–27.
- [8] Cohen J, Nussenzweig V, Nussenzweig R, Vekemans J, Leach A. From the circumsporozoite protein to the RTS, S/AS candidate vaccine. *Human Vaccines* 2010;6:90–6.
- [9] Kester KE, Cummings JF, Ofori-Anyanam O, Ockenhouse CF, Krzych U, Moris P, et al. Randomized, double-blind, phase 2a trial of falciparum malaria vaccines RTS, S/AS01B and RTS, S/AS02A in malaria-naïve adults: safety, efficacy, and immunologic associates of protection. *J Infect Dis* 2009;200:337–46.
- [10] Polhemus ME, Remich SA, Ogutu BR, Waitumbi JN, Otieno L, Apollo S, et al. Evaluation of RTS, S/AS02A and RTS, S/AS01B in adults in a high malaria transmission area. *PLoS ONE* 2009;4:e6465.
- [11] Marty-Roix R, Vladimer GI, Pouliot K, Weng D, Buglione-Corbett R, West K, et al. Identification of QS-21 as an Inflammasome-activating Molecular Component of Saponin Adjuvants. *J Biol Chem* 2016;291:1123–36.
- [12] Coccia M, Collignon C, Herve C, Chalon A, Welsby I, Detienne S, et al. Cellular and molecular synergy in AS01-adjuvanted vaccines results in an early IFN $\gamma$  response promoting vaccine immunogenicity. *NPJ Vaccines* 2017;2:25.
- [13] Rts SCTP, Agnandji ST, Lell B, Fernandes JF, Abossolo BP, Methogo BG, et al. A phase 3 trial of RTS, S/AS01 malaria vaccine in African infants. *New England J Med* 2012;367:2284–95.
- [14] Dendouga N, Fochesato M, Lockman L, Mossman S, Giannini SL. Cell-mediated immune responses to a varicella-zoster virus glycoprotein E vaccine using both a TLR agonist and QS21 in mice. *Vaccine* 2012;30:3126–35.
- [15] Lal H, Poder A, Campora L, Geeraerts B, Oostvogels L, Vanden Abeele C, et al. Immunogenicity, reactogenicity and safety of 2 doses of an adjuvanted herpes zoster subunit vaccine administered 2, 6 or 12 months apart in older adults: Results of a phase III, randomized, open-label, multicenter study. *Vaccine* 2018;36:148–54.
- [16] Regules JA, Cicatelli SB, Bennett JW, Paolino KM, Twomey PS, Moon JE, et al. Fractional third and fourth dose of RTS, S/AS01 malaria candidate vaccine: a phase 2a controlled human malaria parasite infection and immunogenicity study. *J Infect Dis* 2016;214:762–71.
- [17] Aldrich C, Magini A, Emiliani C, Dottorini T, Bistoni F, Crisanti A, et al. Roles of the amino terminal region and repeat region of the *Plasmodium berghei* circumsporozoite protein in parasite infectivity. *PLoS ONE* 2012;7:e32524.
- [18] Bergmann-Leitner ES, Scheiblhofer S, Weiss R, Duncan EH, Leitner WW, Chen D, et al. C3d binding to the circumsporozoite protein carboxy-terminus deviates immunity against malaria. *Int Immunol* 2005;17:245–55.
- [19] Bongfen SE, Ntsama PM, Offner S, Smith T, Felger I, Tanner M, et al. The N-terminal domain of *Plasmodium falciparum* circumsporozoite protein represents a target of protective immunity. *Vaccine* 2009;27:328–35.
- [20] Schwenk R, DeBot M, Porter M, Nikki J, Rein L, Spaccapelo R, et al. IgG2 antibodies against a clinical grade *Plasmodium falciparum* CSP vaccine antigen associate with protection against transgenic sporozoite challenge in mice. *PLoS ONE* 2014;9:e111020.
- [21] Khan F, Porter M, Schwenk R, DeBot M, Saudan P, Dutta S. Head-to-head comparison of soluble vs. Qbeta VLP circumsporozoite protein vaccines reveals selective enhancement of NANP repeat responses. *PLoS ONE* 2015;10:e0142035.
- [22] Beck Z, Matyas GR, Jalah R, Rao M, Polonis VR, Alving CR. Differential immune responses to HIV-1 envelope protein induced by liposomal adjuvant formulations containing monophosphoryl lipid A with or without QS21. *Vaccine* 2015;33:5578–87.
- [23] Genito CJ, Beck Z, Phares TW, Kalle F, Limbach KJ, Stefaniak ME, et al. Liposomes containing monophosphoryl lipid A and QS-21 serve as an effective adjuvant for soluble circumsporozoite protein malaria vaccine FMP013. *Vaccine* 2017;35:3865–74.
- [24] Stewart VA, McGrath SM, Walsh DS, Davis S, Hess AS, Ware LA, et al. Pre-clinical evaluation of new adjuvant formulations to improve the immunogenicity of the malaria vaccine RTS, S/AS02A. *Vaccine* 2006;24:6483–92.
- [25] Stewart VA, McGrath SM, Dubois PM, Pau MG, Mettens P, Shott J, et al. Priming with an adenovirus 35-circumsporozoite protein (CS) vaccine followed by RTS, S/AS01B boosting significantly improves immunogenicity to *Plasmodium falciparum* CS compared to that with either malaria vaccine alone. *Infect Immun* 2007;75:2283–90.
- [26] Ockenhouse CF, Regules J, Tosh D, Cowden J, Kathcart A, Cummings J, et al. S/AS01 Heterologous Prime Boost Vaccine Efficacy against Sporozoite Challenge in Healthy Malaria-Naïve Adults. *PLoS ONE* 2015;10:e0131571.
- [27] Weiss WR, Jiang CG. Protective CD8+ T lymphocytes in primates immunized with malaria sporozoites. *PLoS ONE* 2012;7:e31247.
- [28] Pichyangkul S, Kum-Arb U, Yongvanitchit K, Limsalakpetch A, Gettayacamin M, Lanar DE, et al. Preclinical evaluation of the safety and immunogenicity of a vaccine consisting of *Plasmodium falciparum* liver-stage antigen 1 with adjuvant AS01B administered alone or concurrently with the RTS, S/AS01B vaccine in rhesus primates. *Infect Immun* 2008;76:229–38.
- [29] Stewart VA, Walsh DS, McGrath SM, Kester KE, Cummings JF, Voss G, et al. Cutaneous delayed-type hypersensitivity (DTH) in a multi-formulation comparator trial of the anti-falciparum malaria vaccine candidate RTS,S in rhesus macaques. *Vaccine* 2006;24:6493–502.
- [30] Walsh DS, Gettayacamin M, Leitner WW, Lyon JA, Stewart VA, Marit G, et al. Heterologous prime-boost immunization in rhesus macaques by two, optimally spaced particle-mediated epidermal deliveries of *Plasmodium falciparum* circumsporozoite protein-encoding DNA, followed by intramuscular RTS, S/AS02A. *Vaccine* 2006;24:4167–78.
- [31] Walsh DS, Pichyangkul S, Gettayacamin M, Tongtawe P, Siegrist CA, Hansukjarinya P, et al. Safety and immunogenicity of rts, s+trap malaria vaccine, formulated in the as02a adjuvant system, in infant rhesus monkeys. *Am J Trop Med Hygiene* 2004;70:499–509.
- [32] Phares TW, May AD, Genito CJ, Hoyt NA, Khan FA, Porter MD, et al. Rhesus macaque and mouse models for down-selecting circumsporozoite protein based malaria vaccines differ significantly in immunogenicity and functional outcomes. *Malar J* 2017;16:115.
- [33] Porter MD, Nicki J, Pool CD, DeBot M, Illam RM, Brando C, et al. Transgenic parasites stably expressing full-length *Plasmodium falciparum* circumsporozoite protein as a model for vaccine down-selection in mice using sterile protection as an endpoint. *Clin Vaccine Immunol: CVI* 2013;20:803–10.
- [34] Zou X, House BL, Zyzak MD, Richie TL, Gerbası VR. Towards an optimized inhibition of liver stage development assay (ILSDA) for *Plasmodium falciparum*. *Malar J* 2013;12:394.

- [35] Shen C, Xu H, Liu D, Veazey RS, Wang X. Development of serum antibodies during early infancy in rhesus macaques: implications for humoral immune responses to vaccination at birth. *Vaccine* 2014;32:5337–42.
- [36] Kusi KA, Faber BW, van der Eijk M, Thomas AW, Kocken CH, Remarque EJ. Immunization with different PfAMA1 alleles in sequence induces clonal imprint humoral responses that are similar to responses induced by the same alleles as a vaccine cocktail in rabbits. *Malar J* 2011;10:40.
- [37] Mahdi Abdel Hamid M, Remarque EJ, van Duivenvoorde LM, van der Werff N, Walraven V, Faber BW, et al. Vaccination with *Plasmodium knowlesi* AMA1 formulated in the novel adjuvant co-vaccine HT protects against blood-stage challenge in rhesus macaques. *PLoS ONE* 2011;6:e20547.
- [38] Pichyangkul S, Tongtawe P, Kum-Arb U, Yongvanitchit K, Gettayacamin M, Hollingdale MR, et al. Evaluation of the safety and immunogenicity of *Plasmodium falciparum* apical membrane antigen 1, merozoite surface protein 1 or RTS, S vaccines with adjuvant system AS02A administered alone or concurrently in rhesus monkeys. *Vaccine* 2009;28:452–62.
- [39] Beck Z, Matyas GR, Alving CR. Detection of liposomal cholesterol and monophosphoryl lipid A by QS-21 saponin and *Limulus polyphemus* amoebocyte lysate. *Biochimica et biophysica acta* 2015;1848:775–80.
- [40] Long CA, Zavala F. Malaria vaccines and human immune responses. *Curr Opin Microbiol* 2016;32:96–102.
- [41] Kaptoge S, Di Angelantonio E, Pennells L, Wood AM, White IR, Gao P, et al. C-reactive protein, fibrinogen, and cardiovascular disease prediction. *New England J Med* 2012;367:1310–20.
- [42] Harris DT, Matyas GR, Gomella LG, Talor E, Winship MD, Spitler LE, et al. Immunologic approaches to the treatment of prostate cancer. *Semin Oncol* 1999;26:439–47.
- [43] Kisalu NK, Idris AH, Weidle C, Flores-Garcia Y, Flynn BJ, Sack BK, et al. A human monoclonal antibody prevents malaria infection by targeting a new site of vulnerability on the parasite. *Nat Med* 2018;24:408–16.



# Enhanced Immunogenicity and Protective Efficacy of a *Campylobacter jejuni* Conjugate Vaccine Coadministered with Liposomes Containing Monophosphoryl Lipid A and QS-21

Amritha Ramakrishnan,<sup>a\*</sup> Nina M. Schumack,<sup>b,c</sup> Christina L. Gariepy,<sup>b,c</sup> Heather Eggleston,<sup>b,c</sup> Gladys Nunez,<sup>a</sup> Nereyda Espinoza,<sup>a</sup> Monica Nieto,<sup>a</sup> Rosa Castillo,<sup>a</sup> Jesus Rojas,<sup>a</sup> Andrea J. McCoy,<sup>a</sup> Zoltan Beck,<sup>d</sup> Gary R. Matyas,<sup>e</sup> Carl R. Alving,<sup>e</sup> Patricia Guerry,<sup>c</sup> Frédéric Poly,<sup>c</sup> Renee M. Laird<sup>b,c</sup>

<sup>a</sup>Bacteriology Department, U.S. Naval Medical Research Unit No. 6, Callao, Peru

<sup>b</sup>Henry M. Jackson Foundation for Military Medicine, Bethesda, Maryland, USA

<sup>c</sup>Department of Enteric Diseases, Naval Medical Research Center, Silver Spring, Maryland, USA

<sup>d</sup>U.S. Military HIV Research Program, Henry M. Jackson Foundation for Military Medicine, Bethesda, Maryland, USA

<sup>e</sup>Laboratory of Adjuvant and Antigen Research, U.S. Military HIV Research Program, Walter Reed Army Institute of Research, Silver Spring, Maryland, USA

**ABSTRACT** *Campylobacter jejuni* is among the most common causes of diarrheal disease worldwide and efforts to develop protective measures against the pathogen are ongoing. One of the few defined virulence factors targeted for vaccine development is the capsule polysaccharide (CPS). We have developed a capsule conjugate vaccine against *C. jejuni* strain 81-176 (CPS-CRM) that is immunogenic in mice and nonhuman primates (NHPs) but only moderately immunogenic in humans when delivered alone or with aluminum hydroxide. To enhance immunogenicity, two novel liposome-based adjuvant systems, the Army Liposome Formulation (ALF), containing synthetic monophosphoryl lipid A, and ALF plus QS-21 (ALFQ), were evaluated with CPS-CRM in this study. In mice, ALF and ALFQ induced similar amounts of CPS-specific IgG that was significantly higher than levels induced by CPS-CRM alone. Qualitative differences in antibody responses were observed where CPS-CRM alone induced Th2-biased IgG1, whereas ALF and ALFQ enhanced Th1-mediated anti-CPS IgG2b and IgG2c and generated functional bactericidal antibody titers. CPS-CRM + ALFQ was superior to vaccine alone or CPS-CRM + ALF in augmenting antigen-specific Th1, Th2, and Th17 cytokine responses and a significantly higher proportion of CD4<sup>+</sup> IFN- $\gamma$ <sup>+</sup> IL-2<sup>+</sup> TNF- $\alpha$ <sup>+</sup> and CD4<sup>+</sup> IL-4<sup>+</sup> IL-10<sup>+</sup> T cells. ALFQ also significantly enhanced anti-CPS responses in NHPs when delivered with CPS-CRM compared to alum- or ALF-adjuvanted groups and showed the highest protective efficacy against diarrhea following orogastric challenge with *C. jejuni*. This study provides evidence that the ALF adjuvants may provide enhanced immunogenicity of this and other novel *C. jejuni* capsule conjugate vaccines in humans.

**IMPORTANCE** *Campylobacter jejuni* is a leading cause of diarrheal disease worldwide, and currently no preventative interventions are available. *C. jejuni* is an invasive mucosal pathogen that has a variety of polysaccharide structures on its surface, including a capsule. In phase 1 studies, a *C. jejuni* capsule conjugate vaccine was safe but poorly immunogenic when delivered alone or with aluminum hydroxide. Here, we report enhanced immunogenicity of the conjugate vaccine delivered with liposome adjuvants containing monophosphoryl lipid A without or with QS-21, known as ALF and ALFQ, respectively, in preclinical studies. Both liposome adjuvants significantly enhanced immunity in mice and nonhuman primates and improved protective efficacy of the vaccine compared to alum in a nonhuman primate *C. jejuni*

**Citation** Ramakrishnan A, Schumack NM, Gariepy CL, Eggleston H, Nunez G, Espinoza N, Nieto M, Castillo R, Rojas J, McCoy AJ, Beck Z, Matyas GR, Alving CR, Guerry P, Poly F, Laird RM. 2019. Enhanced immunogenicity and protective efficacy of a *Campylobacter jejuni* conjugate vaccine coadministered with liposomes containing monophosphoryl lipid A and QS-21. *mSphere* 4:e00101-19. <https://doi.org/10.1128/mSphere.00101-19>.

**Editor** Marcela F. Pasetti, University of Maryland School of Medicine

This is a work of the U.S. Government and is not subject to copyright protection in the United States. Foreign copyrights may apply. Address correspondence to Renee M. Laird, [renee.m.laird.ctr@mail.mil](mailto:renee.m.laird.ctr@mail.mil).

\* Present address: Amritha Ramakrishnan, SQZ Biotechnologies, Watertown, Massachusetts, USA.

**Received** 11 February 2019

**Accepted** 15 April 2019

**Published** 1 May 2019



diarrhea model, providing promising evidence that these potent adjuvant formulations may enhance immunogenicity in upcoming human studies with this *C. jejuni* conjugate and other malaria and HIV vaccine platforms.

**KEYWORDS** campylobacter, *Campylobacter jejuni*, adjuvants, conjugate, liposomes, vaccines

**C**ampylobacter infections are major causes of bacterial diarrhea worldwide, with the majority identified as being caused by *Campylobacter jejuni*. *C. jejuni* is a leading cause of foodborne illness in North America and Europe and was identified in the Global Enteric Multicenter Study (GEMS) and Malnutrition and the Consequences for Child Health and Development Project (MAL-ED) multisite birth cohort studies as a significant attributable cause of severe-to-moderate diarrhea that is associated with growth stunting in middle-to-low-income countries (1–4). *C. jejuni* infection typically results in acute inflammatory gastroenteritis that is self-limiting, but in more severe cases, the disease can progress to dysentery. In addition to acute disease, *C. jejuni* infections are associated with long-term sequelae, including reactive arthritis, inflammatory bowel syndrome, and most frequently with Guillain-Barré syndrome (GBS) (5–9). GBS is caused by development of autoantibodies to a subset of *C. jejuni* strains that express lipooligosaccharides (LOS) that mimic human gangliosides in structure, and it is currently estimated that *C. jejuni* infection precedes GBS in 20 to 50% of cases in the developed world and in other regions may be even higher (8).

The global burden imposed by the morbidity of *Campylobacter* disease and its related sequelae drives efforts to develop protective interventions. Measures to influence disease prevention, including source eradication, personal protective measures, and chemoprophylaxis, have been moderately successful thus far. Moreover, the rise of antibiotic-resistant *C. jejuni* point to the need for other types of interventions (10–12). There are no licensed vaccines available for *Campylobacter*. One critical hurdle in vaccine development is that, unlike other enteric pathogens, there are few defined virulence factors that have been targeted as subunit vaccine approaches. *C. jejuni* expresses a polysaccharide capsule (CPS) that is the major serodeterminant of the Penner heat-stable (HS) serotyping scheme (13). There are 47 known HS serotypes of *C. jejuni* resulting from 35 chemically diverse CPS structures (14, 15). Importantly, CPS has been shown to be an important virulence factor modulating invasion and disease and contributing to serum resistance (16, 17). We have developed a CPS conjugate approach utilizing the diphtheria toxin mutant CRM<sub>197</sub> as a carrier protein (18). CPS isolated from strain 81-176 (type HS23/36) was conjugated to CRM<sub>197</sub> (CPS-CRM) as a prototype vaccine candidate. The prototype CPS-CRM vaccine was immunogenic in mice without an adjuvant, generated high levels of anti-CPS IgG and was protective when mice were intranasally challenged with *C. jejuni* strain 81-176. CPS-CRM vaccine efficacy was also tested in a New World nonhuman primate (NHP), *Aotus nancymae*, model. NHPs animals receiving a CPS-CRM dose comparable to 2.5 μg of polysaccharide plus aluminum hydroxide (alum) were protected from diarrhea after challenge with 81-176 (18).

To follow on the success of the preclinical studies, a CPS-CRM conjugate vaccine GMP-manufactured from a mutant strain of 81-176 lacking LOS, known as CJCV1, was tested in a phase 1 study with or without alum at 4-week intervals (ClinicalTrials.gov identifier NCT02067676) (19). Although the vaccine was safe, it was weakly immunogenic, likely because it was delivered in only two doses unlike all the preclinical studies which utilized three doses. In addition, adjuvants other than alum have not been extensively explored with our *C. jejuni* conjugate vaccine in preclinical models, where an immunopotentiating adjuvant might enhance immunogenicity of the CPS-CRM conjugate in humans. These adjuvants often incorporate components that stimulate innate immune system receptors like Toll-like receptors (TLRs) and the inflammasome. The Walter Reed Army Institute of Research Laboratory of Adjuvant and Antigen Research has developed an Army Liposome Formulation (ALF) family of adjuvants that

increase immunogenicity of a number of different vaccine platforms against a variety of pathogens, including HIV, *Plasmodium falciparum*, and *Neisseria meningitidis* (20–24). ALF is a liposome-based formulation containing a potent activator of TLR4, a synthetic form of monophospholipid A (MPLA) known as 3D-PHAD (Avanti Polar Lipids). The addition of components like alum and a detoxified saponin derivative QS-21 has enhanced the effectiveness of MPLA-containing liposomes further. Although both alum and QS-21 can activate the NOD-like receptor P3 (NLRP3) inflammasome complex in antigen-presenting cells (25, 26), they differ in the type of immune response induced; alum primarily skews immunity toward a Th2 response, and QS-21 induces Th1 responses. Here, CPS-CRM was tested with a series of ALF adjuvants: ALF, ALF plus alum (ALFA), ALF plus QS-21 (ALFQ), and ALFQ plus alum (ALFQA). We show that ALF and, to a greater extent, ALFQ enhance the CPS-specific antibody response generated against our CPS-CRM vaccine. Functional bactericidal CPS-specific antibodies were generated at the highest level in ALFQ-adjuvanted mice and NHPs vaccinated with CPS-CRM plus ALFQ (CPS-CRM + ALFQ) showed the greatest protective efficacy against diarrhea in a *C. jejuni* challenge model.

## RESULTS

**Coadministration of ALF adjuvants enhances the immunogenicity of a *C. jejuni* CPS-CRM vaccine.** Previous studies have demonstrated that the CPS-CRM vaccine is immunogenic in mice at three doses without the addition of an adjuvant and in NHPs when delivered with alum (18). However, the vaccine was poorly immunogenic in humans at two doses, even when coadministered with alum. To test the ability of liposome-based immunopotentiating adjuvants to augment immunogenicity of CPS-CRM, we tested four ALF formulation adjuvants and alum with a very low dose of CPS-CRM by immunizing mice three times intramuscularly (i.m.) at 4-week intervals. Serum anti-CPS IgG titers were measured by ELISA prevaccination and 2 weeks after each immunization. Without an adjuvant, 0.1  $\mu$ g of CPS-CRM (based on CPS weight) was not immunogenic in mice after three doses (Fig. 1A). The addition of an adjuvant induced a modest increase in anti-CPS IgG titers after one dose, and titers were boosted by the second and third doses of vaccine plus adjuvant in groups with ALF, ALFA, ALFQ, and alum (Fig. 1A). ALFQA did not enhance CPS-specific responses to the same extent as alum and other ALF formulations. After three doses, all adjuvanted groups had significantly higher CPS-specific total IgG titers than the vaccine-alone group, but no difference was observed in titers between adjuvanted groups. Because differences in qualitative antibody responses have been observed depending on adjuvant properties, we measured IgG subclasses. As expected, alum induced primarily a Th2-mediated antibody response characterized by anti-CPS IgG1 and little IgG2b or IgG2c (Fig. 1B). Conversely, ALF and ALFQ adjuvants induced Th1-biased CPS-specific IgG2b and 2c titers at levels higher than alum-adjuvanted mice. ALF- and ALFQ-adjuvanted mice showed equivalent levels of anti-CPS IgG1 compared to alum. The presence of alum in the ALFA or ALFQA groups dampened the production of CPS-specific IgG2b and 2c in these groups, and the levels were significantly lower than the levels observed in the ALF and ALFQ groups. Based on these results, we selected ALF and ALFQ adjuvants for further testing because they induced a robust CPS-specific antibody response characterized by high titers of anti-CPS IgG1, IgG2b, and IgG2c.

**Dose escalation of CPS-CRM vaccine with ALF and ALFQ.** ALF and ALFQ were further compared in a subsequent study with a dose escalation of CPS-CRM. 1.0, 2.5, and 5.0  $\mu$ g of CPS-CRM (based on CPS weight) was delivered alone or admixed with ALF or ALFQ adjuvants. CPS titers were measured 2 weeks after the third dose. At elevated doses, CPS-CRM vaccine was immunogenic without the use of an adjuvant, and we observed a dose-dependent increase in anti-CPS IgG titers (Fig. 2A). We observed a 2.6-fold increase in IgG titers between the 1.0- and 2.5- $\mu$ g doses, and IgG titers plateaued at 2.5  $\mu$ g with no further increase in anti-CPS IgG at the 5.0- $\mu$ g dose. Administration of CPS-CRM with ALF or ALFQ induced significantly higher titers of anti-CPS IgG at every dose of CPS-CRM tested compared to vaccine alone (Fig. 2A).

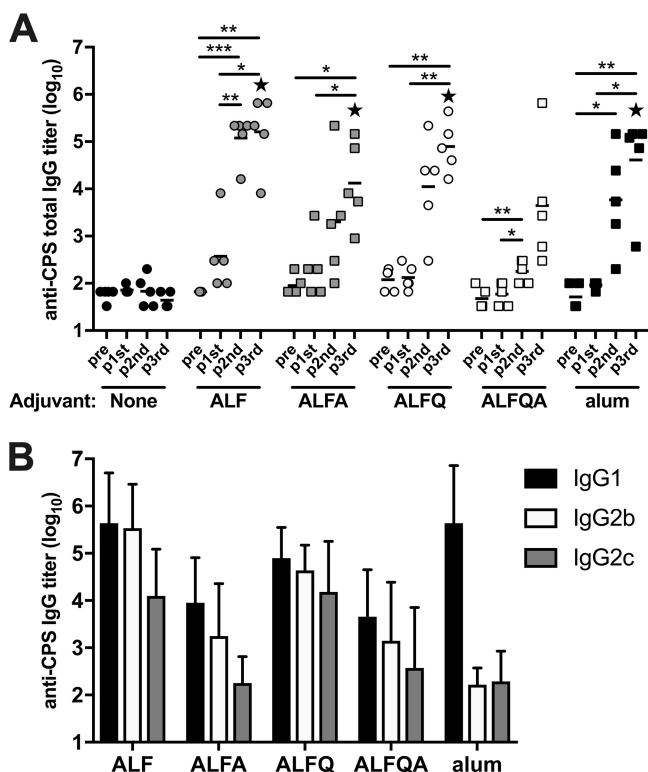


**FIG 1** ALF adjuvant formulations enhance immunogenicity of a *C. jejuni* CPS-CRM vaccine in mice. Mice were immunized i.m. three times at 4-week intervals with 0.1  $\mu\text{g}$  of CPS-CRM alone or with the indicated ALF adjuvant or alum. (A) Kinetics of the CPS-specific antibody response. Anti-CPS IgG titers were measured in serum collected prevaccination and 2 weeks after each immunization. Log<sub>10</sub> titers of individual mice ( $n = 5$  per group) are shown, where the horizontal line indicates median of the group at the respective time point. Repeated-measures one-way ANOVA with multiplicity-adjusted  $P$  values for statistical significance among groups was performed (\*,  $P \leq 0.05$ ; \*\*,  $P \leq 0.01$ ; \*\*\*,  $P \leq 0.001$ ). Statistical significance between groups was determined by ordinary one-way ANOVA with multiplicity-adjusted  $P$  values. Stars indicate significantly different values from CPS-CRM alone ( $P \leq 0.05$ ). (B) Anti-CPS IgG1, IgG2b or IgG2c titers were measured in serum 2 weeks after the third dose. The bar graph represents means plus the standard deviations of five mice per group immunized with CPS-CRM plus the indicated adjuvant.

These results suggest that ALF and ALFQ may allow dose sparing of a *C. jejuni* conjugate vaccine formulation in the clinic. Differences between the vaccine-alone and the ALF or ALFQ treatment groups were not as striking at the 2.5- and 5.0- $\mu\text{g}$  doses, and yet both adjuvants enhanced IgG titers at every dose of vaccine tested. We also measured CPS-specific IgA responses in serum after three doses of CPS-CRM with or without adjuvants (Fig. 2B). Overall, the IgA titers were much lower than those observed for IgG. CPS-CRM alone did not induce substantial levels of anti-CPS IgA at any of the doses tested. Significantly higher IgA titers were observed at the highest 5.0- $\mu\text{g}$  dose of CPS-CRM when coadministered with ALF, whereas ALFQ induced significantly higher levels of anti-CPS IgA at both the 2.5- and 5.0- $\mu\text{g}$  doses compared to vaccine alone. The highest IgA titers were observed with 5.0  $\mu\text{g}$  of CPS-CRM + ALFQ, where titers were significantly higher than those observed with vaccine alone and CPS-CRM + ALF (75- and 14-fold, respectively). Notably, this is the first time that we have observed substantial levels of CPS-specific IgA after vaccination with this CPS-CRM vaccine.

Because we observed differences in CPS-specific IgG subclass responses at a very low dose of 0.1  $\mu\text{g}$  of CPS-CRM + ALF or ALFQ, we measured these responses at the higher vaccine doses (Fig. 2C). CPS-CRM at higher doses delivered without an adjuvant primarily induced CPS-specific IgG1. IgG1, IgG2b, and IgG2c levels were significantly higher in ALF-adjuvanted mice than in mice given vaccine alone. The titers of CPS-specific IgG1, IgG2b, and IgG2c were the highest in the ALFQ groups, with levels that

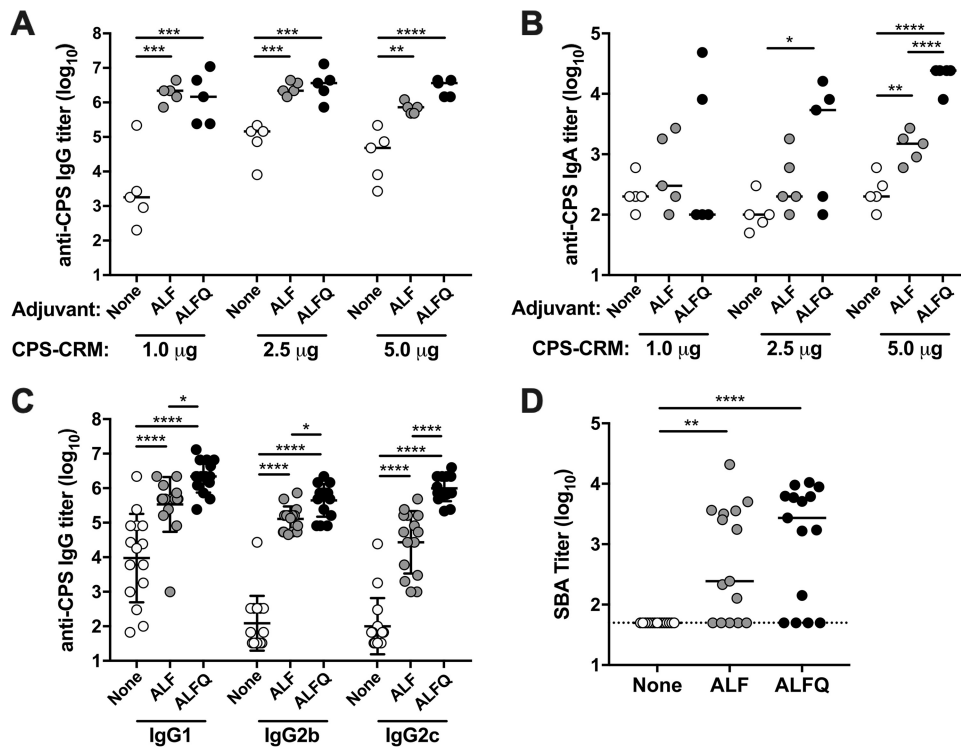


**FIG 2** ALF and ALFQ adjuvants induce high levels of anti-CPS IgG and functional serum bactericidal antibodies at higher doses of CPS-CRM in mice. Mice were immunized i.m. three times at 4-week intervals with 1.0, 2.5, or 5.0  $\mu\text{g}$  of CPS-CRM alone or with ALF or ALFQ. (A and B) Anti-CPS IgG (A) and IgA (B) antibody responses were measured 2 weeks after the third vaccination.  $\text{Log}_{10}$  titers of individual mice ( $n = 5$  per group) are shown, where the horizontal line indicates median of the group. (C) Anti-CPS IgG1, IgG2b, and IgG2c titers were measured 2 weeks after the third vaccination.  $\text{Log}_{10}$  titers of individual mice combining dose levels ( $n = 15$  per group) are shown, where the horizontal line indicates the median of the group. (D) Functional antibody responses were measured after the third immunization by F-SBA.  $\text{Log}_{10}$  F-SBA titers of individual mice with combined dose levels are shown, where the horizontal line indicates the median of the group. The dotted line indicates the limit of detection of F-SBA. Statistical significance between groups was determined by ordinary one-way ANOVA with multiplicity-adjusted  $P$  values (\*,  $P \leq 0.05$ ; \*\*,  $P \leq 0.01$ ; \*\*\*,  $P \leq 0.001$ ; \*\*\*\*,  $P \leq 0.0001$ ).

were significantly higher than both vaccine alone and ALF. Subclass analysis suggests that ALF and, to a greater extent, ALFQ can bias the CPS-specific response toward Th1-mediated IgG2b and IgG2c antibodies.

**Coadministration of CPS-CRM with ALF or ALFQ induces bactericidal antibody responses.** Because CPS conjugate vaccines against other Gram-negative bacteria, such as *Neisseria meningitidis*, have been shown to generate functional serum bactericidal antibody (SBA) responses (27–31) and because bactericidal activity has been described previously after *C. jejuni* infection (32–34), we measured whether our CPS-CRM vaccine generated SBA responses. We developed an improved flow cytometric-based SBA (F-SBA) to measure responses in mice and NHPs (described in detail in the supplementary material and in Fig. S1). No *C. jejuni* F-SBA activity was detected in mouse serum prior to immunization (data not shown). After three immunizations with the CPS-CRM vaccine at 1.0, 2.5, or 5.0  $\mu\text{g}$ , no SBA activity was detected in the serum of mice that received the vaccine without an adjuvant (Fig. 2D). Conversely, functional F-SBA titers were observed in animals vaccinated with CPS-CRM + ALF or ALFQ adjuvants, which is consistent with an increased production of Th1-mediated CPS-specific IgG2b and IgG2c antibody responses in the ALF and ALFQ groups. Indeed, we observed significant correlation of F-SBA and anti-CPS IgG2b or IgG2c titers (see Fig. S2 in the supplemental material). A weaker correlation was observed between anti-CPS IgG1 and F-SBA.

**ALFQ enhances development of multifunctional CD4<sup>+</sup> T cell responses.** To investigate T cell responses in mice immunized with CPS-CRM  $\pm$  ALF or ALFQ, we

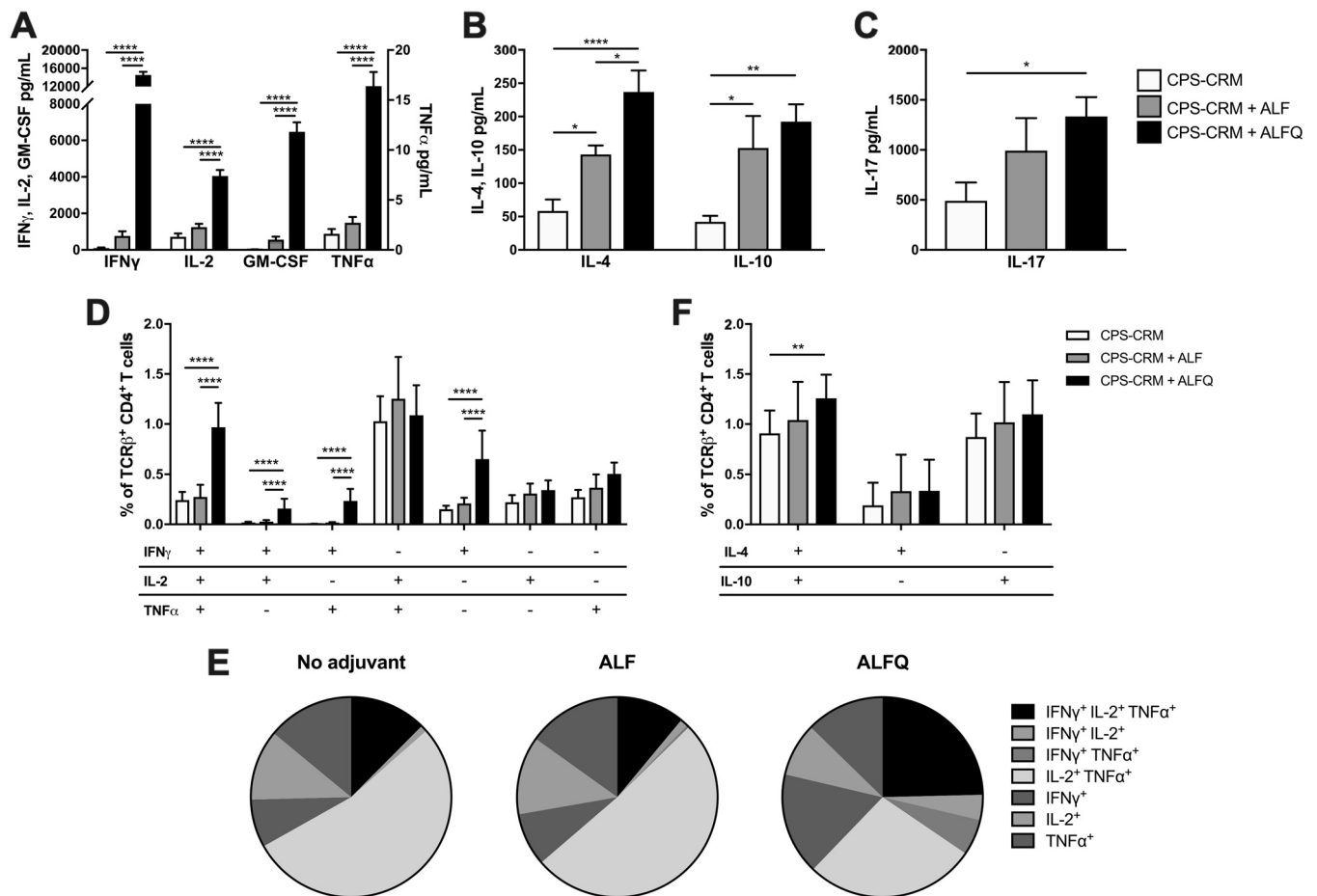


**FIG 3** ALFQ enhances T cell responses to the CPS-CRM vaccine in mice. Splenocytes were harvested 2 weeks after the third vaccination to measure T cell-mediated cytokine production. Splenocytes were cultured for 72 h with medium alone or restimulated with CPS-CRM, and Th1 (A), Th2 (B), and IL-17 (C) cytokines were measured in culture supernatants. Cytokine levels were normalized by subtracting medium-alone from CPS-CRM-stimulated samples. (D) Flow cytometric phenotypic analysis of IFN- $\gamma$ , TNF- $\alpha$ , and IL-2-producing CD4 $^+$  TCR $\beta^+$  T cells in CPS-CRM-restimulated splenocytes. (E) Pie charts show the distribution of Th1-cytokine-producing cells among samples for vaccine-alone/no adjuvant or CPS-CRM delivered with ALF or ALFQ determined by phenotypical analysis. (F) Flow cytometric phenotypic analysis of IL-4- and IL-10-producing CD4 $^+$  TCR $\beta^+$  T cells in CPS-CRM-restimulated splenocytes. In all graphs, data for 1.0-, 2.5-, and 5.0- $\mu$ g CPS-CRM dose levels were combined. Bar graphs represent the means plus the standard deviations of  $n = 15$  for vaccine alone or for CPS-CRM + ALF or ALFQ. Statistical significance between groups was determined by ordinary one-way ANOVA with multiplicity-adjusted  $P$  values (\*,  $P \leq 0.05$ ; \*\*,  $P \leq 0.01$ ; \*\*\*\*,  $P \leq 0.0001$ ).

isolated spleens from animals 2 weeks after the third immunization and restimulated splenocytes with CPS-CRM to measure CRM-specific T cell responses. After 3 days, the Th1, Th2, and IL-17 cytokine levels were measured in the culture supernatant. Mice immunized with CPS-CRM + ALFQ showed superior production of Th1 cytokines gamma interferon (IFN- $\gamma$ ), interleukin-2 (IL-2), granulocyte-macrophage colony-stimulating factor (GM-CSF), and tumor necrosis factor alpha (TNF- $\alpha$ ) compared to vaccine alone or CPS-CRM + ALF (Fig. 3A). No difference in Th1 cytokine production was observed between the vaccine-alone and CPS-CRM + ALF groups, indicating that the inclusion of QS-21 in the ALFQ adjuvant was responsible for the considerable enhancement of Th1 cytokine production. Both ALF and ALFQ augmented production of the Th2 cytokines IL-4 and IL-10 compared to vaccine alone (Fig. 3B). Higher levels of IL-4 were observed in ALFQ-adjuvanted animals compared to both vaccine-alone and CPS-CRM + ALF treatment groups. Similar levels of IL-10 were observed in ALF- and ALFQ-adjuvanted groups. Both ALF and ALFQ induced higher levels of IL-17 production compared to vaccine alone, but only the levels induced by ALFQ were significantly higher (Fig. 3C).

Concurrent with cytokine analysis in the supernatant, we stimulated splenocytes to characterize CD4 $^+$  Th1 and Th2 cell subsets. Consistent with the very high levels of

IFN- $\gamma$  detected in CPS-CRM-restimulated supernatants of CPS-CRM + ALFQ-immunized mice, we observed a significantly higher frequency of IFN- $\gamma$ -producing CD4<sup>+</sup> T cell subsets by flow cytometry (Fig. 3D). Significantly higher frequencies of CD4<sup>+</sup> IFN- $\gamma$ <sup>+</sup> single cytokine-producing cells, double cytokine-producing IFN- $\gamma$ <sup>+</sup> IL-2<sup>+</sup> and IFN- $\gamma$ <sup>+</sup> TNF- $\alpha$ <sup>+</sup> cells, and IFN- $\gamma$ <sup>+</sup> IL-2<sup>+</sup> TNF- $\alpha$ <sup>+</sup> triple-producing CD4<sup>+</sup> T cells were detected compared to both vaccine-alone and CPS-CRM + ALF groups. As a whole, very little difference in CD4<sup>+</sup> Th1 cell phenotypes was observed between nonadjuvanted mice and mice adjuvanted with ALF (Fig. 3E), and similar frequencies of Th1 cytokine-producing cells were generated (Fig. S3). The most striking difference in CD4<sup>+</sup> T cell phenotypes induced in ALFQ-adjuvanted mice was IFN- $\gamma$ <sup>+</sup> IL-2<sup>+</sup> TNF- $\alpha$ <sup>+</sup> triple-producing CD4<sup>+</sup> T cells (Fig. 3E; black pie slice), and a greater frequency of total CD4<sup>+</sup> Th1 cytokine-producing cells was observed (Fig. S3). We also analyzed CD4<sup>+</sup> Th2 cells and found that ALFQ induced higher frequencies of IL-4<sup>+</sup> IL-10<sup>+</sup> double-producing cells compared to vaccine alone, but not higher frequencies of single cytokine-producing CD4<sup>+</sup> Th2 cells compared to vaccine alone or ALF-adjuvanted groups (Fig. 3F). Taken together, the cytokines in the supernatant and the flow phenotypic analysis data support that inclusion of QS-21 in the ALFQ liposome induces the most robust CRM-specific CD4<sup>+</sup> T cell responses.

**ALFQ enhances immunogenicity and efficacy of CPS-CRM in *A. nancymaae*.** ALF and ALFQ adjuvants showed substantial enhancement to CPS-CRM vaccine immunogenicity in our mouse model; however, a reliable wild-type mouse model for *C. jejuni*-mediated diarrhea has only recently been published and has not yet been tested for vaccine efficacy (35). We have previously developed an *A. nancymaae* NHP *C. jejuni* challenge model with HS23/36-expressing strain 81-176 (36) and demonstrated that our prototype CPS-CRM conjugate vaccine is protective when delivered with alum subcutaneously (s.c.) in three doses at 6-week intervals (18). This same strain 81-176 has been utilized in human controlled human infection models (CHIMs); however, since the discovery that LOS mimicry causes GBS and since strain 81-176 expresses LOS capable of inducing this mimicry, 81-176 can no longer be utilized in CHIMs (37, 38). We developed an alternative CHIM with an HS23/36-expressing strain CG8421 (39) and also established an *A. nancymaae* model to unite both human and primate studies. Here, we evaluated the immunogenicity and protective efficacy of our CPS-CRM vaccine adjuvanted with alum, ALF, or ALFQ against CG8421 challenge. For logistic purposes, animals were divided among two separate cohorts. For comparison against the historic vaccine experiment (18), we immunized NHP with 3.5  $\mu$ g of CPS-CRM + alum s.c. We delivered 3.5  $\mu$ g of CPS-CRM  $\pm$  ALF or ALFQ or phosphate-buffered saline (PBS) sham i.m. All groups received three doses at 4-week intervals, which is consistent with the dosing schedule in our mouse model. Anti-CPS IgG titers developed in animals immunized with CPS-CRM + alum after two doses, and no boost was observed after the third dose (Fig. 4A). Titers were significantly higher than PBS sham-immunized animals after the second and third doses. In NHPs treated with CPS-CRM + ALF, similar levels of anti-CPS IgG were observed compared to alum-adjuvanted animals after the second dose, and titers decreased slightly between the second and third dose of CPS-CRM + ALF. Titers were significantly lower in ALF-adjuvanted animals compared to alum-adjuvanted animals after the third dose, although the difference was not striking (mean log<sub>10</sub> titer of 4.2 in alum versus 3.8 in the ALF group). The most prominent enhancement of CPS-specific IgG was observed in animals immunized with CPS-CRM + ALFQ (Fig. 4A). After a single immunization, anti-CPS IgG titers were significantly higher than baseline and PBS-immunized animals. After two doses, titers were significantly higher than both alum- and ALF-adjuvanted groups (mean log<sub>10</sub> ALFQ titer of 5.1). Although we observed a small but significant drop in titers between doses 2 and 3 in ALFQ-adjuvanted animals (log<sub>10</sub> titer of 5.1 versus 4.8), the titers remained higher than both alum- and ALF-treated animals at the same time point.

In a cohort that included a PBS sham-, ALF-, and ALFQ-vaccinated NHPs, we had the opportunity to measure CPS-specific IgG antibody-secreting cells (ASCs) in peripheral

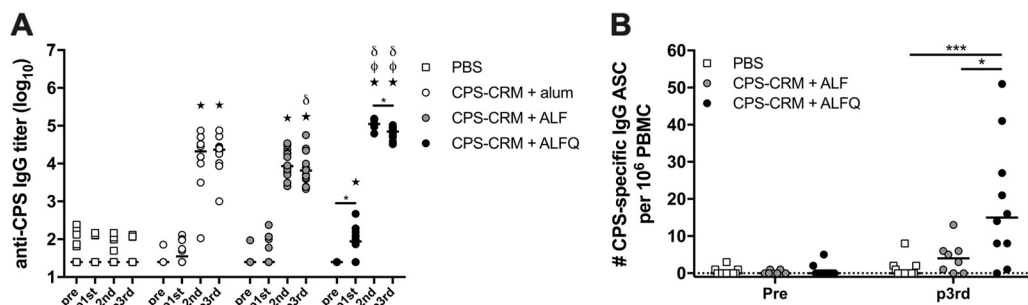


**FIG 4** ALFQ significantly enhances the CPS-specific antibody responses in *A. nancymae* immunized with CPS-CRM. NHPs were immunized three times at 4-week intervals with PBS or 3.5  $\mu$ g of CPS-CRM coadministered with alum, ALF, or ALFQ. Animals were divided among two cohorts. (A) Serum anti-CPS IgG titers were measured pre- and postvaccination in individual animals from both cohorts. Log<sub>10</sub> titers of individual animals are shown, where the horizontal line indicates median of the group (PBS, *n* = 20; alum, *n* = 10; ALF, *n* = 17; ALFQ, *n* = 10). Statistical differences among each group were determined by repeated-measures one-way ANOVA with multiplicity-adjusted *P* values (\*, *P*  $\leq$  0.05). Statistical significance between groups was determined by ordinary one-way ANOVA with multiplicity-adjusted *P* values. Stars indicate significant differences from PBS,  $\delta$  symbols indicate significantly different from alum, and  $\phi$  symbols indicate significant differences from ALF (*P*  $\leq$  0.05). (B) Number of CPS-specific IgG ASCs detected in peripheral blood pre-vaccination and 7 days after the third vaccination in cohort 2 NHPs immunized with PBS or CPS-CRM + ALF or ALFQ. The numbers of ASCs per 10<sup>6</sup> PBMC of individual animals are shown, where the horizontal line indicates the median of the group. Ordinary one-way ANOVA with multiplicity-adjusted *P* values for statistical significance between groups were determined (\*, *P*  $\leq$  0.05; \*\*\*, *P*  $\leq$  0.001).

blood by enzyme-linked immunospot (ELISPOT) assay (Fig. 4B). At 7 days after the third immunization, CPS-specific IgG ASCs were detectable in ALF-adjuvanted NHPs at levels higher than in PBS-immunized animals, although the difference was not statistically significant (values for CPS-specific IgG ASCs per 10<sup>6</sup> peripheral blood mononuclear cells (PBMC): PBS [median, 0; range, 0 to 8] and ALF [median, 4; range, 0 to 13]). Consistent with the highest levels of anti-CPS IgG observed in the serum after vaccination, NHPs immunized with CPS-CRM + ALFQ had significantly higher levels of CPS-specific IgG ASCs compared to animals immunized with PBS and CPS-CRM + ALF (ASCs: ALFQ [median, 15; range, 0 to 51]).

All sham-immunized and CPS-CRM-immunized animals were challenged with *C. jejuni* strain CG8421 at 4 weeks after the last immunization and monitored for diarrhea development (Table 1). The attack rate in PBS-immunized animals was 70%, as expected. The protective efficacy (PE) of NHPs immunized with CPS-CRM + alum was 29%, which is lower than previously reported for our prototype HS23/36 conjugate delivered at approximately 2.5  $\mu$ g (based on CPS, not the total conjugate weight) with alum at 6-week intervals (18). Enhanced protective efficacies were observed with the liposome adjuvants, where ALF-adjuvanted animals showed 66% PE, and ALFQ-adjuvanted animals showed 86% PE. No differences in diarrhea duration, levels of colonization or duration of colonization were observed among the all groups.

**ALFQ induces high levels of functional CPS-specific bactericidal antibodies in NHPs that are associated with protection from *C. jejuni*-mediated diarrhea.** Because we observed enhanced PE in NHPs that were immunized with CPS-CRM + ALF or CPS-CRM + ALFQ, we measured F-SBA responses before and after the third immunization to look for association of bactericidal activity with protection from diarrhea (Fig. 5A). A few animals in each group had background F-SBA titers against *C. jejuni* strain 81-176 detectable before vaccination potentially indicating a previous environ-

**TABLE 1** Protective efficacy of the CPS-CRM vaccine in *A. nancymae* NHPs using various adjuvants

Group	No. of animals	Diarrhea attack rate, <i>n</i> (%)	Protective efficacy against diarrhea (%) <sup>a</sup>	<i>P</i> <sup>b</sup>
CPS-CRM + alum	10	5 (50)	29	0.43
CPS-CRM + ALF	17	4 (24)	66	0.008
CPS-CRM + ALFQ	10	1 (10)	8	0.005
PBS	20	14 (70)		

<sup>a</sup>Protective efficacy was calculated as follows: [(attack rate of PBS-treated animals – attack rate of vaccinated animals)/attack rate of PBS-treated animals]  $\times$  100.

<sup>b</sup>Determined using a Fisher exact test with no adjustment for multiple comparisons.

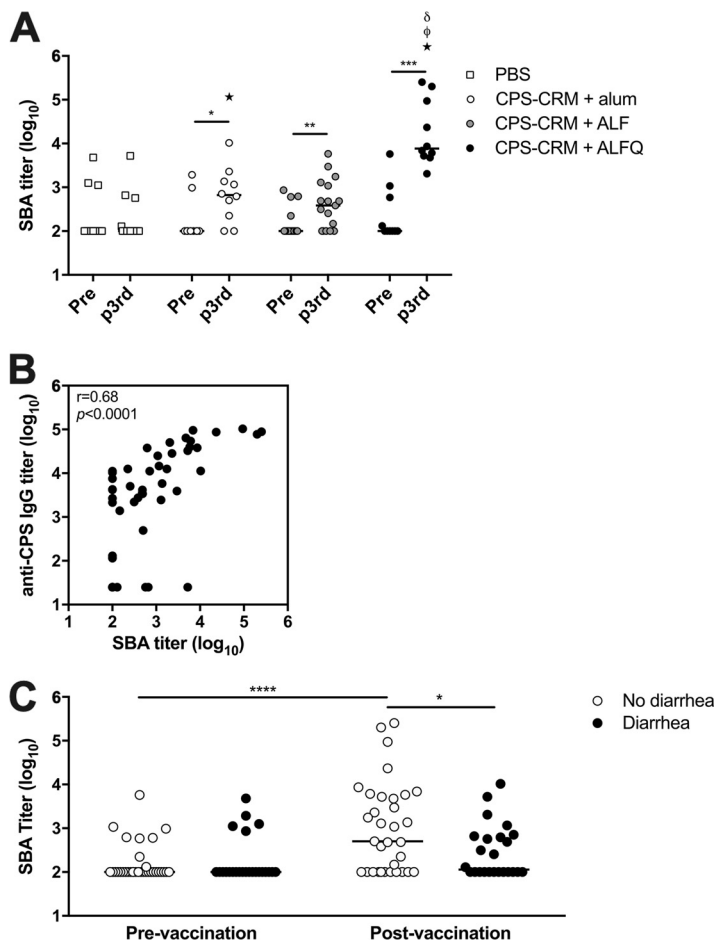


**FIG 5** Functional antibody responses are induced in *A. nancymae* immunized with CPS-CRM. (A) Functional antibody responses were measured by F-SBA against strain 81-176 in NHPs prevaccination and after the third vaccination.  $\log_{10}$  F-SBA titers of individual animals are shown, where the horizontal line indicates the median of the group. Paired *t* tests were performed to determine the significance between pre- and post-third vaccinations (\*,  $P \leq 0.05$ ; \*\*,  $P \leq 0.01$ ; \*\*\*,  $P \leq 0.001$ ). Statistical significance between groups was determined at each time point by ordinary one-way ANOVA with multiplicity-adjusted *P* values. Stars indicate significant differences from PBS,  $\delta$  symbols indicate significant differences from alum, and  $\phi$  symbols indicate significant differences from ALF ( $P \leq 0.05$ ). (B) Pearson correlation analysis of F-SBA responses after the third vaccination versus anti-CPS IgG responses. The correlation coefficient and *P* value are shown within the plot. (C) Association of functional F-SBA titer with disease outcome. Pre- and postvaccination F-SBA titers were analyzed in animals with or without diarrhea after challenge with CJ strain CG8421 (paired *t* test for significance; \*\*\*\*,  $P \leq 0.0001$ ; unpaired *t* test for significance; \*,  $P \leq 0.05$ ).

mental exposure to *C. jejuni*. No change in bactericidal activity was observed between pre- and postvaccination in PBS sham-immunized NHPs. CPS-CRM + alum-vaccinated animals developed F-SBA titers against *C. jejuni* strain 81-176 after the third dose, where 50% (5/10) of the NHPs were classified as responders by a 4-fold rise in F-SBA titers from prevaccination, and 41% (7/17) of ALF-adjuvanted animals developed F-SBA responses. ALFQ-adjuvanted animals showed the most robust increase in F-SBA responses after three vaccinations with a 100% (10/10) response rate and an average of 499-fold rise in bactericidal activity over baseline (fold increase, 6 to 2,524). Although alum- and ALF-adjuvanted animals had higher F-SBA titers compared to PBS controls after vaccination, ALFQ-adjuvanted NHPs had significantly higher titers than did the PBS-, alum-, or ALF-treated groups (147-, 35-, and 64-fold higher, respectively).

We verified the HS23/36 CPS specificity of the F-SBA response in a number of NHP responders by measuring bactericidal activity against an 81-176 mutant *C. jejuni* strain that does not express CPS (*kpsM* mutant) and in strain CG8486, which expresses an



unrelated CPS of the HS4 type (16, 18, 40). Bactericidal activity is readily detected against the HS23/36 CPS<sup>+</sup> 81-176 strain; however, there is no F-SBA response against the CPS<sup>-</sup> *kpsM* mutant or against the unrelated CG8486 strain (Fig. S1E). In addition, similar F-SBA titers were generated against the challenge strain CG8421, which also expresses a HS23/36 CPS type (Fig. S1E). Importantly, F-SBA titers measured after the third vaccination show a significant correlation with anti-CPS IgG titers measured at the same time point (Fig. 5B). To investigate the effect of bactericidal activity on disease outcome, we compared the F-SBA titers before and after the third vaccination to whether the animals did or did not develop diarrhea and found that there was a statistically significant trend toward higher F-SBA titers in animals who did not develop diarrhea after challenge (Fig. 5C). These data suggest that CPS-specific bactericidal activity may play a role in protection against *C. jejuni*-mediated diarrhea in the *A. nancymae* model.

## DISCUSSION

Given the previous lack of immunogenicity with a *C. jejuni* conjugate delivered with or without alum in humans, we sought here to identify potential immunomodulatory adjuvants to enhance both humoral and cellular immune responses to CPS conjugate vaccines in animal models. We evaluated the Army Liposome Formulation adjuvants, ALF and ALFQ, admixed with soluble CPS-CRM or the conjugate vaccine adsorbed to alum before combination with the liposome adjuvants forming ALFA or ALFQA. Initial analysis compared these adjuvants to CPS-CRM + alum. Although alum has been the adjuvant that has dominated the vaccine field for decades, there are now a number of potent adjuvants that are being evaluated and even licensed for human use. Most notably, the proprietary adjuvant system AS01 has been licensed as Shingrix (zoster vaccine recombinant; GlaxoSmithKline). AS01 is a liposome-based adjuvant formulation containing MPLA and QS-21 that is similar to the liposome adjuvants utilized in this study, specifically ALFQ. The two adjuvants that best enhanced immunogenicity to the *C. jejuni* CPS conjugate in mice and NHPs were ALF and ALFQ. Both ALF and ALFQ contain the TLR4 agonist MPLA, and ALFQ also incorporates QS-21. Although alum induced high anti-CPS IgG titers in mice at a low dose of 0.1  $\mu$ g of CPS-CRM, the response was dominated by IgG1, whereas ALF and ALFQ induced IgG2b and IgG2c CPS responses at all doses of CPS-CRM evaluated. These data are consistent with reports that MPLA favors induction of IFN- $\gamma$ -producing CD4<sup>+</sup> T cells and antibody class switching to Th1-mediated subtypes (41–44). In preliminary studies, the addition of alum to ALF and ALFQ to form ALFA and ALFQA in mice, respectively, did not provide an advantage over ALF and ALFQ and were not pursued for further analysis.

Dose escalation of the CPS-CRM vaccine with ALF and ALFQ in mice showed that high IgG titers were achieved at 1.0  $\mu$ g of CPS-CRM and were not significantly increased by escalating the levels to 2.5 or 5.0  $\mu$ g. These data suggest that potent adjuvants like ALF or ALFQ may allow dose sparing of polysaccharide conjugate vaccines, which is a noteworthy consideration for a multivalent *C. jejuni* conjugate vaccine. Our current estimate of the valency required for an effective *C. jejuni* CPS vaccine would be 8 (45; F. Poly et al., unpublished data). This is likely achievable based upon the successful licensure of the *S. pneumoniae* CPS conjugate vaccine Prevnar13, where the total amount of capsule delivered is approximately 30.8  $\mu$ g (4.4  $\mu$ g of serotype 6B saccharides and 2.2  $\mu$ g of each of the remaining 12 serotypes). Future studies will test whether inclusion of ALF or ALFQ with a multivalent *C. jejuni* conjugate vaccine might allow dose sparing of each CPS conjugate. One notable difference in the antibody response at the high 5- $\mu$ g dose of CPS-CRM + ALFQ was the generation of high levels of anti-CPS IgA antibodies (mean log<sub>10</sub> titer of 4.29). These IgA levels are higher than we had previously observed in mice vaccinated with CPS-CRM (18), although the IgA levels were lower than the IgG levels. It is not clear whether CPS-specific mucosal IgA can play a role in protection against *C. jejuni*-mediated disease since we did not measure fecal IgA. However, serum anti-CPS IgA was undetectable in CPS-CRM + ALFQ-vaccinated NHPs (data not shown), where we observed 86% PE against diarrhea, suggesting that

IgA may not be important for protection in this NHP model. Future studies will further investigate the role of anti-CPS IgA in the mouse and NHP models by measuring mucosal IgA responses.

Previous work with the prototype CPS-CRM vaccine demonstrated that the vaccine alone at approximately 2.5  $\mu\text{g}$  (based on CPS weight, 25  $\mu\text{g}$  of total conjugate weight) at 4-week intervals was protective against strain 81-176 in a mouse intranasal challenge model and 2.5  $\mu\text{g}$  of CPS-CRM + alum delivered s.c. at 6-week intervals was 100% efficacious against diarrhea in *A. nancymaae* NHPs (18). In this study, we observed reduced protective efficacy against diarrhea (29% PE) in the group given 3.5  $\mu\text{g}$  of CPS-CRM + alum and challenged with strain CG8421, but what caused reduced PE compared to the historic experiments with strain 81-176 is not clear. In this study, vaccination intervals were reduced from 6 to 4 weeks to mirror intervals in the mouse studies and to align with 4-week intervals used in the CJC1 phase 1 clinical study. Interestingly, reduced vaccination intervals had a positive effect on anti-CPS IgG titers after the third vaccination in CPS-CRM + alum-treated animals with a mean  $\log_{10}$  titer of 4.2 at 4-week intervals compared to 2.6 ( $\log_e$  titer of 6) in the historic experiment (18). PE was measured against a different *C. jejuni* strain CG8421 in this study, although the CPS type expressed by CG8421 is also of the HS23/36 type, and we have observed cross-reactivity of anti-CPS antibodies between 81-176 and CG8421 in vaccinated animals by F-SBA, Western blotting, and flow cytometry binding experiments (Fig. S1E and data not shown). Nonetheless, ALF and, to a greater extent, ALFQ enhanced the immunogenicity of the conjugate vaccine in both animal models. In NHPs, CPS-CRM + ALFQ generated the highest levels of anti-CPS IgG, CPS-specific ASCs, and the highest F-SBA titers.

We currently do not know what immune mechanism(s) provide protection from *C. jejuni*-mediated disease in the NHP model or following human infection. Humoral responses certainly play a role in protection as evidenced by persistent *C. jejuni* infections in agammaglobulinemic and immunocompromised individuals (46, 47). Bactericidal activity mediated by complement activation by *C. jejuni*-specific antibodies in serum has been reported (32–34). SBA appears as early as 36 to 48 h after the onset of diarrhea and can be detected in convalescent-phase sera 40 days later (34). Capsule conjugate vaccines have been shown to induce bactericidal activity against other Gram-negative pathogens (48–50). We hypothesize that similar to *Neisseria meningitidis*, *Haemophilus influenzae* type B, and *Shigella* conjugate vaccines, the *C. jejuni* CPS conjugate vaccine induces functional antibody titers against the CPS that can be measured in a bactericidal assay. Here, we report that SBA responses develop against the homologous 81-176 strain in mice and NHPs immunized with the CPS-CRM conjugate vaccine and that higher SBA titers in NHPs are associated with protection from diarrhea. Unlike other studies that utilize culture-based SBA methods to measure bactericidal activity, we have developed a flow cytometry-based SBA assay that allows rapid, high-throughput analysis. Due to the specialized culture requirements for *C. jejuni* growth, we experienced problems developing a culture-based SBA assay where multiple repeats were necessary due to control failures. The F-SBA method is time-conserving and serum-sparing. These methods can be easily adapted to measure bactericidal responses against different *C. jejuni* strains, other bacteria, and in multiple animal models and is currently being developed for human sera. We report here that the CPS-CRM vaccine delivered without an adjuvant does not induce functional bactericidal responses in mice. Only with the addition of ALF and ALFQ does SBA activity develop, likely due to the generation of CPS-specific IgG2b and IgG2c that are present in ALF- and ALFQ-adjuvanted mice, but not in animals receiving vaccine alone. We observed a significant correlation between SBA and anti-CPS IgG2b and IgG2c titers ( $P \leq 0.0001$ ; Pearson  $r = 0.60$  and  $0.62$ , respectively). In NHPs, CPS-CRM delivered with alum, ALF, and ALFQ induced bactericidal activity against 81-176. The SBA activity was CPS specific since F-SBA titers correlated with the anti-CPS IgG response and higher SBA titers were associated with protection from diarrhea after three immunizations. Because *A. nancymaae* is an understudied NHP model, IgG subclasses have not yet been

identified, and there are no reagents available to measure these responses. No SBA responses were measurable against a nonencapsulated 81-176 mutant, indicating that anti-CPS antibodies alone are able to bind CPS and activate the complement cascade to kill wild-type *C. jejuni*. Although complement-dependent activity was previously described following infection in humans (33, 34), the target(s) of the functional antibody response remains unidentified. Antigens suggested as targets include outer membrane proteins and flagellin, although there is no direct evidence that antibodies specific for any one *C. jejuni* protein are bactericidal. *C. jejuni*'s outermost surface is covered by CPS, and we report here for the first time that vaccination with a conjugate vaccine induces CPS-specific antibodies with bactericidal activity against *C. jejuni*. Future studies with multivalent *C. jejuni* capsule conjugate vaccine will measure SBA responses against multiple CPS types and look for potential association with protection.

One of the most striking effects of the ALF liposome adjuvants was their effect on T cell responses measured in mice. While it was evident from the production of anti-CPS IgG2b and IgG2c titers measured in the serum that both ALF and ALFQ induced Th1 cell development, phenotypic analysis revealed a striking difference in the quantity and quality of the T cell response between these two adjuvants. The inclusion of QS-21 in the ALFQ adjuvant significantly enhanced the development of multifunctional CD4<sup>+</sup> T cell responses to the carrier protein CRM in mice to a greater extent than ALF. ALFQ induced higher levels of Th1 cytokines compared to vaccine alone and vaccine plus ALF, with the most notable increase observed in IFN- $\gamma$ <sup>+</sup> IL-2<sup>+</sup> TNF- $\alpha$ <sup>+</sup> triple-producing Th1 cells. Interestingly, ALFQ also induced higher levels of IL-4<sup>+</sup> IL-10<sup>+</sup> Th2 cells and the production of IL-17 measured in cell supernatants. Further phenotypic analysis is needed to determine whether ALFQ specifically induces Th17 cell development or if IL-17 production is being produced by a different cell subset. Nonetheless, this study sheds light on ALFQ as a potent adjuvant to enhance T cell responses. We were unable to measure T cell responses in *A. nancymaae* due to limited sample availability and because few T cell assays and reagents have been developed for this NHP model. Nonetheless, enhanced T cell responses in *A. nancymaae* are inferred in this model in CPS-CRM + ALFQ-immunized animals, as evidenced by higher CPS-specific IgG levels and significantly higher numbers of ASCs measured in peripheral blood. Future work in clinical studies will focus on defining T cell responses to CPS-CRM plus ALFQ to include Th1, Th2, and Th17 development, as well as antigen-specific T follicular helper responses.

Taken together, these studies demonstrate that ALF and ALFQ liposome-based adjuvants are compatible with a bacterial polysaccharide conjugate vaccine platform. ALF and, to a greater extent, ALFQ significantly enhanced anti-polysaccharide antibody responses, which lends promise to their usefulness to induce immunity to polysaccharide antigens in traditionally difficult populations such as children or the elderly. In addition, ALFQ administration with CRM-containing conjugate vaccines may overcome any immune cell anergy or interference in humans from earlier administration of childhood diphtheria-containing vaccines. CRM<sub>197</sub> was chosen for our prototype *C. jejuni* polysaccharide conjugate vaccine due to its well-characterized and safe use as a licensed carrier protein. There are now many reports using alternate carrier proteins in an effort to include other important antigenic targets and expand the effectiveness of conjugate vaccines (51–54). The administration of ALFQ with our recently developed multipathogen conjugate vaccine platform combining *C. jejuni* and *Shigella* polysaccharides with recombinant enterotoxigenic *Escherichia coli* tip-adhesin proteins (55) has great potential to enhance vaccine-mediated immunity to not only *C. jejuni* but also two other important enteric pathogens.

## MATERIALS AND METHODS

**Ethics statement.** All animal experiments were performed under an Institutional Animal Care and Use Committee (IACUC) approved protocol at the Naval Medical Research Center (mouse) or NAMRU-6, Peru (*A. nancymaae*), in compliance with all applicable Federal regulations governing the protection of animals in research.

**Bacterial strains and growth conditions.** *C. jejuni* strains 81-176 and CG8421 have been described previously, and both express an HS23/36 CPS type (37). For the bactericidal assays, *C. jejuni* strain 81-176 was grown on Muller-Hinton (MH) agar plates (MH broth [21 g/liter] and Bacto agar [15 g/liter]; BD, Sparks, MD) at 37°C in a microaerobic environment (nitrogen, 85%; carbon dioxide, 10%; oxygen, 5%) for 20 h. Cells were harvested in dextrose-gelatin-Veronal buffer (DGV; Lonza, Walkersville, MD) and set to an optical density at 600 nm of 0.1, equivalent to a concentration of  $3 \times 10^8$  CFU/ml. For the *A. nancymae* challenge, *C. jejuni* strain CG8421 was grown on MH plates at 42°C under microaerobic conditions and expanded over a 2-day period. Bacteria from MH plates were pooled in ice-cold PBS, and the concentration was adjusted photometrically with PBS to reach the target dose of  $5 \times 10^{11}$  CFU in 5 ml. The actual doses determined by serial dilution onto MH plates were  $4.3 \times 10^{11}$  and  $4.5 \times 10^{11}$  CFU in cohorts 1 and 2, respectively.

**Capsule conjugate vaccine.** Capsules were extracted from strain 81-176 and conjugated to CRM<sub>197</sub> as previously described (18). The CPS content was determined by anthrone assay (56), and the protein content was determined by a bicinchoninic acid assay. Two lots of vaccines (batch 4 and CJC1) were produced by Dalton Pharma Services (Toronto, Ontario, Canada) under contract.

**Vaccine and adjuvant formulations.** The following CPS-CRM vaccines were utilized: lot CJC1 for all mouse studies and lot batch 4 for *A. nancymae* studies. Lyophilized CPS-CRM was reconstituted in sterile water to an isotonic concentration. ALF and ALF plus QS-21 (ALFQ) were prepared by the U.S. Military HIV Research Program and have been described previously (21, 57, 58). Mouse doses of ALF and ALFQ contained 20 µg/mouse 3D-PHAD and 10 µg/mouse QS-21. *A. nancymae* doses of ALF and ALFQ contained 50 µg/NHP 3D-PHAD and 25 µg/NHP QS-21. For formulation with ALF or ALFQ, reconstituted CPS-CRM was added to dried liposomes or liquid formulation, respectively. For ALFA and ALFQA formulations, 0.1 µg of reconstituted CPS-CRM was adsorbed to 30 µg of alum (Brenntag Biosector; Brenntag, Frederikssund, Denmark) for 1 h at room temperature before being added to dried ALF or liquid ALFQ liposomes. All ALF, ALFQ, ALFA, and ALFQA formulations were vortexed at a slow speed for 10 min at room temperature and then incubated at 4°C for an additional hour with occasional shaking. Mouse vaccines were delivered in a total volume of 50 µl per dose. Each CJC1 conjugate dose contained a total of 0.1, 1.0, 2.5, or 5.0 µg based on CPS weight. *A. nancymae* vaccines were delivered in a total volume of 500 µl per dose for CPS-CRM + alum and 250 µl per dose for the PBS sham, CPS-CRM + ALF, or CPS-CRM + ALFQ treatment groups. Each CPS-CRM batch 4 conjugate dose contained a total of 3.5 µg based on CPS weight. A total of 300 µg/NHP of alum was adsorbed to CPS-CRM (batch 4) in the *A. nancymae* study.

**Animal immunizations.** Groups of five 6- to 8-week-old female C57BL6/J mice (The Jackson Laboratory, Bar Harbor, ME) were immunized i.m. in alternating rear thighs at 0, 4, and 8 weeks. Mice were tail bled 2 weeks after each immunization and bled by cardiac puncture without recovery 2 weeks after the third immunization. *A. nancymae* NHPs (captive-born) were purchased from the Instituto Veterinario de Investigaciones Tropicales y de Altura (Iquitos, Peru). Male and female animals (29 male, 28 female; average age, 15 months; weight, 670 to 980 g) were randomized into vaccine or control groups before immunization. The animals were stool culture negative for *Campylobacter* and seronegative (i.e., IgG titer < 1:400) against glycine-extracted surface antigens of *C. jejuni* strain CG8421, as measured by enzyme-linked immunosorbent assay (ELISA) (59). Prior to immunizations or blood draw, NHPs were anesthetized with ketamine hydrochloride (10 mg/kg). Vaccine plus ALF or ALFQ or PBS was administered i.m. in 250 µl in alternating thighs, and vaccine plus alum was administered s.c. at 0, 4, and 8 weeks. NHP studies were separated into two cohorts due to facility size restrictions: cohort 1 was composed of CPS-CRM + alum ( $n = 10$ ), CPS-CRM + ALF ( $n = 10$ ), or PBS ( $n = 9$ ) treatments, and cohort 2 was composed of CPS-CRM + ALF ( $n = 7$ ), CPS-CRM + ALFQ ( $n = 10$ ), or PBS ( $n = 11$ ) treatments.

**Oral challenge of *A. nancymae* with CG8421.** NHPs were challenged with  $5 \times 10^{11}$  CFU of strain CG8421 delivered in 5.0 ml saline via an oral-gastric tube with procedures as previously described for challenge with *C. jejuni* strain 81-176 (18, 36). Stools were monitored three times daily for 10 days for signs of diarrhea. Animals with two consecutive days of loose to watery stools met the endpoint criteria of diarrhea. *C. jejuni* colonization was monitored daily for 10 days by serially diluting stool in PBS and cultured on BBL *Campylobacter* CSM agar (BD) with CCDA selective supplement (Thermo Fisher, Waltham, MA) under microaerobic conditions at 42°C for 48 h.

**Anti-CPS ELISA.** Anti-CPS total IgG or IgG subclass analysis was performed using oxidized CPS and Carbo-BIND plates as previously described (60). The following horseradish peroxidase-conjugated secondary antibodies were used for detection: goat anti-mouse IgG or goat anti-mouse IgA and *A. nancymae* anti-CPS IgG responses were measured using goat anti-human IgG (SeraCare, Gaithersburg, MD). Mouse IgG subclass secondary antibodies and isotype controls were purchased from SouthernBiotech (Birmingham, AL).

**Mouse splenocyte restimulation and T cell cytokine expression analysis.** Single-cell suspensions from individual mouse spleens were generated, and  $5 \times 10^5$  cells per well were cultured in duplicate in complete Dulbecco modified Eagle medium (cDMEM) with either cDMEM alone, 5 µg/ml CPS-CRM (based on protein content), or on immobilized 0.5 µg of anti-CD3 (145-2C11) plus 0.1 µg of anti-CD28 (37.51) at 37°C in 5% CO<sub>2</sub>. Supernatants were harvested after 72 h and analyzed using a Bio-Plex mouse cytokine Th1/Th2 kit spiked with IL-17A, and plates were read using a Bio-Plex 100 (Bio-Rad, Hercules, CA). Cytokine expression was normalized by subtracting the pg/ml in control medium-alone wells from CPS-CRM-restimulated wells.

T cell phenotypic analysis was performed on splenocytes stimulated for 24 h under the conditions described above. After 18 h, GolgiPlug and GolgiStop (BD Biosciences) were added for the last 5 h of culture. Samples were fixed in formaldehyde, Fc blocked with anti-CD16/32 (93), and then surface stained

with the antibodies TCR $\beta$  (H57-597), CD4 (GK1.5), and CD8 $\alpha$  (53-6.7). Cells were permeabilized with BD Perm/Wash buffer (BD Biosciences) and stained intracellularly with IL-2 (JES6-5H4), IL-4 (11B11), IL-10 (JES5-16E3), IFN- $\gamma$  (XMG1.2), and TNF- $\alpha$  (MP6-XT22). Data were acquired using a LSRFortessa (BD Biosciences) and analyzed using FlowJo 10 software (Tree Star, Ashland, OR). CD4<sup>+</sup> TCR $\beta$ <sup>+</sup> T cells were gated on cytokine positive cells, and Boolean gating analysis was applied to determine multifunctional T cell populations.

**A. *nancymae* PBMC isolation and ELISPOT analysis.** To isolate PBMCs, whole blood by density gradient centrifugation was performed. Freshly isolated PBMCs were directly used in an ELISPOT assay. Multiscreen HTS plates (Millipore, catalog no. MSIPS4W10) were coated with CPS conjugated to bovine serum albumin at a concentration of 15  $\mu$ g/ml diluted in 1 $\times$  PBS overnight at 4°C. Plates were blocked for 1 h with complete RPMI. Freshly isolated PBMCs were added at  $0.5 \times 10^6$  cells/well, followed by incubation overnight at 37°C and 5% CO<sub>2</sub>. Plates were washed three times with 1 $\times$  PBS–0.05% Tween and incubated for 3 h at room temperature with anti-human IgG (SeraCare, catalog no. 474-1006). Spots were developed using TMB substrate (Mabtech, Cincinnati, OH). The number of CPS-specific antigen-secreting cells (ASCs) are expressed as the number of CPS-specific IgG ASCs per 10<sup>6</sup> PBMC.

**Serum bactericidal assay.** Heat-inactivated (HI) sera were serially diluted in DGV in a 96-well plate, and baby rabbit complement (BRC [Cedarlane, Burlington, NC]; 4 or 6% by volume for NHP or mice, respectively) was added to a total volume of 90  $\mu$ l. Then, 10  $\mu$ l of  $3 \times 10^8$  CFU/ml ( $3 \times 10^6$  CFU) 81-176 was added to serum + BRC (final volume, 100  $\mu$ l), followed by incubation at 37°C for 1 h. Next, 100  $\mu$ l of a propidium iodide (PI; Molecular Probes, Eugene, OR) dye solution was added directly to the wells, followed by incubation at room temperature for 15 min in the dark. Samples were acquired immediately after PI staining on a FACSCanto II cytometer (BD), and the percentages of PI<sup>+</sup> 81-176 cells in controls and experimental SBA samples were analyzed using FlowJo. The data were normalized to the control for the amount of nonspecific killing by HI sera alone by subtracting the percentage of PI<sup>+</sup> cells in the HI sera without BRC (0%) from the percentage of PI<sup>+</sup> cells in HI sera plus BRC at each serum dilution. The normalized percentage of PI<sup>+</sup> cells was plotted versus the log<sub>10</sub> serum dilution and analyzed by four-parameter logistic curve fitting model for four-parameter logistic (4PL) analysis using Prism (v7; GraphPad, La Jolla, CA), and the F-SBA titer was defined as the calculated 50% inhibitory concentration (IC<sub>50</sub>).

**Statistics.** Data points were analyzed using GraphPad Prism (v7). ELISA and F-SBA titers were log<sub>10</sub> transformed. Paired *t* tests were used to compare preimmune to postimmune titers. A repeated-measure one-way analysis of variance (ANOVA) with Tukey's multiplicity-adjusted *P* values was used to compare titers at different time points among a vaccine group. An ordinary one-way ANOVA with Tukey's multiplicity-adjusted *P* values was used to test for statistical significance for data sets with multiple groups. *P* values if  $\leq 0.05$  were considered statistically significant. The Pearson's correlation coefficient was used to describe the correlation between 81-176 F-SBA and anti-CPS IgG ELISA titers. For all NHP experiments, the proportion of animals with diarrhea in each test group was compared to that in the control PBS group with a Fisher exact test. Frequency analyses were not adjusted for multiple comparisons.

## SUPPLEMENTAL MATERIAL

Supplemental material for this article may be found at <https://doi.org/10.1128/mSphere.00101-19>.

**TEXT S1**, DOCX file, 0.03 MB.

**FIG S1**, TIF file, 1.1 MB.

**FIG S2**, EPS file, 0.2 MB.

**FIG S3**, EPS file, 0.1 MB.

## ACKNOWLEDGMENTS

This study was funded by Navy Work Unit 6000.RAD1.DA3.A0308.

A.R., R.M.L., F.P., A.J.M., and P.G. designed all experiments and prepared the manuscript. Z.B., G.R.M., and C.R.A. provided expertise and all ALF adjuvant materials. N.M.S., C.L.G., H.E., G.N., N.E., M.N., R.C., and J.R. performed animal experiments and collected and analyzed all data.

The views expressed here are those of the authors and do not necessarily reflect the official policy or position of the Department of the Navy, the Department of the Army, the Department of Defense, or the U.S. government. G.R.M., F.P., and P.G. are/were employees of the U.S. government, and this work was performed as part of their official duties. Title 17 USC 105 provides that "copyright protection under this title is not available for any work of the United States government." Title 17 USC 101 defines a U.S. government work as a work prepared by an employee of the U.S. government as part of that person's official duties.


P.G. is a coinventor on a capsule conjugate vaccine patent. C.R.A. is a coinventor on pending patents for ALFQ and ALFA, and Z.B. is a coinventor on ALFQ.

## REFERENCES

- Amour C, Gratz J, Mduma E, Svensen E, Rogawski ET, McGrath M, Seidman JC, McCormick BJ, Shrestha S, Samie A, Mahfuz M, Qureshi S, Hotwani A, Babji S, Trigoso DR, Lima AA, Bodhidatta L, Bessong P, Ahmed T, Shakoor S, Kang G, Kosek M, Guerrant RL, Lang D, Gottlieb M, Houpt ER, Platts-Mills JA, Etiology Risk Factors, Interactions of Enteric Infections and Malnutrition and the Consequences for Child Health Development Project Network Investigators. 2016. Epidemiology and impact of campylobacter infection in children in 8 low-resource settings: results from the MAL-ED Study. *Clin Infect Dis* 63:1171–1179. <https://doi.org/10.1093/cid/ciw542>.
- Coker AO, Isokpehi RD, Thomas BN, Amisu KO, Obi CL. 2002. Human campylobacteriosis in developing countries. *Emerg Infect Dis* 8:237–244. <https://doi.org/10.3201/eid0803.010233>.
- Kotloff KL, Nataro JP, Blackwelder WC, Nasrin D, Farag TH, Panchalingam S, Wu Y, Sow SO, Sur D, Breiman RF, Faruque AS, Zaidi AK, Saha D, Alonso PL, Tamboura B, Sanogo D, Onwuchekwa U, Manna B, Ramamurthy T, Kanungo S, Ochieng JB, Omere R, Oundo JO, Hossain A, Das SK, Ahmed S, Qureshi S, Quadri F, Adegbola RA, Antonio M, Hossain MJ, Akinsola A, Mandomando I, Nhampossa T, Acacio S, Biswas K, O'Reilly CE, Mintz ED, Berkeley LY, Muhsen K, Sommerfelt H, Robins-Browne RM, Levine MM. 2013. Burden and aetiology of diarrhoeal disease in infants and young children in developing countries (the Global Enteric Multicenter Study, GEMS): a prospective, case-control study. *Lancet* 382:209–222. [https://doi.org/10.1016/S0140-6736\(13\)60844-2](https://doi.org/10.1016/S0140-6736(13)60844-2).
- Platts-Mills JA, Babji S, Bodhidatta L, Gratz J, Haque R, Havt A, McCormick BJ, McGrath M, Olortegui MP, Samie A, Shakoor S, Mondal D, Lima IF, Hariraju D, Rayamajhi BB, Qureshi S, Kabir F, Yori PP, Mufamadi B, Amour C, Carreon JD, Richard SA, Lang D, Bessong P, Mduma E, Ahmed T, Lima AA, Mason CJ, Zaidi AK, Bhutta ZA, Kosek M, Guerrant RL, Gottlieb M, Miller M, Kang G, Houpt ER, Investigators M-E. 2015. Pathogen-specific burdens of community diarrhoea in developing countries: a multisite birth cohort study (MAL-ED). *Lancet Glob Health* 3:e564–e575. [https://doi.org/10.1016/S2214-109X\(15\)00151-5](https://doi.org/10.1016/S2214-109X(15)00151-5).
- Pope JE, Krizova A, Garg AX, Thiessen-Philbrook H, Ouimet JM. 2007. Campylobacter reactive arthritis: a systematic review. *Semin Arthritis Rheum* 37:48–55. <https://doi.org/10.1016/j.semarthrit.2006.12.006>.
- Yuki N. 2010. Human gangliosides and bacterial lipo-oligosaccharides in the development of autoimmune neuropathies. *Methods Mol Biol* 600: 51–65. [https://doi.org/10.1007/978-1-60761-454-8\\_4](https://doi.org/10.1007/978-1-60761-454-8_4).
- Mortensen NP, Kuijff ML, Ang CW, Schiellerup P, Krogfelt KA, Jacobs BC, van Belkum A, Endtz HP, Bergman MP. 2009. Sialylation of *Campylobacter jejuni* lipo-oligosaccharides is associated with severe gastro-enteritis and reactive arthritis. *Microbes Infect* 11:988–994. <https://doi.org/10.1016/j.micinf.2009.07.004>.
- Nachamkin I, Szymanski CM, Blaser MJ. 2008. *Campylobacter*, 3rd ed. ASM Press, Washington, DC.
- Marshall JK, Thabane M, Garg AX, Clark WF, Salvadori M, Collins SM, Walkerton Health Study Investigators. 2006. Incidence and epidemiology of irritable bowel syndrome after a large waterborne outbreak of bacterial dysentery. *Gastroenterology* 131:445–450. quiz 660. <https://doi.org/10.1053/j.gastro.2006.05.053>.
- Engberg J, Neimann J, Nielsen EM, Aerestrup FM, Fussing V. 2004. Quinolone-resistant *Campylobacter* infections: risk factors and clinical consequences. *Emerg Infect Dis* 10:1056–1063. <https://doi.org/10.3201/eid1006.030669>.
- Pickering LK. 2004. Antimicrobial resistance among enteric pathogens. *Semin Pediatr Infect Dis* 15:71–77. <https://doi.org/10.1053/j.spid.2004.01.009>.
- Ruiz J, Marco F, Oliveira I, Vila J, Gascon J. 2007. Trends in antimicrobial resistance in *Campylobacter* spp. causing traveler's diarrhea. *APMIS* 115: 218–224. [https://doi.org/10.1111/j.1600-0463.2007.apm\\_567.x](https://doi.org/10.1111/j.1600-0463.2007.apm_567.x).
- Karlyshev AV, Linton D, Gregson NA, Lastovica AJ, Wren BW. 2000. Genetic and biochemical evidence of a *Campylobacter jejuni* capsular polysaccharide that accounts for Penner serotype specificity. *Mol Microbiol* 35:529–541.
- Penner JL, Hennessy JN. 1980. Passive hemagglutination technique for serotyping *Campylobacter fetus* subsp. *jejuni* on the basis of soluble heat-stable antigens. *J Clin Microbiol* 12:732–737.
- Poly F, Serichantalergs O, Kuroiwa J, Pootong P, Mason C, Guerry P, Parker CT. 2015. Updated *Campylobacter jejuni* capsule PCR multiplex typing system and its application to clinical isolates from South and Southeast Asia. *PLoS One* 10:e0144349. <https://doi.org/10.1371/journal.pone.0144349>.
- Bacon DJ, Szymanski CM, Burr DH, Silver RP, Alm RA, Guerry P. 2001. A phase-variable capsule is involved in virulence of *Campylobacter jejuni* 81-176. *Mol Microbiol* 40:769–777. <https://doi.org/10.1046/j.1365-2958.2001.02431.x>.
- Maue AC, Mohawk KL, Giles DK, Poly F, Ewing CP, Jiao Y, Lee G, Ma Z, Monteiro MA, Hill CL, Ferderber JS, Porter CK, Trent MS, Guerry P. 2013. The polysaccharide capsule of *Campylobacter jejuni* modulates the host immune response. *Infect Immun* 81:665–672. <https://doi.org/10.1128/IAI.01008-12>.
- Monteiro MA, Baqar S, Hall ER, Chen YH, Porter CK, Bentzel DE, Applebee L, Guerry P. 2009. Capsule polysaccharide conjugate vaccine against diarrheal disease caused by *Campylobacter jejuni*. *Infect Immun* 77: 1128–1136. <https://doi.org/10.1128/IAI.01056-08>.
- Poly F, Noll AJ, Riddle MS, Porter CK. 2018. Update on *Campylobacter* vaccine development. *Hum Vaccin Immunother* 25:1–12. <https://doi.org/10.1080/21645515.2018.1528410>.
- Beck Z, Matyas GR, Jalah R, Rao M, Polonis VR, Alving CR. 2015. Differential immune responses to HIV-1 envelope protein induced by liposomal adjuvant formulations containing monophosphoryl lipid A with or without QS21. *Vaccine* 33:5578–5587. <https://doi.org/10.1016/j.vaccine.2015.09.001>.
- Genito CJ, Beck Z, Phares TW, Kalle F, Limbach KJ, Stefaniak ME, Patterson NB, Bergmann-Leitner ES, Waters NC, Matyas GR, Alving CR, Dutta S. 2017. Liposomes containing monophosphoryl lipid A and QS-21 serve as an effective adjuvant for soluble circumsporozoite protein malaria vaccine FMP013. *Vaccine* 35:3865–3874. <https://doi.org/10.1016/j.vaccine.2017.05.070>.
- Seth L, Bingham Ferlez KM, Kaba SA, Musser DM, Emadi S, Matyas GR, Beck Z, Alving CR, Burkhard P, Lanar DE. 2017. Development of a self-assembling protein nanoparticle vaccine targeting *Plasmodium falciparum* circumsporozoite protein delivered in three arm liposome formulation adjuvants. *Vaccine* 35:5448–5454. <https://doi.org/10.1016/j.vaccine.2017.02.040>.
- Zollinger WD, Babcock JG, Moran EE, Brandt BL, Matyas GR, Wassef NM, Alving CR. 2012. Phase I study of a *Neisseria meningitidis* liposomal vaccine containing purified outer membrane proteins and detoxified lipooligosaccharide. *Vaccine* 30:712–721. <https://doi.org/10.1016/j.vaccine.2011.11.084>.
- Torres OB, Matyas GR, Rao M, Peachman KK, Jalah R, Beck Z, Michael NL, Rice KC, Jacobson AE, Alving CR. 2017. Heroin-HIV-1 (H2) vaccine: induction of dual immunologic effects with a heroin hapten-conjugate and an HIV-1 envelope V2 peptide with liposomal lipid A as an adjuvant. *NPJ Vaccines* 2:13. <https://doi.org/10.1038/s41541-017-0013-9>.
- Li H, Willingham SB, Ting JP, Re F. 2008. Cutting edge: inflammasome activation by alum and alum's adjuvant effect are mediated by NLRP3. *J Immunol* 181:17–21. <https://doi.org/10.4049/jimmunol.181.1.17>.
- Marty-Roix R, Vladimer GI, Pouliot K, Weng D, Buglione-Corbett R, West K, MacMicking JD, Chee JD, Wang S, Lu S, Lien E. 2016. Identification of QS-21 as an inflammasome-activating molecular component of saponin adjuvants. *J Biol Chem* 291:1123–1136. <https://doi.org/10.1074/jbc.M115.683011>.
- World Health Organization. 1976. Requirements for meningococcal polysaccharide vaccine. World Health Organization, Geneva, Switzerland.
- Wong KH, Barrera O, Sutton A, May J, Hochstein DH, Robbins JD, Robbins JB, Parkman PD, Seligmann EB, Jr. 1977. Standardization and control of meningococcal vaccines, group A and group C polysaccharides. *J Biol Stand* 5:197–215. [https://doi.org/10.1016/S0092-1157\(77\)80005-X](https://doi.org/10.1016/S0092-1157(77)80005-X).
- Campbell JD, Edelman R, King JC, Jr, Papa T, Ryall R, Rennels MB. 2002. Safety, reactogenicity, and immunogenicity of a tetravalent meningococcal polysaccharide-diphtheria toxoid conjugate vaccine given to healthy adults. *J Infect Dis* 186:1848–1851. <https://doi.org/10.1086/345763>.
- Gill CJ, Baxter R, Anemona A, Ciavarrò G, Dull P. 2010. Persistence of immune responses after a single dose of Novartis meningococcal serogroup A, C, W-135 and Y CRM-197 conjugate vaccine (Menveo®) or Menaactra® among healthy adolescents. *Hum Vaccin* 6:881–887. <https://doi.org/10.4161/hv.6.11.12849>.
- World Health Organization. 1999. Standardization and validation of serological assays for evaluation of immune responses to *Neisseria*

- meningitidis serogroup A/C vaccines. World Health Organization, Geneva, Switzerland.
32. Jones DM, Eldridge J, Dale B. 1980. Serological response to *Campylobacter jejuni/coli* infection. *J Clin Pathol* 33:767–769. <https://doi.org/10.1136/jcp.33.8.767>.
  33. Blaser MJ, Smith PF, Kohler PF. 1985. Susceptibility of *Campylobacter* isolates to the bactericidal activity of human serum. *J Infect Dis* 151:227–235. <https://doi.org/10.1093/infdis/151.2.227>.
  34. Pennie RA, Pearson RD, Barrett LJ, Lior H, Guerrant RL. 1986. Susceptibility of *Campylobacter jejuni* to strain-specific bactericidal activity in sera of infected patients. *Infect Immun* 52:702–706.
  35. Giallourou N, Medlock GL, Bolick DT, Medeiros PH, Ledwaba SE, Kolling GL, Tung K, Guerry P, Swann JR, Guerrant RL. 2018. A novel mouse model of *Campylobacter jejuni* enteropathy and diarrhea. *PLoS Pathog* 14:e1007083. <https://doi.org/10.1371/journal.ppat.1007083>.
  36. Jones FR, Baqar S, Gozalo A, Nunez G, Espinoza N, Reyes SM, Salazar M, Meza R, Porter CK, Walz SE. 2006. New World monkey *Aotus nancymaae* as a model for *Campylobacter jejuni* infection and immunity. *Infect Immun* 74:790–793. <https://doi.org/10.1128/IAI.74.1.790-793.2006>.
  37. Poly F, Read TD, Chen YH, Monteiro MA, Serichantalergs O, Pootong P, Bodhidatta L, Mason CJ, Rockabrand D, Baqar S, Porter CK, Tribble D, Darsley M, Guerry P. 2008. Characterization of two *Campylobacter jejuni* strains for use in volunteer experimental-infection studies. *Infect Immun* 76:5655–5667. <https://doi.org/10.1128/IAI.00780-08>.
  38. Tribble DR, Baqar S, Scott DA, Oplinger ML, Trespalacios F, Rollins D, Walker RI, Clements JD, Walz S, Gibbs P, Burg EF, III, Moran AP, Applebee L, Bourgeois AL. 2010. Assessment of the duration of protection in *Campylobacter jejuni* experimental infection in humans. *Infect Immun* 78:1750–1759. <https://doi.org/10.1128/IAI.01021-09>.
  39. Tribble DR, Baqar S, Carmolli MP, Porter C, Pierce KK, Sadigh K, Guerry P, Larsson CJ, Rockabrand D, Ventone CH, Poly F, Lyon CE, Dakdouk S, Fingar A, Gilliland T, Daunais P, Jones E, Rymarchyk S, Huston C, Darsley M, Kirkpatrick BD. 2009. *Campylobacter jejuni* strain CG8421: a refined model for the study of campylobacteriosis and evaluation of *Campylobacter* vaccines in human subjects. *Clin Infect Dis* 49:1512–1519. <https://doi.org/10.1086/644622>.
  40. Chen YH, Poly F, Pakulski Z, Guerry P, Monteiro MA. 2008. The chemical structure and genetic locus of *Campylobacter jejuni* CG8486 (serotype HS:4) capsular polysaccharide: the identification of 6-deoxy-D-idoheptopyranose. *Carbohydr Res* 343:1034–1040. <https://doi.org/10.1016/j.carres.2008.02.024>.
  41. Casella CR, Mitchell TC. 2008. Putting endotoxin to work for us: monophosphoryl lipid A as a safe and effective vaccine adjuvant. *Cell Mol Life Sci* 65:3231–3240. <https://doi.org/10.1007/s00018-008-8228-6>.
  42. Fattom A, Li X, Cho YH, Burns A, Hawwari A, Shepherd SE, Coughlin R, Winston S, Naso R. 1995. Effect of conjugation methodology, carrier protein, and adjuvants on the immune response to *Staphylococcus aureus* capsular polysaccharides. *Vaccine* 13:1288–1293. [https://doi.org/10.1016/0264-410X\(95\)00052-3](https://doi.org/10.1016/0264-410X(95)00052-3).
  43. Moore A, McCarthy L, Mills KH. 1999. The adjuvant combination monophosphoryl lipid A and QS21 switches T cell responses induced with a soluble recombinant HIV protein from Th2 to Th1. *Vaccine* 17:2517–2527. [https://doi.org/10.1016/S0264-410X\(99\)00062-6](https://doi.org/10.1016/S0264-410X(99)00062-6).
  44. Neuzil KM, Johnson JE, Tang YW, Prieels JP, Slaoui M, Gar N, Graham BS. 1997. Adjuvants influence the quantitative and qualitative immune response in BALB/c mice immunized with respiratory syncytial virus FG subunit vaccine. *Vaccine* 15:525–532. [https://doi.org/10.1016/S0264-410X\(97\)00218-1](https://doi.org/10.1016/S0264-410X(97)00218-1).
  45. Pike BL, Guerry P, Poly F. 2013. Global distribution of *Campylobacter jejuni* Penner serotypes: a systematic review. *PLoS One* 8:e67375. <https://doi.org/10.1371/journal.pone.0067375>.
  46. Freeman AF, Holland SM. 2007. Persistent bacterial infections and primary immune disorders. *Curr Opin Microbiol* 10:70–75. <https://doi.org/10.1016/j.mib.2006.11.005>.
  47. Johnson RJ, Nolan C, Wang SP, Shelton WR, Blaser MJ. 1984. Persistent *Campylobacter jejuni* infection in an immunocompromised patient. *Ann Intern Med* 100:832–834. <https://doi.org/10.7326/0003-4819-100-6-832>.
  48. Kayhty H, Makela O, Eskola J, Saarinen L, Seppala I. 1988. Isotype distribution and bactericidal activity of antibodies after immunization with *Haemophilus influenzae* type b vaccines at 18-24 months of age. *J Infect Dis* 158:973–982. <https://doi.org/10.1093/infdis/158.5.973>.
  49. Miller E, Salisbury D, Ramsay M. 2001. Planning, registration, and implementation of an immunization campaign against meningococcal serogroup C disease in the UK: a success story. *Vaccine* 20(Suppl 1):S58–S67. [https://doi.org/10.1016/S0264-410X\(01\)00299-7](https://doi.org/10.1016/S0264-410X(01)00299-7).
  50. Riddle MS, Kaminski RW, Di Paolo C, Porter CK, Gutierrez RL, Clarkson KA, Weerts HE, Duplessis C, Castellano A, Alaimo C, Paolino K, Gormley R, Gambillara Fonck V. 2016. Safety and immunogenicity of a candidate bioconjugate vaccine against *Shigella flexneri* 2a administered to healthy adults: a single-blind, randomized phase I study. *Clin Vaccine Immunol* 23:908–917. <https://doi.org/10.1128/CI.00224-16>.
  51. Prymula R, Peeters P, Chrobok V, Kriz P, Novakova E, Kaliskova E, Kohl I, Lommel P, Poolman J, Prieels J-P, Schuerman L. 2006. Pneumococcal capsular polysaccharides conjugated to protein D for prevention of acute otitis media caused by both *Streptococcus pneumoniae* and nontypable *Haemophilus influenzae*: a double blind efficacy study. *Lancet* 367:740–748. [https://doi.org/10.1016/S0140-6736\(06\)68304-9](https://doi.org/10.1016/S0140-6736(06)68304-9).
  52. Yang H-H, Mascuch SJ, Madoff LC, Paoletti LC. 2008. Recombinant group B streptococcus alpha-like protein 3 is an effective immunogen and carrier protein. *Clin Vaccine Immunol* 15:1035–1041. <https://doi.org/10.1128/CI.00030-08>.
  53. Baraldo K, Mori E, Bartoloni A, Petracca R, Giannozzi A, Norelli F, Rappuoli R, Grandi G, Del Giudice G. 2004. N19 polyepitope as a carrier for enhanced immunogenicity and protective efficacy of meningococcal conjugate vaccines. *Infect Immun* 72:4884–4887. <https://doi.org/10.1128/IAI.72.8.4884-4887.2004>.
  54. Szu SL, Schneerson R, Vickers JH, Bryla D, Robbins JB. 1989. Comparative immunogenicities of Vi polysaccharide protein conjugates composed of cholera toxin or its B subunit as a carrier bound to high or lower molecular weight Vi. *Infect Immun* 57:3823–3827.
  55. Laird RM, Ma Z, Dorabawila N, Pequegnat B, Omari E, Liu Y, Maue AC, Poole ST, Maciel M, Satish K, Garipey CL, Schumack NM, McVeigh AL, Poly F, Ewing CP, Prouty MG, Monteiro MA, Savarino SJ, Guerry P. 2018. Evaluation of a conjugate vaccine platform against enterotoxigenic *Escherichia coli* (ETEC), *Campylobacter jejuni*, and *Shigella*. *Vaccine* 36:6695–6702. <https://doi.org/10.1016/j.vaccine.2018.09.052>.
  56. Leyva A, Quintana A, Sanchez M, Rodriguez EN, Cremata J, Sanchez JC. 2008. Rapid and sensitive anthrone-sulfuric acid assay in microplate format to quantify carbohydrate in biopharmaceutical products: method development and validation. *Biologicals* 36:134–141. <https://doi.org/10.1016/j.biologicals.2007.09.001>.
  57. Matyas GR, Muderhwa JM, Alving CR. 2003. Oil-in-water liposomal emulsions for vaccine delivery. *Methods Enzymol* 373:34–50. [https://doi.org/10.1016/S0076-6879\(03\)73003-1](https://doi.org/10.1016/S0076-6879(03)73003-1).
  58. Matyas GR, Mayorov AV, Rice KC, Jacobson AE, Cheng K, Iyer MR, Li F, Beck Z, Janda KD, Alving CR. 2013. Liposomes containing monophosphoryl lipid A: a potent adjuvant system for inducing antibodies to heroin hapten analogs. *Vaccine* 31:2804–2810. <https://doi.org/10.1016/j.vaccine.2013.04.027>.
  59. Baqar S, Rice B, Lee L, Bourgeois AL, El Din AN, Tribble DR, Heresi GP, Mourad AS, Murphy JR. 2001. *Campylobacter jejuni* enteritis. *Clin Infect Dis* 33:901–905. <https://doi.org/10.1086/322594>.
  60. Pequegnat B, Laird RM, Ewing CP, Hill CL, Omari E, Poly F, Monteiro MA, Guerry P. 2017. Phase-variable changes in the position of O-methyl phosphoramidate modifications on the polysaccharide capsule of *Campylobacter jejuni* modulate serum resistance. *J Bacteriol* 199:e00027-17. <https://doi.org/10.1128/JB.00027-17>.

# SCIENTIFIC REPORTS



OPEN

## Identification of Immune Signatures of Novel Adjuvant Formulations Using Machine Learning

Sidhartha Chaudhury<sup>1</sup>, Elizabeth H. Duncan<sup>2</sup>, Tanmaya Atre<sup>2</sup>, Casey K. Storme<sup>2</sup>, Kevin Beck<sup>3</sup>, Stephen A. Kaba<sup>2</sup>, David E. Lanar<sup>2</sup> & Elke S. Bergmann-Leitner<sup>2</sup>

Adjuvants have long been critical components of vaccines, but the exact mechanisms of their action and precisely how they alter or enhance vaccine-induced immune responses are often unclear. In this study, we used broad immunoprofiling of antibody, cellular, and cytokine responses, combined with data integration and machine learning to gain insight into the impact of different adjuvant formulations on vaccine-induced immune responses. A Self-Assembling Protein Nanoparticles (SAPN) presenting the malarial circumsporozoite protein (CSP) was used as a model vaccine, adjuvanted with three different liposomal formulations: liposome plus Alum (ALFA), liposome plus QS21 (ALFQ), and both (ALFOA). Using a computational approach to integrate the immunoprofiling data, we identified distinct vaccine-induced immune responses and developed a multivariate model that could predict the adjuvant condition from immune response data alone with 92% accuracy ( $p = 0.003$ ). The data integration also revealed that commonly used readouts (i.e. serology, frequency of T cells producing IFN- $\gamma$ , IL2, TNF $\alpha$ ) missed important differences between adjuvants. In summary, broad immune-profiling in combination with machine learning methods enabled the reliable and clear definition of immune signatures for different adjuvant formulations, providing a means for quantitatively characterizing the complex roles that adjuvants can play in vaccine-induced immunity. The approach described here provides a powerful tool for identifying potential immune correlates of protection, a prerequisite for the rational pairing of vaccines candidates and adjuvants.

Adjuvants have long been recognized as a crucial component in vaccine formulations<sup>1</sup>. Currently, access to, and availability of, adjuvants suitable for clinical use are limited; licensed vaccines are typically formulated with Alum, and there are only a few licensed novel vaccines, such as AS04 or AS01B. In an effort to develop vaccines without the need to depend on commercial partners, our institute has developed several liposomal adjuvant formulations<sup>2–4</sup>. These formulations contain liposomes as carriers for adjuvants monophospholipid A (MPLA) and either Alum and/or QS21). Liposomes containing MPLA induce high antibody titers as well as strong cellular responses<sup>5</sup>. Formulations of circumsporozoite protein (CSP) with QS21 have been used for the leading malaria vaccine RTS,S, which provides up to 83% vaccine efficacy depending on the vaccination regimen<sup>6</sup>. In the field, however, this formulation only provides limited and short-lived efficacy<sup>7</sup>. Therefore, new approaches to increase vaccine efficacy are needed.

Recently, a self-assembling protein nanoparticle (SAPN) platform displaying the C-terminus (denoted here as peptide 16 (PF16)), as well as six copies of the central repeat region motif of *Plasmodium falciparum* CSP (PfCSP), was manufactured for testing in humans<sup>4</sup>. This construct also contains two universal CD4<sup>+</sup> T cell helper epitopes, derived from the Lymphocytic Choriomeningitis virus and the Influenza A matrix protein 1, to increase the immunogenicity of the SAPN. This SAPN, formulated with the commercially available analogue of MF59 (AddaVax), demonstrated the ability to mediate sterile protection in mice after challenge with a *P. berghei* transgenic parasite that expresses PfCSP<sup>8</sup>, providing support for the vaccine's clinical development. The mechanism of protection in mice was found to be based, at least in part, on antibody-mediated sporozoite neutralization. Although the role of cellular responses has not yet been fully explored, SAPNs have been shown to be taken up and processed by dendritic cells, suggesting the possibility of a role for cellular immunity in protection.

<sup>1</sup>Biotechnology High Performance Computing Software Applications Institute, Telemedicine and Advanced Technology Research Center, U.S. Army Medical Research and Materiel Command, Fort Detrick, MD, USA. <sup>2</sup>Malaria Vaccine Branch, US Military Malaria Research Program, Walter Reed Army Institute of Research, Silver Spring, MD, USA. <sup>3</sup>Miltenyi Biotec Inc., San Diego, CA, USA. Correspondence and requests for materials should be addressed to S.C. (email: [sidhartha.chaudhury.civ@mail.mil](mailto:sidhartha.chaudhury.civ@mail.mil)) or E.S.B.-L. (email: [elke.s.bergmann-leitner.civ@mail.mil](mailto:elke.s.bergmann-leitner.civ@mail.mil))



Cellular immunity is reportedly important for protection in the RTS,S malaria vaccine, another subunit vaccine based on the CSP antigen. Previous studies have shown that protection in RTS,S depends, at least in part, on CD4<sup>+</sup> T cells, especially those producing IFN- $\gamma$ , IL2, TNF $\alpha$ <sup>9</sup>, and antibodies (especially, certain isotype classes)<sup>10,11</sup>. Although induction of CD8<sup>+</sup> responses in humans has proven difficult when immunizing with recombinant vaccines, such as RTS,S, DNA-based vaccines, such as the heterologous prime-boost DNA/Ad4 CSP-based vaccine, have demonstrated that CSP-specific CD8<sup>+</sup> T cells can be induced. Likewise, a study using humanized mice demonstrated that CD8<sup>+</sup> T cells can mediate protection when RTS,S is delivered with the CAF09 liposomal adjuvant<sup>12</sup>.

CD8<sup>+</sup> T cells may increase the efficacy of a CSP-based vaccine because they could potentially eliminate *Plasmodium*-infected hepatocytes. Such an effect would complement antibody-based neutralization. While it is clear that the appropriate selection of adjuvant and vaccine delivery platform may be able to induce the desired cellular immunity, there are several challenges to identifying the correct vaccine formulation is challenging. First, adjuvants can induce a wide range of complex and subtle changes to vaccine-induced immunity. Quantification of these adjuvant effects can help guide the selection of adjuvants to achieve the desired mode of immunity. Second, experimental assessment of cellular immunity is complicated by the fact that certain cell types may migrate out of the blood compartment and into other organs, such as the liver, lymph node, or spleen, where they could be difficult to detect<sup>13</sup>.

In this study, we measure a wide range of serological, cellular, and cytokine properties in tissue samples taken from multiple physiological compartments, including the blood, liver, spleen, and lymph node, to generate a broad immunoprofile of non-human primates (NHPs) following vaccination with different SAPN/adjuvant formulations consisting of Alum, QS21, or a combination of both. The goal of the study was to determine the potency of different adjuvant formulations in a primate preclinical model. The resulting immunoprofile consisted of over 120 immune measures collected for each animal in the study. Machine-learning methods, such as the random forest model, offer powerful tools for analyzing large immune data sets and for characterizing how different immune features or combinations of immune features are linked to vaccination conditions or immunological outcomes<sup>14–16</sup>. This is particularly useful in immunology studies, where group-level or population-level effect sizes can be modest, and where sample sizes are relatively small compared to the number of immune parameters being measured<sup>16</sup>. We employed a range of multivariate analysis techniques to characterize immune responses with respect to adjuvant formulation and antigen dose, and thereby define a distinct immune ‘signature’ for each adjuvant and adjuvant/SAPN dosage combination used in the study.

Immune correlates – or even surrogates – of protection continue to remain elusive for most diseases, including malaria. Efforts to define immune parameters responsible for protection against infection or disease have been hampered by a focus on a limited number of “standard” immune parameters, most commonly serum antibody titers and/or the secretion of certain cytokines by antigen-specific T cells in select immune compartments (in case of NHP or humans, most commonly PBMC). While the choice of adjuvant can determine whether or not a vaccine is capable of inducing protective immunity by altering a vaccine’s immune profile, adjuvants continue to be selected based on factors such as availability, since rational adjuvant-vaccine pairing requires insights into both immune correlates of protection and immunoprofiles induced by adjuvants. The study presented here represents a first step towards this goal by providing the tools, namely laboratory assays, statistical methods, and mathematical models, capable of identifying characteristic immune profiles imprinted upon a vaccine by different adjuvant formulations.

## Results

**Vaccinations with SAPN.** Vaccinations were carried out in 22 rhesus monkeys (*Macaca mulatta*) randomly assigned to nine cohorts (Supplemental Table S1). Each vaccine and adjuvant cohort consisted of three animals, except the control cohorts which each had a single animal. Three different adjuvant conditions were compared side-by-side: ALFA, ALFQ, and the combination ALFQA formulation. The SAPN-based vaccine (FMP014) was administered at two antigen doses: 10  $\mu$ g (“low dose”) and 40  $\mu$ g (“high dose”), for the low-dose and high-dose cohorts, respectively. The immunization schedule for both vaccinated and control animals was three intramuscular injections at four week intervals. Because of the relatively small sample sizes in each cohort, we pooled vaccinated subjects by adjuvant (ALFA, ALFQ, and ALFQA) and antigen dose (low dose and high dose). For comparison, we also pooled the adjuvant-only and saline conditions as a combined ‘non-vaccinated’ group. Although this sample size is relatively small, it is typical for many NHP studies. In order to apply more sophisticated data analysis methods such as machine-learning methods and regression analysis on this limited sample size, we employed a number of strategies including feature reduction and boot-strapping to minimize the risk of overfitting and assess the variability in the model estimates.

**Immunoprofiling.** Our profiling panel includes serological tests (i.e. ELISA titers to the CSP-SAPN, the repeat region, and the C-terminus of CSP), cellular assays measuring the frequency of CD4<sup>+</sup> and CD8<sup>+</sup> T cell subpopulations, as well as arrays profiling the cytokine response in antigen-stimulated leukocytes (Fig. 1).

Vaccine-induced responses were monitored by bleeding the animals prior to the start of the study and after each vaccination. Sera from these time points were used to determine the potency of the vaccine formulations. IFN- $\gamma$ /IL2 Fluorospot assays were used to measure changes in the frequency of CSP-specific cells between pre-immune, post-vaccination, and terminal time points. After completing the vaccination regimen, animals were euthanized and blood, livers, draining lymph nodes, and spleens were collected. Cryopreserved leukocytes from the various compartments were either unstimulated or stimulated with CSP-SAPN or CSP peptide pools. Animals receiving saline/adjuvant formulations were used to determine vaccine-specific responses.

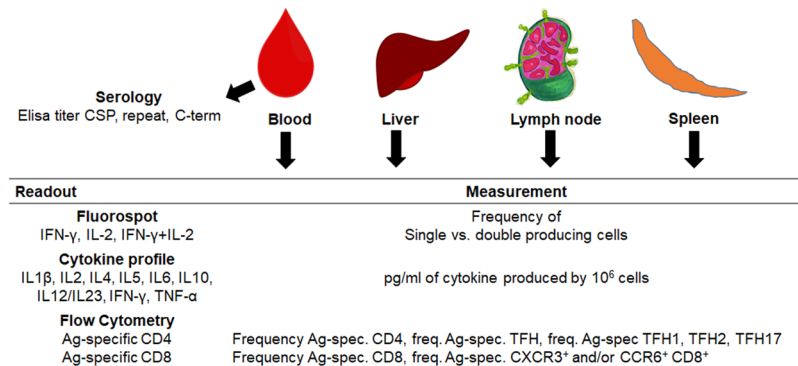


**Figure 1.** Overview of all measurements collected in this study. Samples were collected from blood, liver, lymph node, and spleen. Serology, Fluorospot, cytokine, and flow cytometry assays were carried out for all tissues and different time points for peripheral blood mononuclear cells (PBMCs).

**Hierarchical clustering.** Integrating all measurements allowed the analysis of data in regards to which responses were (1) vaccine-induced by comparison with either pre-immune (where available) or adjuvant-saline control animals; (2) sensitive to vaccine dose; and (3) sensitive to the adjuvant formulation (Fig. 2).

We carried out univariate analyses of all immune measures in the study, compared to either their corresponding pre-immune measures or the pooled non-vaccinated control cohort, in order to identify vaccine-induced immune responses. We found vaccine-induced responses in all serological data, as well as in the majority of cytokine responses (IL4, IL5 responses in Ag-stimulated lymphocytes resident in the liver and spleen, as well as IL5 responses in Ag-stimulated PBMCs). Vaccine-induced changes in the frequency of Ag-specific, IL2-producing T cells were statistically significant and higher than for Ag-specific IFN- $\gamma$ -producing cells. Interestingly, a relatively small number of vaccine-induced responses were observed when analyzing the changes in the T cell subsets (flow cytometric phenotyping of responding cells). These changes could be detected in the frequency of CSP-specific CD4<sup>+</sup> cells in the lymph nodes, CSP-specific cTFH2 CD4<sup>+</sup> cells in the liver, and CSP-specific cTFH1 cells in the blood.

We carried out univariate analyses on the vaccine-induced immune responses comparing the pooled adjuvant groups (ALFA vs. ALFQ) and the pooled antigen dose groups (low-dose and high-dose). We found 12 immune responses that showed significant differences with respect to adjuvant ( $p < 0.05$  and  $q < 0.20$ ), but no differences in immune responses with respect to antigen dose. The adjuvant-specific differences included serum antibody response to the CSP C-terminal region at multiple time points, as well as differences in the cytokine response for IL4 and IL5 in both PBMCs and the liver, and for IL6, IL8, and TNF $\alpha$  in the liver.

We carried out a 2-way ANOVA to compare adjuvant and dose conditions for all immune parameters that were classified as vaccine-induced. Among the 12 parameters that showed adjuvant-specific differences in the univariate analysis, 8 of 12 were found to have significant adjuvant effect in the ANOVA ( $p < 0.05$ ). We did not observe any significant dose effects or adjuvant-dose interaction effects. Supplemental Table S2 provides a summary of the univariate analysis and the ANOVA analysis for the 12 parameters that showed adjuvant-specific differences.

Overall, we found 53 immune measures that we classified as vaccine-induced. We carried a correlation analysis for all vaccine-induced immune measures (Supplemental Fig. S1) followed by hierarchical clustering and found that 10 immune clusters represented almost 80% of the vaccine-induced immune responses. Representative parameters from each of the 10 clusters are shown in Table 1.

**Principal Component Analysis.** We carried out principal component analyses (PCA) on the representative vaccine-induced immune measures identified by univariate analysis (Fig. 2) (Table 1) and plotted the first two principal components (Fig. 3). The measures for non-vaccinated animals and vaccinated animals formed distinct clusters in the PCA plot, consistent with our classification of these immune measures as vaccine-induced. In agreement with the univariate analysis, the measures for low-dose and high-dose animals showed large overlap in the PCA plot, indicating that there were no significant dose-specific differences in the vaccine-induced immune responses. However, the measures for ALFA and ALFQ animals clustered in distinctly different regions of the PCA plot, indicating a systematic difference in immune responses between these two groups. Interestingly, immune measures for the combination ALFQA animals overlapped considerably with those for both ALFA and ALFQ animals, suggesting both a wider variety of immune responses in the ALFQA condition as well as a commonality in immune responses with both adjuvant groups. We carried out PCA using all 53 vaccine-induced measures (Supplemental Fig. S2) and saw largely similar trends.

**Machine learning.** The above analyses confirmed that that ALFA and ALFQ induce distinctly different immune responses when formulated with SAPN. To assess which combination of immune parameters most clearly defines the differences between these two adjuvant conditions, we used a machine-learning method known as the random forest model<sup>17</sup>. We carried out a leave-one-out analysis to train the random forest model and test its accuracy in predicting an animal's adjuvant condition from its immune response data alone. First, when we used all 53 vaccine-induced immune responses, the resultant model achieved 83% accuracy ( $\kappa = 0.67$ ,  $p = 0.01$ ) in predicting which animals were given the ALFA- or ALFQ-adjuvanted vaccine. Analyzing for variable importance

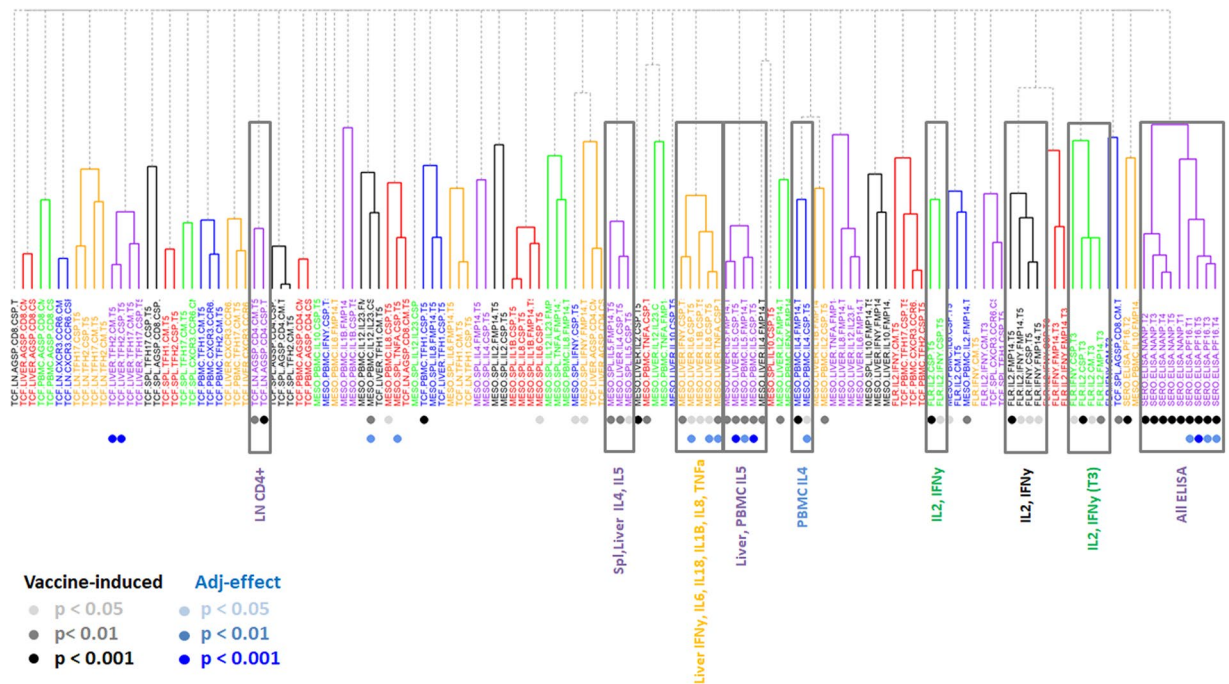


**Figure 2.** Hierarchical clustering of vaccine-induced immune responses. Hierarchical clustering of immune responses based on their correlation coefficients is shown, colored by immune cluster. Shaded circles below the immune measures indicate statistical significance as a vaccine-induced response or an adjuvant effect. Cluster names are shown, and clusters that predominantly show vaccine-induced measures are highlighted.

Cluster Name <sup>a</sup>	Assay <sup>b</sup>	Compartment <sup>c</sup>	Phenotype <sup>d</sup>	Representative Parameter <sup>e</sup>
TCFLN.CD4	T cell flow cytometry	LN	CD4	TCFLn.AgSp.CD4.CSP.T5
MESO.IL4	Mesoscale	Spl, Liver	IL4, IL5	MESO.liver.IL4.CSP.T5
MESO.IL5		Liver, PBMC	IL5	MESO.liver.IL5.CSP.T5
MESO.Multi		Liver	IFN-γ, IL6, IL18, IL1β, IL8, TNFα	MESO.liver.IFNy.CSP.T5
MESO.PBMC.IL4		PBMC	IL4	MESO.pbmc.IL4.FMP14.T5
FLR.IL2	Fluorospot	PBMC	IL2, IL2 + IFN-γ	FLR.IL2.CSP.T5
FLR.IFNy		PBMC	IL2, IL2 + IFN-γ	FLR.IFNy.CSP.T5
FLR.IL2.T3		PBMC	IL2	FLR.IL2.CSP.T3
FLR.IFNy.T3		PBMC	IFN-γ	FLR.IFNy.CSP.T3
SERO.ELISA	ELISA	Serum	NANP, C-term	SERO.ELISA.NANP.T5

**Table 1.** Clusters and representative parameters for vaccine induced responses. <sup>a</sup>Cluster name based on readout (TCF = Flow cytometry; MESO = mesoscale cytokine array; FLR = Fluorospot assay; SERO = serological response measured by ELISA). T3 = time point after last vaccination; T5 = terminal time point (euthanasia); <sup>b</sup>Readout method used to detect Ag-specific immune responses; <sup>c</sup>Source of lymphocytes for analysis; <sup>d</sup>Ag-specific parameter significantly different compared to vaccine controls or pre-immune; <sup>e</sup>Parameter identifier based on readout method, source of immune cells, significant measurement, time point. <sup>f</sup>The list of all parameters analyzed as well as the various clusters that are vaccine- or adjuvant-induced is shown in Fig. 2.

in the model (Table 2), we found that IL5 responses in the liver and PBMCs, as well as ELISA C-term responses, contributed most to prediction accuracy.

To see if we could improve the prediction accuracy, we ran a new random forest model by training it with the 12 immune measures we had identified as having adjuvant-specific differences. The model accuracy improved (92% accuracy, with kappa = 0.83 and p < 0.001) and the variable importance analysis showed good agreement with the random forest model generated using all 53 vaccine-induced measures (Table 2). We also carried out 5-fold and 10-fold internal validation of the model. For the 12-parameter model, we achieved 94% accuracy (kappa = 0.90) in 5-fold internal validation and 97% accuracy (kappa = 0.92) in 10-fold internal validation. For the 53-parameter model, we achieved 85% accuracy (kappa = 0.70) in 5-fold internal validation and 83% accuracy (kappa = 0.65) in 10-fold internal validation. Overall, we found general agreement with all three validation methods, suggesting that these models are able to reliably distinguish between the ALFA and ALFQ adjuvant conditions from vaccine-induced immune responses alone.

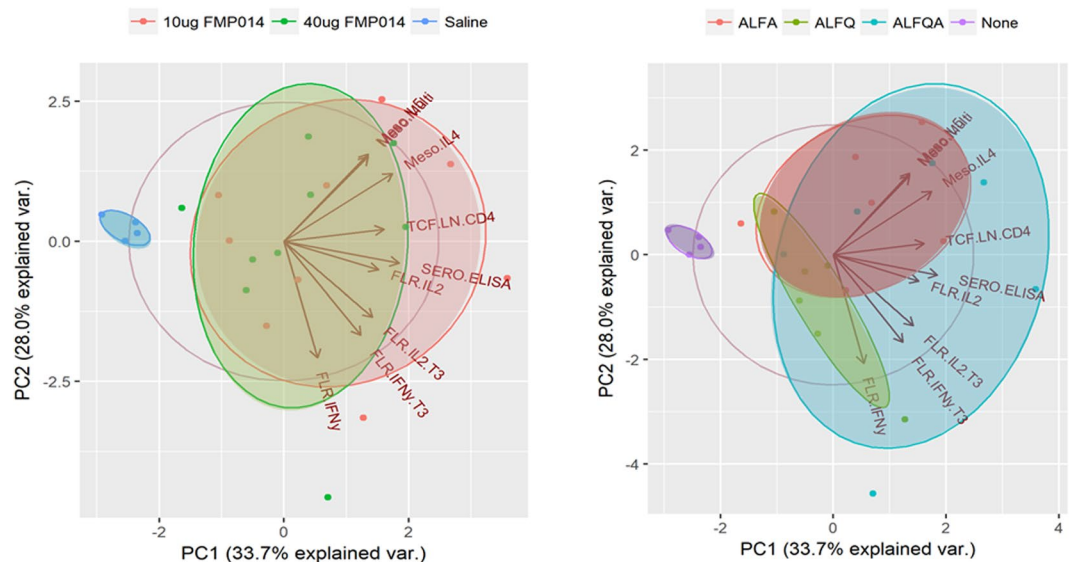


**Figure 3.** Principal component analysis of vaccine-induced immune responses. The first two principal components (PC1, PC2) are plotted comparing subjects with different antigen doses (left) and different adjuvant conditions (right), compared to non-vaccinated controls. Vectors corresponding to the projection of each immune measure along the two components are shown.

Assay	Phenotype	Parameter	Weight (53 param model)	Weight (12 param model)
MESO	IL5	MESO.pbmc.IL5.CSP.T5	100.0	100.0
		MESO.liver.IL5.CSP.T5	51.6	36.0
		MESO.pbmc.IL5.FMP14.T5	35.1	28.8
		MESO.liver.IL5.FMP14.T5	32.5	27.3
	IL6	MESO.liver.IL6.CSP.T5	39.6	31.5
	IL4	MESO.pbmc.IL4.CSP.T5	28.0	2.0
	IFNy	MESO.liver.IFNy.CSP.T5	26.0	—
IL12, IL23	MESO.pbmc.IL12.IL23.CSP.T5	22.9	43.1	
	FLR	IL2, IFNy	FLR.IIL2.IFNy.CSP.T5	52.6
FLR.IIL2.IFNy.FMP14.T5			28.0	—
SERO	C-term spec	SERO.ELISA.PF16.T1	60.3	28.5
		SERO.ELISA.PF16.T5	27.6	16.5

**Table 2.** Variable importance in Random Forest Model using all vaccine-induced parameters.

We identified responses that significantly distinguished ALFA- from ALFQ-adjuvanted vaccines when analyzing the cytokine profile of Ag-specific, liver-resident lymphocyte responses, in particular, of IL1 $\beta$ , IL6, and TNF $\alpha$ , as well as Ag-specific IL5 responses in liver-resident and PBMC lymphocytes of vaccinated NHPs. Moreover, the frequency of Ag-specific CD4<sup>+</sup> T cells was also a hallmark feature of recipients of the ALFA-adjuvanted vaccine. In contrast, ALFQ appears to drive higher antibody responses, especially against the C-terminus (PF16) of CSP (Supplemental Fig. S3 and Supplemental Fig. S4). Figure 4 shows representative immune measures for these responses for the three adjuvant conditions.

**Linear regression analysis.** Results from both the PCA (Fig. 3) and univariate analysis of immune parameters that distinguish ALFA from ALFQ (Fig. 4) suggest that the ALFQA adjuvant leads to immune responses that have the hallmarks of both ALFA- and ALFQ-specific responses. In order to quantify the relative contribution of ALFA and ALFQ to the ALFQA immune response, we modeled the ALFQA response as a linear combination of ALFA and ALFQ responses.

Starting from the 12 immune parameters that showed adjuvant-specific differences in the univariate analysis (C-terminus-specific antibody titers at all five time points; IL5, IL6, IL8, TNF $\alpha$  responses of CSP-specific liver-resident lymphocytes; IL4, IL5, and IL12/23p40 responses of CSP-specific PBMCs), we carried out a correlation analysis and clustered all parameters that showed a Pearson correlation coefficient of greater than 0.80, and selected a representative parameter for each cluster. This resulted in 8 clusters (Supplemental Table S3). We fit a linear regression model to median values for the 8 representative immune parameters. We fit the following equation, where  $M$  corresponds to a vector of median values for the 8 immune measures for each adjuvant condition

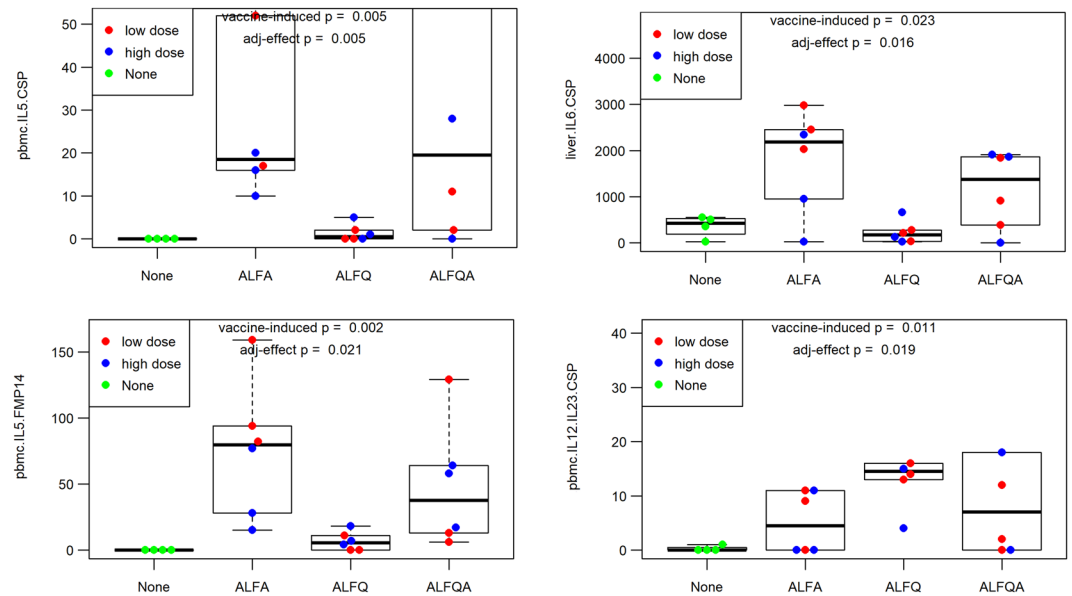


**Figure 4.** Adjuvant-specific differences in the SAPN-based vaccine. The ALFA-specific response in CSP-specific IL5- and IL6-producing cells (top left and right, respectively). ALFQ-biased and ALFQ-specific responses in CSP C-term-specific ELISA and CSP-specific IL12/IL23p40-producing cells (bottom left and right, respectively).

(ALFA, ALFQ, and ALFQA), and  $\beta$  corresponds to the weighted contribution of each component adjuvant (ALFA and ALFQ) to the combination adjuvant (ALFQA).

$$M_{ALFQA} = \beta_{ALFA}M_{ALFA} + \beta_{ALFQ}M_{ALFQ}$$

We found that the immune response measures in the ALFQA condition could be accurately modeled as a linear combination of ALFA and ALFQ responses, obtaining a best fit with  $\beta_{ALFA} = 0.54$  and  $\beta_{ALFQ} = 0.49$  ( $p < 10^{-4}$  and  $p < 0.01$ , respectively). We defined three types of adjuvant interactions involving two adjuvants that interfere with and diminish one another's responses, and can be expressed quantitatively by the condition  $\beta_{ALFA} + \beta_{ALFQ} \ll 1$ ; 2) additive interactions involving two adjuvants that 'average' their respective immune responses ( $\beta_{ALFA} + \beta_{ALFQ} \approx 1$ ); and 3) synergistic interactions involving two adjuvants that fully combine and/or enhance one another's immune responses ( $\beta_{ALFA} + \beta_{ALFQ} \gg 1$ ). Within this regime, we found that the ALFQA adjuvant combination is largely additive, with a balanced contribution of both ALFA and ALFQ components.

To show how each of the eight immune measures differ between adjuvants ALFA and ALFQ, we plotted the normalized median values in a radar plot (Fig. 5). For the linear regression model, we calculated the expected median values for the immune measures of ALFQA based on the experimental immune measures of ALFA and ALFQ, and compared them with the actual measured values for ALFQA. We found good agreement between the modeled and actual measurements for the ALFQA condition ( $R^2 = 0.61$ ), suggesting that a linear model is sufficient to describe the interaction between ALFA and ALFQ in this condition.

We generated a 95% confidence interval for the estimated values for ALFQA based on the linear regression model using a resampling technique (see Methods). Overall, we found that the linear model for the combined ALFQA adjuvant predicted antibody responses at multiple time points, as well as most cytokine measures in the PBMC and liver within the 95% confidence interval, indicating that the combined ALFQA adjuvant can be modeled as a linear combination of ALFQ and ALFA-specific responses. However, we found that two PBMC cytokine measures, IL-4 and IL-5, fell well outside the estimated range. In these cases, the ALFQA adjuvant showed responses very close to the ALFA, suggesting some degree of synergy instead of additivity.

## Discussion

The current report is the first to characterize the impact of adjuvant formulations on the complex immunoprofile of responses in a non-human primate malaria vaccine study, using both adjuvants and vaccine from a clinical development pipeline. The animals had received a high (40  $\mu$ g) or low dose (10  $\mu$ g) of FMP014 vaccine formulated with the recently developed adjuvants ALFA, ALFQ, and ALFQA<sup>3,4</sup>. The antigen-specific responses of lymphocytes from multiple anatomical sites (blood, liver, spleen, and draining lymph node) were characterized using cytokine arrays, flow cytometry, and Fluorospot assays. Compiling 120 different measurements from these assays resulted in the definition of distinct immune signatures of these novel adjuvants and a modeling tool capable of predicting the immunoprofile of the vaccine-induced immune response. These signatures can guide the selection of adjuvants, not only for malaria but potentially for vaccines against other pathogens as well by establishing immunological fingerprints of different adjuvants which can be matched with the requirements of vaccine candidates.

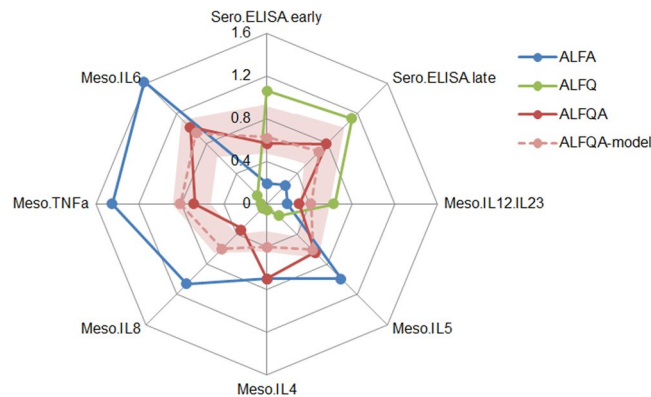


**Figure 5.** Linear regression model of combination ALFQA adjuvant. Median values for eight representative immune parameters that showed significant differences with respect to adjuvant are displayed in a radar plot using normalized values for ALFA (blue), ALFQ (green), and ALFQA (red). The estimated values based on the linear regression model for ALFQA (pink) is shown along with the 95% confidence interval for the estimated values (shaded pink).

Army Liposome Formulations (ALFs) are anionic liposomes<sup>18</sup> comprised of synthetic phospholipids, cholesterol, monophosphoryl lipids, QS-21 (ALFQ), and/or Alhydrogel (ALFQA and ALFA respectively). These formulations were developed to address the limited availability of adjuvants for clinical use and are based on formulations that have already been extensively used in humans: ALFQ has similarities to AS01<sup>19</sup>, an adjuvant used in Zostervax, which was recently approved by the FDA. AS01 formulations promote the induction of both antibody and cellular responses, and have extensively been tested in the clinic with the RTS,S malaria vaccine, the first licensed malaria vaccine<sup>6,20</sup>. ALFA has similarities to AS04, which is used in Cervarix, an FDA approved HPV vaccine. Alhydrogel-based adjuvants are potent inducers of humoral immune responses. Indeed, testing ALFA with various vaccines against malaria<sup>2,4</sup>, HIV, and heroin<sup>21</sup> confirmed that this adjuvant induces significant antibody titers. Liposome formulations containing QS21 have been shown to result in strong Th1 responses in mice<sup>3</sup> and non-human primates (Kaba *et al.*, manuscript in preparation). Combining QS21 and Alhydrogel has been reported to increase the potency of the vaccine formulation as well as broaden the immune response to a balanced Th1/Th2 profile in mice<sup>3</sup>. Given the similarities of the ALF formulations to other clinically tested adjuvants, we believe that the defined parameters and modeling approach presented here will be applicable to their clinically used counterparts, and hence provide guidance for the selection of adjuvants for vaccine formulations when immune correlates are known.

Immunoprofiling greatly increases our understanding of the potency of vaccine formulations and holds promise for identifying immune correlates, or at least surrogate markers of, protection. For the present study, we collected 120 different measurements characterizing antigen-specific CD4<sup>+</sup> (with special emphasis on follicular T helper cells) and CD8<sup>+</sup> T cell subsets, using specialized flow cytometry<sup>22</sup>, cytokine arrays on culture supernatants of antigen-specifically stimulated lymphocytes, characterization of serological responses regarding fine specificity, and anti-parasite activity in a passive-transfer setting.

Evaluating serological responses, we noticed two major adjuvant-driven differences: (1) CSP-antigen formulated with QS21 (ALFQ and ALFQA) induced significantly more antibodies directed to the C-terminus of the CSP than did that formulated with ALFA; and (2) CSP-antigen formulated with ALFA induced higher antibody titers to the central repeat region of CSP. It is not clear why ALFQ promotes responses to the C-terminal region. Possible explanations are that QS21 has an impact on antigen-presentation to B cells, or that the formulation affects the epitope structure, accessibility, or density and arrangement on the nanoparticle in a manner that alters its relative immunogenicity.

Fluorospot assays that measure the frequency of IFN $\gamma$ , IL2, and IFN $\gamma$ /IL2 double-producing cells revealed that all three adjuvants induce IL2 single-producing cells equally, while ALFQ and especially ALFQA induce significantly higher numbers of IFN $\gamma$  single-producing cells. Vaccination with ALFQ-adjuvanted antigen results in significantly higher frequencies of IFN $\gamma$ /IL2 double-producing cells. The addition of QS21 appears to favor poly-functional T cells, whereas Alhydrogel promotes the induction of terminally differentiated effector cells. Others have reported that IL2 single-producing cells are linked to the generation of memory cells<sup>23</sup>. This suggests that all three formulations are comparable in their ability to induce T cell memory and terminally differentiated effector T cells. The association of poly-functional T cells with protection has been reported for RTS,S when an Ad35-CSP prime was part of the regimen<sup>24</sup>. Similarly, immunization with adjuvants targeting TLR4 favored the induction of poly-functional T cells in mice protected against challenge with live *Plasmodium* sporozoites<sup>25</sup>. That the ALFQ-adjuvanted vaccine formulation resulted in a higher frequency of poly-functional T cells suggests that this formulation may induce higher protective efficacy.

Data integration and hierarchical clustering demonstrated several findings. First, 53 of the 120 immune measures showed a significant change following vaccination. The 10 immune clusters comprising 38 of the vaccine-induced measures could predict systemic differences between adjuvants, but not dose. Second, classic and commonly used readouts (*i.e.* serology, enumeration of CD4<sup>+</sup> and CD8<sup>+</sup> cells producing IFN $\gamma$ , IL2, and TNF $\alpha$ ) missed important differences between the adjuvants. Alhydrogel in ALFA and ALFQA led to significantly

higher IL4 and IL5 cytokine responses of antigen-specific lymphocytes at different anatomical sites. This observation is consistent with previous findings that Alhydrogel tends to induce Th2-type immune responses<sup>1</sup>. Third, Alhydrogel induced a pronounced antigen-specific cytokine pattern in the liver that was significantly different from that of ALFQ-induced responses—namely, the induction of pro-inflammatory IL1 $\beta$ , IL6, and IL8 and the Th1 cytokines IFN $\gamma$  and TNF $\alpha$ . The immunological milieu of the liver tends to down-regulate persistent local immune responses by silencing antigen-specific CD8<sup>+</sup> T cells through TGF $\beta$  and IL10. These immune-dampening cytokines are primarily produced by liver-resident CD4<sup>+</sup> T cells<sup>26</sup>. Our finding suggests that Alhydrogel-containing vaccine formulations may overcome this tolerance by inducing antigen-specific lymphocytes with pro-inflammatory cytokine profiles.

The current study reveals that immunoprofiling provides the breadth of immune measurements needed for the development of predictive modeling tools. Here, we first performed univariate analyses to identify significant vaccine-specific responses. Next, we carried out correlation analyses followed by hierarchical clustering to identify associations between measurements. Clustering identified 10 groups of correlated immune parameters, or clusters that capture the vaccine-induced responses for the SAPN vaccine candidate. PCA using representative parameters for these immune clusters revealed systematic differences between animals with respect to adjuvant condition, but not vaccine dose. To determine if these parameters could be used to generate an ‘immune signature’ that could clearly define the adjuvant condition, we used a random forest model to create a mathematical model that predicts adjuvant condition from immune data alone. When we used all 53 vaccine-induced parameters to build the model, we achieved an accuracy of 83% for predicting which signature was associated with a specific adjuvant. When we used the 12 parameters that differed between the adjuvants, the predictive accuracy of the model improved to 92%. The random forest model results suggest that these 12 parameters, spread between serological responses such as the ELISA antibody titers, as well as cellular responses such as IL4 and IL6 responses in the liver, are sufficient to discriminate between the ALFA and ALFQ adjuvants. Furthermore, using linear regression modeling, we showed that these parameters were sufficient to quantify the relative contribution of ALFA and ALFQ to the ALFQA combination adjuvant.

In conclusion, this NHP study represents the first comprehensive immunoprofiling effort for three adjuvant formulations that are based on previously described proprietary adjuvants which had not only been tested extensively in humans, but are part of three vaccines licensed for use in humans (Zostervax, Mosquirix, Cervarix). By using a wide range of immune data combined with multivariate analysis and machine learning, we were to identify immune “fingerprints” unique to specific adjuvant formulations and reflect their respective biases towards promoting different types of serological and cellular responses. In upcoming clinical studies with these adjuvant formulations, these immune fingerprints can serve as a guide for defining a more limited selection of accessible human immune parameters that can be used to identify potential correlates of protection. More generally, this approach of applying machine-learning methods to vaccine-induced immune responses can be applied to define complex multi-variate immune signatures that reliably distinguish subjects based on characteristics such as vaccine dose, vaccine regimen, or protection status, and provide insights into the immunological mechanisms that underlie vaccine efficacy.

## Methods

**Study design and samples.** Twenty-two non-human primates (NHPs, *Macaca mulatta*) were divided into nine vaccine cohorts and immunized three times in four-week intervals (Supplemental Table S1). Serum and PBMC samples were collected two weeks after each vaccination and cryopreserved. NHPs were euthanized 4–6 weeks after the last immunization; spleens, lymph nodes, liver, and bone marrow were collected; and lymphocytes were prepared and cryopreserved. The research was conducted under an approved animal use protocol in an AAALAC accredited facility, in compliance with the Animal Welfare Act and other federal statutes and regulations relating to animals and experiments involving animals; it also adheres to the principles stated in the *Guide for the Care and Use of Laboratory Animals* (NRC Publication, 2011 edition).

**Immunizations.** All vaccines were administered by intramuscular injection into the rectus femoris muscles, with injection sites alternating following each immunization. Serum and blood samples were collected 14 days prior to the first immunization and each subsequent immunization, 35 days after the third immunization, and at the time of euthanasia for tissue collection.

**Mesoscale 10-plex Cytokine U-plex Panel.** Cryopreserved pre-immune PBMCs (when available) and post-immune PBMCs (collected at the final time point), splenocytes, lymph node cells, and liver-resident lymphocytes from each NHP were stimulated with a CSP mega-pool representing the FMP014 vaccine peptide pools (15-mer peptides overlapping by 11 AA) at a final concentration of 1  $\mu$ g/mL for 48 h. A U-PLEX<sup>®</sup> Biomarker Group 1 (NHP) Assays, SECTOR 10-plex kit (IL1 $\beta$ , IL6, IL8, IL4, IL5, IL10, IL12/IL23p40, IL2, IFN $\gamma$ , TNF $\alpha$ , Mesoscale Discovery, Gaithersburg, MD) was used to analyze culture supernatants according to the manufacturer’s protocol. Plates were read using a QuickPlex SQ120 plate reader.

**Polychromatic Flow Cytometry Staining.** All monoclonal antibodies for cell culture and analysis were purchased from Miltenyi Biotec (San Diego, CA) unless otherwise stated. Cryopreserved pre-immune and final time-point PBMCs, splenocytes, liver-resident lymphocytes, and lymph node cells were cultured for 16 h (37°C, 5% CO<sub>2</sub>) at a concentration of 2.5  $\times$  10<sup>7</sup> cells/ml in complete medium (RPMI-1640 with 10% fetal bovine serum, Pen/Strep, L-glutamine, NEAA, Sodium Pyruvate, 2-mercaptoethanol) with CD28 and CD49d (both from BD Biosciences, San Jose, CA) at 1.0  $\mu$ g/mL, anti-human CCR6-APC (REA190) at 1:10, and CD40 pure (HB14) at 1:100, or in the presence of CSP Megapool (pool representing the *P. falciparum* CSP sequence) at 1.0  $\mu$ g/mL in addition to the aforementioned. Following stimulation, cells were washed, resuspended, and stained 1:10 with

anti-human CD154-biotin (5C8) for 15 min at 4 °C in FACS solution (1.0% fetal bovine serum and 0.1% sodium azide in DPBS). Cells were further incubated 1:5 with anti-biotin microbeads, ultrapurified for 15 min at 4 °C. After washing, a pre-titrated and optimized antibody cocktail with fluorochrome-conjugated antibodies [CD3-BV421 (BD Biosciences), CD4-PerCPVio700 (M-T466), CD185-PE-Cyanine7 (MU5UBEE) (eBioscience, San Diego, CA), CD183-VioBrightFITC (REA232), anti-biotin-PE (5C8), and Zombie Aqua Fixable dye (BioLegend, San Diego, CA)] was added, and the cells were incubated for 45 min at 4 °C. After washing in flow buffer, the cells were resuspended in DPBS/0.5% BSA containing 2 mM EDTA, enriched over a magnetic column, and acquired on a MACSQuant Analyzer 10 (Miltenyi Biotec).

The gating strategy is depicted in Supplemental Fig. S5. Lymphocytes were first gated by scatter, then singlets, and finally viability and the lineage marker CD3. Enriched antigen-specific cells were gated by co-expression of CD4 and CD154, followed by the co-expression of CD4 and CXCR5. Within the CD4<sup>+</sup>CXCR5<sup>+</sup> cells, subsets were further identified—based on CCR6 and CXCR3 expression—as Tfh1, Tfh2, and Tfh17 cells. Enriched antigen-specific CD8<sup>+</sup> T cells were also analyzed for the expression of CXCR3 and CCR6. The quantitative analysis was performed using FlowJo 10 (Treestar, Ashland, OR).

**ELISA.** Assessment of humoral immune responses was performed by ELISA, as previously described<sup>4</sup>. Briefly, ELISA plates were coated with 25 ng of peptide representing either the repeat region (NANP)<sub>6</sub> or the C-terminus of CSP (PF16). Plates were blocked with 1% casein buffer (ThermoFisher Scientific, Waltham, MA), and tested with serially diluted mouse sera. OD = 1 antibody titers were determined using HRP-labeled goat-anti-mouse IgG (KPL, Gaithersburg, MD) as the secondary antibody and the ABTS substrate (KPL) for detection.

**IL2/IFN- $\gamma$  Fluorospot assay.** Antigen-specific interferon (IFN)- $\gamma$ , interleukin 2 (IL2), and IFN- $\gamma$ /IL2 cytokine-secreting T cells were measured by Fluorospot (U-CyTech Biosciences, Utrecht, Netherlands) following the manufacturer's instructions. Briefly, activated Fluorospot plates were coated with a solution of IL2- and IFN- $\gamma$ -coating antibodies and incubated overnight at 4 °C. Stimulating antigens were diluted in culture medium (RPMI-1640 containing 10% fetal bovine serum, Pen/Strep, L-glutamine, NEAA, Sodium Pyruvate, 2-mercaptoethanol). Monkey anti-CD3 mAb (Mabtech Inc., Cincinnati, OH) was used as an internal positive control. Each well was treated with 25  $\mu$ l of CD28 and CD49d (BD Biosciences, San Diego, CA) cell stimulants, 25  $\mu$ l of antigen, and 50  $\mu$ l of cells. Cells were plated at a cell concentration of  $2.5 \times 10^5$  cells/well. Plates were incubated at 37 °C, 5% CO<sub>2</sub>, 100% humidity for 40 to 48 h. Fluorospot plates were analyzed using the Autoimmun Diagnostica (AID) GmbH Fluorospot reader (Strassberg, Germany) equipped with filters for FITC (excitation 490 nm/emission 510 nm) and Cy3 (excitation 550 nm/emission 570 nm).

**Univariate analysis.** To determine which immune responses showed vaccine-induced changes, we carried out univariate analysis for each immune measure. For the serology and Fluorospot data, we had subject-matched pre-immune data and used the paired t-test to calculate statistical significance. For the Mesoscale and T cell flow cytometry data, no pre-immune data were available; therefore, we carried out t-tests between vaccination cohorts pooled by adjuvant (ALFA, ALFQ, and ALFQA) and dose (10  $\mu$ g and 40  $\mu$ g). Prior to any t-test, we carried out a Shapiro-Wilks test to determine if the to-be-compared distributions were normally distributed. If both were normally distributed ( $p < 0.05$  by the Shapiro-Wilks test) we applied a Student's t-test; if either distribution was not normally distributed, we applied the Wilcoxon signed-rank test. After calculating p-values for immune parameters in the data set, we calculated an adjusted p-value using the Benjamini-Hochberg correction<sup>27</sup>. Immune measures in which comparison to either pre-immune or control group data showed a significant difference at  $p < 0.05$  and a false discovery rate of  $q < 0.20$  were classified as vaccine-induced immune responses.

To identify immune measures that differed with respect to adjuvant and antigen dose, we pooled the vaccinated cohorts by adjuvant (ALFA, ALFQ, ALFQA) and antigen dose (10  $\mu$ g and 40  $\mu$ g), respectively. We then compared the adjuvant (ALFA vs. ALFQ) and antigen dose (10  $\mu$ g vs. 40  $\mu$ g) as described above, by applying either Student's t-test or the Wilcoxon signed-rank test following a multiple test correction. Immune measures that showed a significant difference between pooled adjuvant groups or pooled antigen dose groups at  $p < 0.05$  and  $q < 0.20$  were classified as measures showing adjuvant-specific and dose-dependent differences, respectively.

**Multivariate Analysis.** Correlation matrices for the data set were generated by calculating the Spearman correlation coefficient between each immune measure and every other immune measure. Subjects with missing data for any pair of immune measures were omitted from that particular correlation calculation. Spearman's  $\rho$  statistic was used to calculate p-values for each correlation estimate. Only correlation coefficients with  $p < 0.05$  were retained for further analysis to ensure that only high-confidence correlations were used in subsequent analyses; all others were set to '0'. Hierarchical clustering (R package *hclust* function) was used to group correlated immune measures and to define immune clusters based on a cutoff criterion of having a correlation coefficient of at least 0.40, using the *cutree* function. A dendrogram of the hierarchical cluster was generated using the *A2Rplot* function in R package *addicted*.

Representative immune measures from the ten largest clusters (representing almost 80% of all vaccine-induced immune responses) containing at least one vaccine-induced immune measure were used for additional analyses. Principal component analysis (PCA) was performed on these ten representative immune measures, using the R function *ir.pca* to separate subjects with respect to adjuvant (ALFA, ALFQ, and ALFQA) and antigen dose (10  $\mu$ g and 40  $\mu$ g). Using the R package *ggbiplot*, the first two principal components were visualized as two-dimensional PCA plots.

The random forest model was generated using all vaccine-induced immune responses (R *caret* package). We trained the model using the repeated *cv* method, subsampling the data set by 5-fold and resampling ten times. The random forest model was tuned using the *caret* R package. Specifically the number of branches of the tree (*mtry*),



the rule for splitting (*gini* or *extratrees*), was adjusted to identify the optimal accuracy and kappa values during internal 10-fold cross validation, repeated 10 times. The *oneSE* method was used to select the optimal model. For both the 53 parameter model and 12 parameter model, the optimal parameter was *mtry* = 2 and *splitrule* = *gini*. To test the predictive accuracy of the random forest modeling approach, we carried out a leave-one-out analysis, where one subject was removed from the data set, after which the model was trained on the remaining subjects and then used to predict the adjuvant condition of the excluded subject based on its immune data. We performed this for all subjects in the data set, and calculated both the accuracy and kappa value of the prediction model. We used the *varImp* function to determine the variable importance for each generated model, and reported the average variable importance across all models to assess the relative importance of each vaccine-induced immune measure to predicting the adjuvant condition.

We used linear regression modeling to determine the relative contributions of ALFA and ALFQ adjuvants to the combined ALFQA adjuvant condition. We carried out correlation analysis of all 12 immune parameters that showed adjuvant-specific differences in the univariate analysis, and generated clusters for immune measures that showed a Pearson correlation coefficient > 0.80 (Supplemental Table S3). From each cluster, the parameter that showed the greatest effect-size in the univariate analysis between the ALFA and ALFQ conditions was selected as the representative parameter for that group. We found that all eight parameters were normally distributed in at least one of the adjuvant cohorts using the Shapiro test ( $p > 0.05$ ). We defined immune responses for ALFA and ALFQ as vectors of median values of the pooled ALFA and ALFQ vaccinated cohorts, respectively, for the eight representative immune measures. We then fitted the median ALFQA response across those same 12 measures ( $M_{ALFQA}$ ) as the sum of the ALFA and ALFQ responses ( $M_{ALFA}$  and  $M_{ALFQ}$ ), weighted by  $\beta_{ALFA}$  and  $\beta_{ALFQ}$ , respectively. Because we sought to express the ALFQA response as entirely a function of the ALFQ and ALFA responses, we suppressed the constant term from the equation.

$$M_{ALFQA} = \beta_{ALFA}M_{ALFA} + \beta_{ALFQ}M_{ALFQ}$$

The coefficients  $\beta_{ALFA}$  and  $\beta_{ALFQ}$  reflect the relative contributions of ALFA and ALFQ, respectively, to the ALFQA adjuvant condition. We classified the interaction of these two adjuvants by its relative contribution to the combined adjuvant condition, using the following criteria:

$$\beta_{ALFA} + \beta_{ALFQ} \ll 1 \text{ (antagonistic)}$$

$$\beta_{ALFA} + \beta_{ALFQ} \approx 1 \text{ (additive)}$$

$$\beta_{ALFA} + \beta_{ALFQ} \gg 1 \text{ (synergistic)}$$

In order to generate an estimate of the 95% confidence interval for the linear regression model, we carried out a boot-strapping approach where we re-sampled the ALFA and ALFQ data set, with replacement, 1000 times, and generated a linear regression model for each re-sampled data set. We modeled the ALFQA response based on the coefficients and the median ALFA and ALFQ values generated from each of the re-sampled data sets, and report the 2.5 percentile and 97.5 percentile values for each immune parameter.

All the analysis scripts used in this study were written in R and are available freely for download at <https://github.com/BHSAI/immstat>. Please contact the corresponding author for technical support or further information.

## References

- Bergmann-Leitner, E. S. & Leitner, W. W. Adjuvants in the Driver's Seat: How Magnitude, Type, Fine Specificity and Longevity of Immune Responses Are Driven by Distinct Classes of Immune Potentiators. *Vaccines (Basel)* **2**, 252–296, <https://doi.org/10.3390/vaccines2020252> (2014).
- Genito, C. J. *et al.* Liposomes containing monophosphoryl lipid A and QS-21 serve as an effective adjuvant for soluble circumsporozoite protein malaria vaccine FMP013. *Vaccine* **35**, 3865–3874, <https://doi.org/10.1016/j.vaccine.2017.05.070> (2017).
- Beck, Z. *et al.* Differential immune responses to HIV-1 envelope protein induced by liposomal adjuvant formulations containing monophosphoryl lipid A with or without QS21. *Vaccine* **33**, 5578–5587, <https://doi.org/10.1016/j.vaccine.2015.09.001> (2015).
- Seth, L. *et al.* Development of a self-assembling protein nanoparticle vaccine targeting Plasmodium falciparum Circumsporozoite Protein delivered in three Army Liposome Formulation adjuvants. *Vaccine* **35**, 5448–5454, <https://doi.org/10.1016/j.vaccine.2017.02.040> (2017).
- De Serrano, L. O. & Burkhart, D. J. Liposomal vaccine formulations as prophylactic agents: design considerations for modern vaccines. *J. Nanobiotechnology* **15**, 83, <https://doi.org/10.1186/s12951-017-0319-9> (2017).
- Regules, J. A. *et al.* Fractional Third and Fourth Dose of RTS,S/AS01 Malaria Candidate Vaccine: A Phase 2a Controlled Human Malaria Parasite Infection and Immunogenicity Study. *J. Infect. Dis.* **214**, 762–771, <https://doi.org/10.1093/infdis/jiw237> (2016).
- Olotu, A. *et al.* Seven-Year Efficacy of RTS,S/AS01 Malaria Vaccine among Young African Children. *N. Engl. J. Med.* **374**, 2519–2529, <https://doi.org/10.1056/NEJMoa1515257> (2016).
- McCoy, M. E. *et al.* Mechanisms of protective immune responses induced by the Plasmodium falciparum circumsporozoite protein-based, self-assembling protein nanoparticle vaccine. *Malar. J.* **12**, 136, <https://doi.org/10.1186/1475-2875-12-136> (2013).
- Lumsden, J. M. *et al.* Protective immunity induced with the RTS,S/AS vaccine is associated with IL-2 and TNF-alpha producing effector and central memory CD4 T cells. *PLOS ONE* **6**, e20775, <https://doi.org/10.1371/journal.pone.0020775> (2011).
- Chaudhury, S. *et al.* Delayed fractional dose regimen of the RTS,S/AS01 malaria vaccine candidate enhances an IgG4 response that inhibits serum opsonophagocytosis. *Sci. Rep.* **7**, 7998, <https://doi.org/10.1038/s41598-017-08526-5> (2017).
- White, M. T. *et al.* The relationship between RTS,S vaccine-induced antibodies, CD4(+) T cell responses and protection against Plasmodium falciparum infection. *PLOS ONE* **8**, e61395, <https://doi.org/10.1371/journal.pone.0061395> (2013).
- Espinosa, D. A. *et al.* Robust antibody and CD8(+) T-cell responses induced by P. falciparum CSP adsorbed to cationic liposomal adjuvant CAF09 confer sterilizing immunity against experimental rodent malaria infection. *NPJ Vaccines* **2**, <https://doi.org/10.1038/s41541-017-0011-y> (2017).

13. Ishizuka, A. S. *et al.* Protection against malaria at 1 year and immune correlates following PfSPZ vaccination. *Nat. Med.* **22**, 614–623, <https://doi.org/10.1038/nm.4110> (2016).
14. Choi, I. *et al.* Machine learning methods enable predictive modeling of antibody feature: function relationships in RV144 vaccinees. *PLoS Comput. Biol.* **11**, e1004185, <https://doi.org/10.1371/journal.pcbi.1004185> (2015).
15. Trtica-Majnaric, L., Zekic-Susac, M., Sarlija, N. & Vitale, B. Prediction of influenza vaccination outcome by neural networks and logistic regression. *J. Biomed. Inf.* **43**, 774–781, <https://doi.org/10.1016/j.jbi.2010.04.011> (2010).
16. Valletta, J. J. & Recker, M. Identification of immune signatures predictive of clinical protection from malaria. *PLoS Comput. Biol.* **13**, e1005812, <https://doi.org/10.1371/journal.pcbi.1005812> (2017).
17. Breiman, L. Random Forests. *Mach. Learn.* **45**, 5–32, <https://doi.org/10.1023/a:1010933404324> (2001).
18. Forssen, E. A. & Tokes, Z. A. Use of anionic liposomes for the reduction of chronic doxorubicin-induced cardiotoxicity. *Proc. Natl. Acad. Sci. USA* **78**, 1873–1877 (1981).
19. Didierlaurent, A. M. *et al.* Adjuvant system AS01: helping to overcome the challenges of modern vaccines. *Expert Rev. Vaccines* **16**, 55–63, <https://doi.org/10.1080/14760584.2016.1213632> (2017).
20. Ockenhouse, C. F. *et al.* Ad35.CS.01-RTS,S/AS01 Heterologous Prime Boost Vaccine Efficacy against Sporozoite Challenge in Healthy Malaria-Naive Adults. *PLoS ONE* **10**, e0131571, <https://doi.org/10.1371/journal.pone.0131571> (2015).
21. Alving, C. R., Matyas, G. R., Torres, O., Jalah, R. & Beck, Z. Adjuvants for vaccines to drugs of abuse and addiction. *Vaccine* **32**, 5382–5389, <https://doi.org/10.1016/j.vaccine.2014.07.085> (2014).
22. Farooq, F. *et al.* Circulating follicular T helper cells and cytokine profile in humans following vaccination with the rVSV-ZEBOV Ebola vaccine. *Sci. Rep.* **6**, 27944, <https://doi.org/10.1038/srep27944> (2016).
23. Bejon, P. *et al.* Early gamma interferon and interleukin-2 responses to vaccination predict the late resting memory in malaria-naive and malaria-exposed individuals. *Infect. Immun.* **74**, 6331–6338, <https://doi.org/10.1128/IAI.00774-06> (2006).
24. Kazmin, D. *et al.* Systems analysis of protective immune responses to RTS,S malaria vaccination in humans. *Proc. Natl. Acad. Sci. USA* **114**, 2425–2430, <https://doi.org/10.1073/pnas.1621489114> (2017).
25. Kastentmuller, K. *et al.* Full-length Plasmodium falciparum circumsporozoite protein administered with long-chain poly(I.C) or the Toll-like receptor 4 agonist glucopyranosyl lipid adjuvant-stable emulsion elicits potent antibody and CD4+ T cell immunity and protection in mice. *Infect. Immun.* **81**, 789–800, <https://doi.org/10.1128/IAI.01108-12> (2013).
26. Crispe, I. N. The liver as a lymphoid organ. *Annu. Rev. Immunol.* **27**, 147–163, <https://doi.org/10.1146/annurev.immunol.021908.132629> (2009).
27. Benjamini, Y. & Hochberg, Y. Controlling the False Discovery Rate: A Practical and Powerful Approach to Multiple Testing. *J. Roy. Stat. Soc. Ser. B. (Stat. Method.)* **57**, 289–300 (1995).

## Acknowledgements

The authors would like to thank the members of the USMHRP program (Dr. Gary Matyas, Dr. Carl Alving, and Dr. Zoltan Beck) and Dr. Peter Burkhardt (University of Connecticut) for their contribution in designing the vaccine and adjuvant formulations and Dr. Tatsuya Oyama (BHSAI) for his help in revising and editing the manuscript. Material has been reviewed by the Walter Reed Army Institute of Research. There is no objection to its presentation and/or publication. The research was conducted under an approved animal use protocol in an AAALAC accredited facility, in compliance with the Animal Welfare Act and other federal statutes and regulations relating to animals and experiments involving animals; it also adheres to the principles stated in the Guide for the Care and Use of Laboratory Animals, NRC Publication, 2011 edition. This work was supported by the U.S. Military Infectious Disease Research Program, the Joint Warfighter Medical Research Program, and the U.S. Army Medical Research and Materiel Command. The opinions and assertions contained herein are the private views of the authors and are not to be construed as official or as reflecting the views of the U.S. Army or the U.S. Department of Defense. This paper has been approved for public release with unlimited distribution.

## Author Contributions

S.C. performed the data analysis and the computational portion of the work, E.H.D. performed the flow cytometric analysis and cytokine array experiments, T.A. performed the Fluorospot analysis, C.K.S. conducted pilot experiments for the cellular work, K.B. designed the flow cytometric panels and consulted on rare cell detection, S.A.K. performed the ELISAs, D.E.L. and S.A.K. designed and conducted the N.H.P. immunizations, E.B.-L. designed the immunological wet-lab experiments and compiled the manuscript. All authors read and approved the final manuscript. All authors read and approved the final manuscript.

## Additional Information

**Supplementary information** accompanies this paper at <https://doi.org/10.1038/s41598-018-35452-x>.

**Competing Interests:** Dr. Kevin Beck is an employee of Miltenyi Biotec Inc. (San Diego, CA).

**Publisher's note:** Springer Nature remains neutral with regard to jurisdictional claims in published maps and institutional affiliations.



**Open Access** This article is licensed under a Creative Commons Attribution 4.0 International License, which permits use, sharing, adaptation, distribution and reproduction in any medium or format, as long as you give appropriate credit to the original author(s) and the source, provide a link to the Creative Commons license, and indicate if changes were made. The images or other third party material in this article are included in the article's Creative Commons license, unless indicated otherwise in a credit line to the material. If material is not included in the article's Creative Commons license and your intended use is not permitted by statutory regulation or exceeds the permitted use, you will need to obtain permission directly from the copyright holder. To view a copy of this license, visit <http://creativecommons.org/licenses/by/4.0/>.

© The Author(s) 2018